Studies on Supply and Demand Side Energy Management in Low-Voltage Distribution Systems for Maximum Utilization of Photovoltaic Generation

太陽光発電の最大利用に向けた低圧配電系統の需要・供給側におけるエネルギーマネジメントに関する研究

February 2018

Hiroshi Kikusato

喜久里 浩之

Studies on Supply and Demand Side Energy Management in Low-Voltage Distribution Systems for Maximum Utilization of Photovoltaic Generation

太陽光発電の最大利用に向けた低圧配電系統の需要・供給側におけるエネルギーマネジメントに関する研究

February 2018

Waseda University
Graduate School of Advanced Science and Engineering
Department of Advanced Science and Engineering,
Research on Electrical Engineering and Bioscience A

Hiroshi Kikusato

喜久里 浩之

Abstract

We propose energy management methods for maximum utilization of photovoltaic (PV) generation in supply and demand side. The rapid increase of PV penetration increases reverse power flow and causes overvoltage in low-voltage distribution systems (LVDSs), so that the PV output tends to be curtailed. Our proposed methods utilize a low-voltage regulator (LVR) for voltage control in the LVDS to mitigate overvoltage and an electric vehicle (EV) for increasing the self-consumption of PV generation to reduce reverse power flow. In our supply side energy management method using the LVR, we determine an appropriate deployment and control parameters of LVRs to coordinate with the existing voltage control devices and mutually improve the voltage control performance. We also propose a method for rapidly determining control parameters of LVR by using classifiers based on machine learning technique for an upgraded voltage control scheme. Moreover, in our demand side EV management scheme, an auction mechanism is introduced to effectively reduce the PV curtailment and residential operation cost, while securing the autonomy and the equity of customers.

The proposed coordinated voltage control method of the LVR significantly reduced the voltage violation (up to 99%) while avoiding interference with existing voltage control devices. Additionally, the rapid determination method reduced the computational time required for obtaining the control parameters of LVR up to 96%, and it can be applied to the upgraded voltage control scheme for handling the frequently varying voltage trend by periodically updating the control parameters. It can be also applied to the simultaneous optimization for the huge number of LVRs. In our EV charging management method, introduction of the auction mechanism secured the autonomy and equity, which will promote the customers' contribution, and effectively reduced the PV curtailment and residential operation cost. The PV curtailment issue will become more and more obvious in many countries in the near future. Since the introduction of the LVR is simple and that of the EV will be promoted whether willing or not, how to effectively utilize these devices will have more important role in these countries.

This thesis is composed as follows. A coordinated voltage control scheme of the LVR is proposed in Chapter 2. As an upgraded supply side voltage control scheme, a method for rapidly determining the control parameters of LVR using classifiers is proposed in Chapter 3. A demand side EV charging management scheme using auction mechanism is introduced in Chapter 4. Finally, we discuss the conclusion in Chapter 5.

Acknowledgements

I have received immeasurable support and encouragement from many collaborators in completing this work. First of all, I would like to express the deepest appreciation to my supervisor, Professor Yasuhiro Hayashi for providing the significant support to this work, and I am sure that the work could not have been completed anywhere except Hayashi Laboratory. He always provided us infinite precious opportunities that have enriched my six-year research life.

I would like to thank the thesis referees, Professor Noboru Murata, Professor Hideo Ishii, and Professor Toru Asahi. Their insightful advice and comments for this thesis often provided me new viewpoints and refined the contents.

I would like to thank my major collaborators on the research projects. I am deeply grateful to Associate Professor Yu Fujimoto, Dr. Jun Yoshinaga, Mr. Naoyuki Takahashi, Mr. Noriyuki Motegi, Dr. Shinichi Kusagawa, Associate Professor Shinichi Hanada, Dr. Daiya Isogawa, and Professor Hiroshi Ohashi. The discussion with the great researchers definitely enhanced this work.

I express special thanks to successive PhD students in Hayashi Laboratory, Dr. Shinya Yoshizawa, Dr. Shunsuke Kawano, Mr. Satoru Akagi, Mr. Yuji Takenobu, Mr. Akihisa Kaneko, Mr. Kohei Murakami, and Mr. Anto Ryu. Although the research life was sometimes very tough, the time with them was always very exciting and one of the greatest supports for me. The relationship will last forever to improve each other. May the Force be with you.

I am also very grateful to the research collaborators, Mr. Kohei Mori, and Mr. Masaya Kobayashi, all members in Hayashi Laboratory and in Leading Graduate Program in Science and Engineering, Waseda University for their assistance.

Finally, I show the greatest appreciation to my family, friends, and the parties concerned for their endless support and encouragement.

Table of Contents

List of figures

List of tables

Chapter 1
Introduction

1.1 Energy outlook in the power sector

The maximum utilization of renewables is essential for future sustainability of the earth. Energy from the sun is special for us because it is the only one energy source that we can get from outside of the earth. The original source of most renewable energies, i.e., solar, solar thermal, wind, biomass, tidal, is provided by the sun. As a consequence, renewables are under spatial and temporal constraints; that is, we need to overcome these constraints in order to make use of the renewables. In the power sector, which is the primary user of the renewables, electricity will account for almost a quarter of the total energy consumption by 2040 [1-1]. Therefore, it is strongly required to promote renewables while dealing with these constraints.

In this section, the trends of energy usage in the world and Japan is reviewed, focusing on the power sector and on the installation of renewables on the basis of statistical data in the "World Energy Outlook 2015" reported by the International Energy Agency (IEA) [1-1].

1.1.1 World energy outlook in the power sector

After the Paris agreement was adopted in December 2015, the implementation plans of new policies and improved technologies have been discussed and announced all over the world. The goal is to suppress the average global temperature rise below 2°C throughout this century and pursue efforts to limit the temperature rise to 1.5°C before the industrial revolution [1-2]. Quantitative projections of long-term energy trends are presented in [1-1] according to three scenarios: the new policies scenario, the current policies scenario, and the 450 scenario, each assuming different progress of energy policies of the world. The **new policies scenario** takes into consideration polices and measures that affect the energy trends that were adopted by mid-2015. Additionally, it incorporates other relevant intentions that were announced but when implemented is not clearly defined. The **current policies scenario** considers only policies and measures that were formally adopted by mid-2015 and assumes that nothing new will be added, which is not realistic. The **450 scenario** adopts a different approach, an outcome-oriented scenario. It adopts the international goal, which is to suppress the global average temperature rise below 2°C, and illustrates how that might be achieved. In this scenario, the concentration of the greenhouse gas in the atmosphere is assumed to reach 450 parts per million (ppm) and to be stabilized at around 450 ppm after 2100. The projections of total primary energy demand (TPED) and total CO_2 emissions in the world are shown in Fig. 1.1 and Fig. 1.2. Although all scenarios assume that the TPED will continue to increase towards 2040 (Fig. 1.1), in the 450 scenario, the CO_2 emissions are suggested to decrease to a level below that in 1990 (Fig. 1.2). It has been recognized that a large number of energy

sources whose CO_2 emissions are less than conventional energy sources are essential to achieve the 2°C target. Fig. 1.3 and Fig. 1.4 show that this movement to alter the energy sources is strongly required in the power sector.

The projections of world's share of the power sector in TPED and in total CO_2 emissions are shown in Fig. 1.3 and Fig. 1.4, respectively. This shows that the share of the power sector will increase beyond 40% by 2040 along with the increasing TPED (Fig. 1.3). On the other hand, in the 450 scenario the share of the power sector in total CO_2 emissions significantly decreases. This lower share in 2040, which is approximately half of 2013 and much smaller still compared with 1990, implies that deployment of energy sources with less or no CO_2 emissions is expected in the power sector. This is a significant contribution to the reduction of CO_2 emissions and important for achieving the 2°C goal.

The 450 scenario trend for achieving a significant reduction of CO_2 emissions in the power sector also appeared in the world's share of total electricity generation types as shown in Fig. 1.5. Although coal was used to generate energy almost more than twice than the other sources until 2013, the share of renewables sharply increased after 2013. As a result, the share of renewables in the electricity generation is described to exceed 30% and become the largest even discounting hydro power. That will become more than twice share of coal. Regarding the amount of electricity generation of each renewable energy source shown in Fig. 1.6, the amount of wind generation sharply increases from 2013. In 2040, wind power will become almost 2.5 times larger than all others whereas the solar photovoltaic (PV) and concentrating solar power (CSP) will follow closely behind.

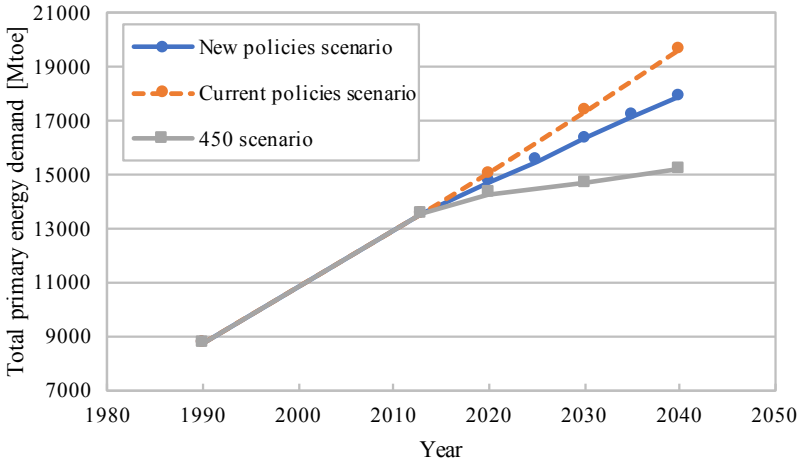

Fig. 1.1 Total primary energy demand in the world

(created based on [1-1], pp. 584–585).

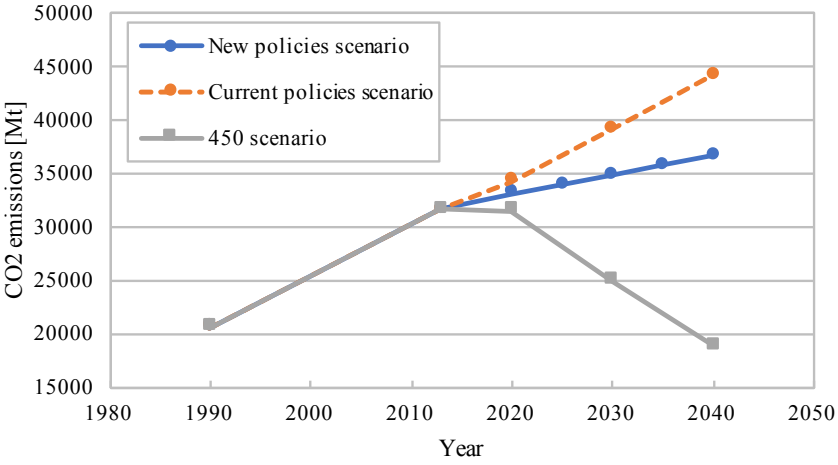

Fig. 1.2 Total CO_2 emissions in the world

(created based on [1-1], pp. 586–587).

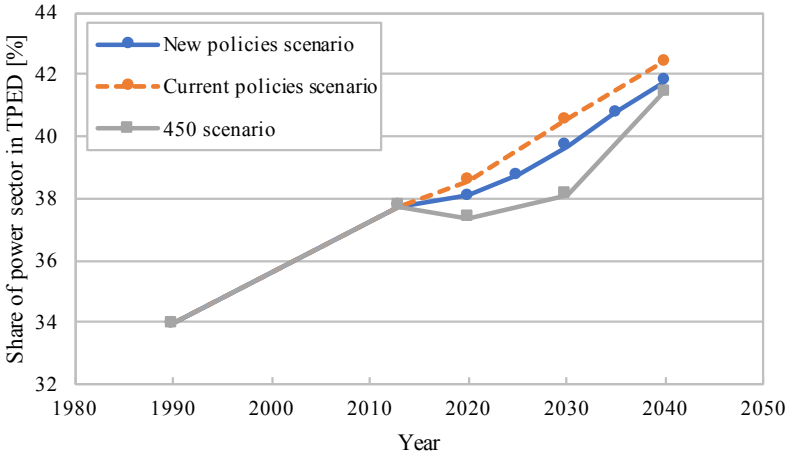

Fig. 1.3 Share of power sector in total primary energy demand in the world

(created based on [1-1], pp. 584–585).

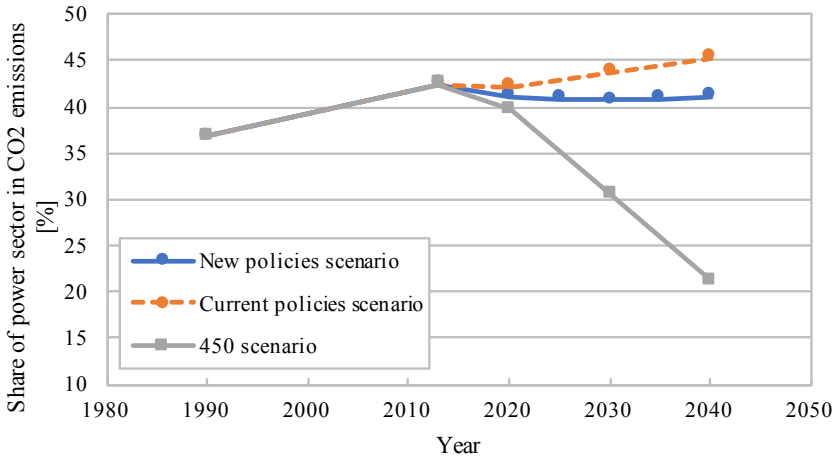

Fig. 1.4 Share of the power sector in total CO_2 emissions in the world (created based on [1-1], pp. 586–587).

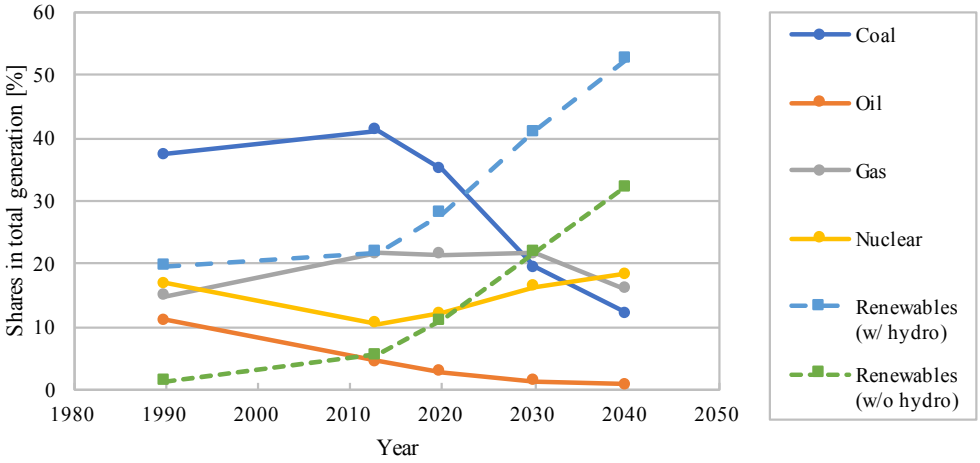

Fig. 1.5 Share of renewables in total electricity generation of 450 scenario in the world (created based on [1-1], pp. 587).

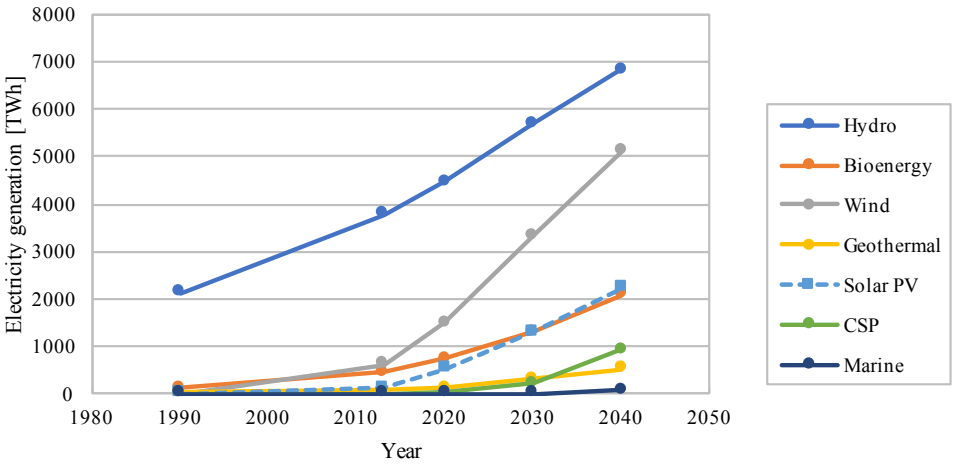

Fig. 1.6 Electricity generation of renewables in 450 scenario in the world (created based on [1-1], pp. 587).

1.1.2 Japanese energy outlook in the power sector

Some energy projections are different between Japan and the world. Japanese TPED and total CO_2 emissions are shown in Fig. 1.7 and Fig. 1.8. The TPED of Japan, which is assumed to increase in the world, decreases along with the total CO_2 emissions in all scenarios. It is considered that the critical reason of the reduction is a population decrease. On the other hand, in scenario 450 the share of the power sector in the TPED along with total CO_2 emissions will increase towards 2040 though the total share of the power sector will dramatically decrease (see Fig. 1.9 and Fig. 1.10). These projections are now similar to the world projections. Therefore, it can be recognized that this similar issue of requiring power resources with lowered CO_2 emissions is essential and common between Japan and the world.

Regarding to the Japanese share of energy resource types in total electricity generation in the 450 scenario, renewables and nuclear power sharply increase in order to achieve the 2°C goal. The share of renewables will reach approximately 50% of all energy generation by 2040 while gas and coal account for the majority in 2013 (see Fig. 1.11). Moreover, a characteristic point in Japanese electricity generation of renewables in the 450 scenario is that solar PV is the largest of all renewables except hydro power. This trend had happened suddenly and caused some problems in Japan.

In Japan, in addition to CO2 emissions, primary energy self-sufficiency is a large issue. Energy self-sufficiency has stayed at only 6% after the Great East Japan earthquake and the Fukushima Daiichi nuclear accident in 2011. In order to break down this emergency, the government is aiming to increase it to approximately 25% by 2030 [1-3]. Also, the introduction of PV is promoted by implementing the Feed-in Tariff (FIT) program to significantly pursue a future best mix of power supply configuration [1-4]. The implementation of the FIT program has led to the rapid PV introduction. The certificated and operating amount of PV capacity in Japan is depicted in Fig. 1.13 [1-5]. The certificated PV capacity rapidly increased and has already exceeded the target of FY2030: 64 [GW] in March 2014. In addition, it reached 80 [GW] in 2017. The operating PV capacity is maintaining an increase following the certificated PV capacity. This trend suggests that solutions to these issues that has already occurred and are likely enhanced by expanding the operating PV capacity is expected to develop.

In our research, we focus on the maximum utilization of PV generation. PV is the largest share of renewables in Japan and a large share of power generation in the world when excluding hydro. The next section discusses issues caused by the massive introduction of PV in the power system.

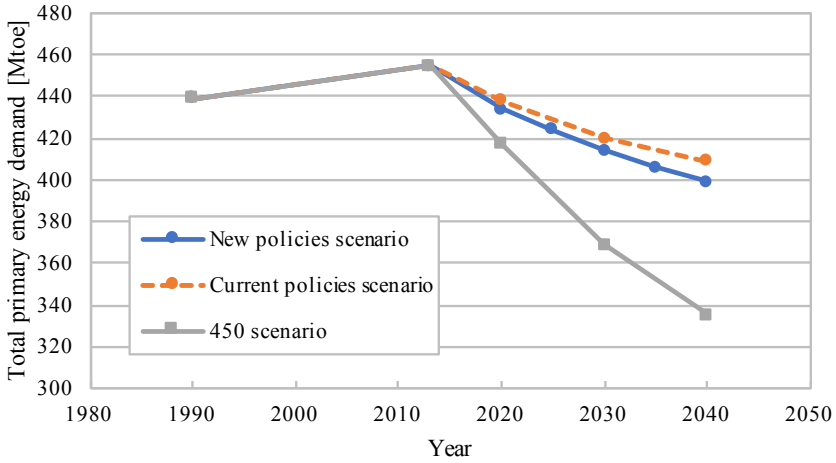

Fig. 1.7 Total primary energy demand in Japan
(created based on [1-1], pp. 612–613).

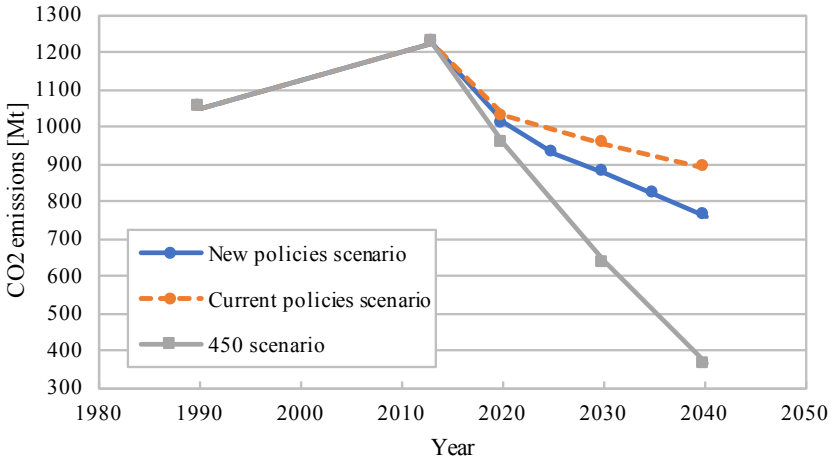

Fig. 1.8 Total CO_2 emissions in Japan
(created based on [1-1], pp. 614–615).

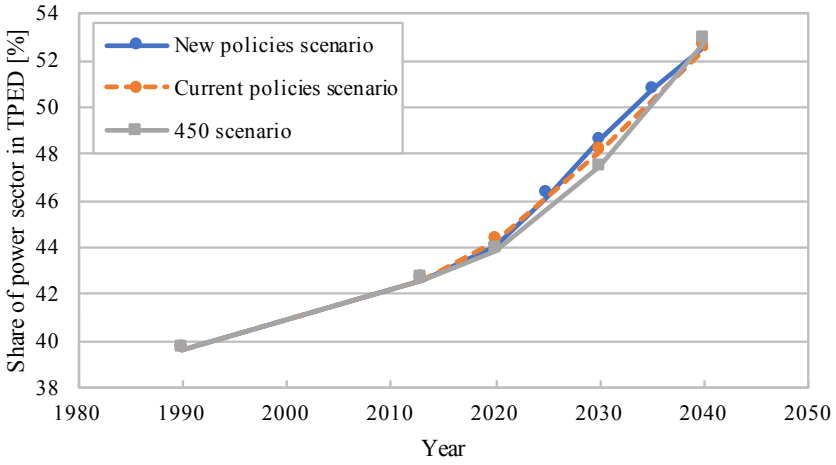

Fig. 1.9 Share of power sector in total primary energy demand in Japan
(created based on [1-1], pp. 612–613).

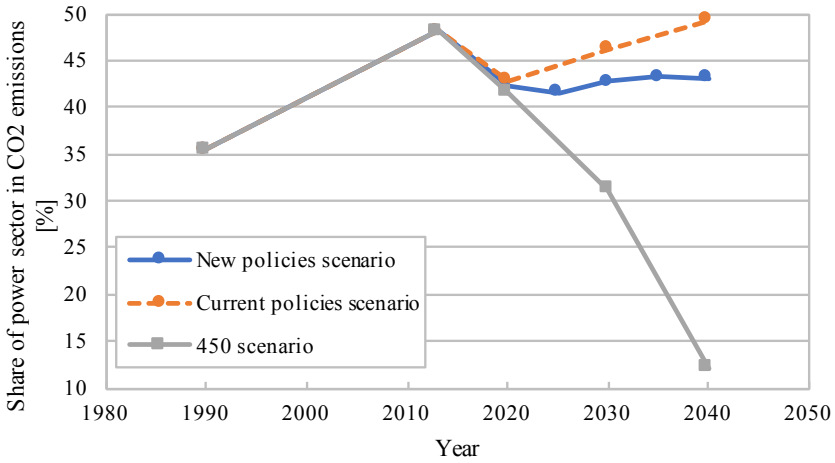

Fig. 1.10 Share of power sector in total CO_2 emissions in Japan (created based on [1-1], pp. 614–615).

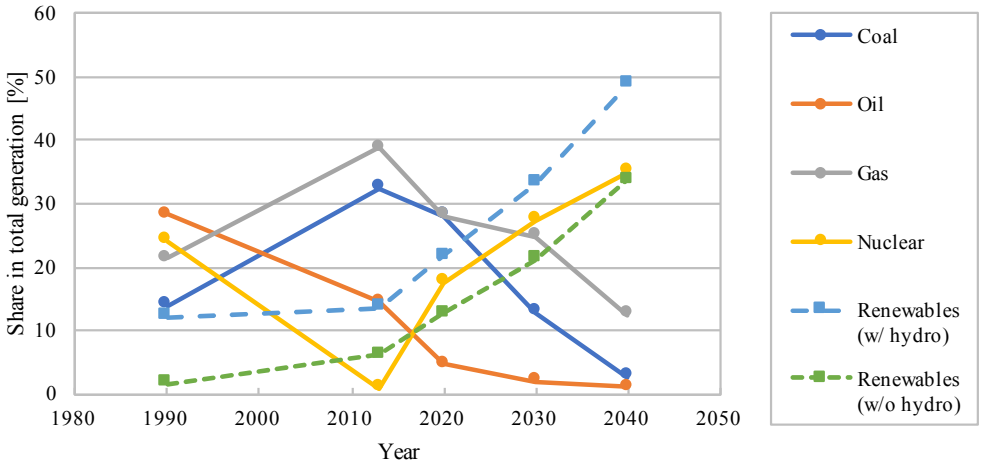

Fig. 1.11 Share of renewables in total electricity generation of the 450 scenario in Japan (created based on [1-1], pp. 615).

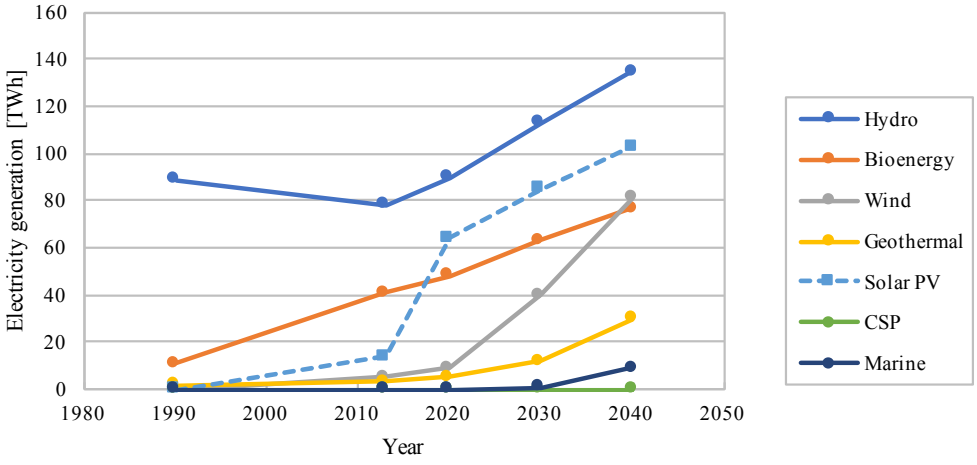

Fig. 1.12 Electricity generation of renewables in the 450 scenario in Japan (created based on [1-1], pp. 615).

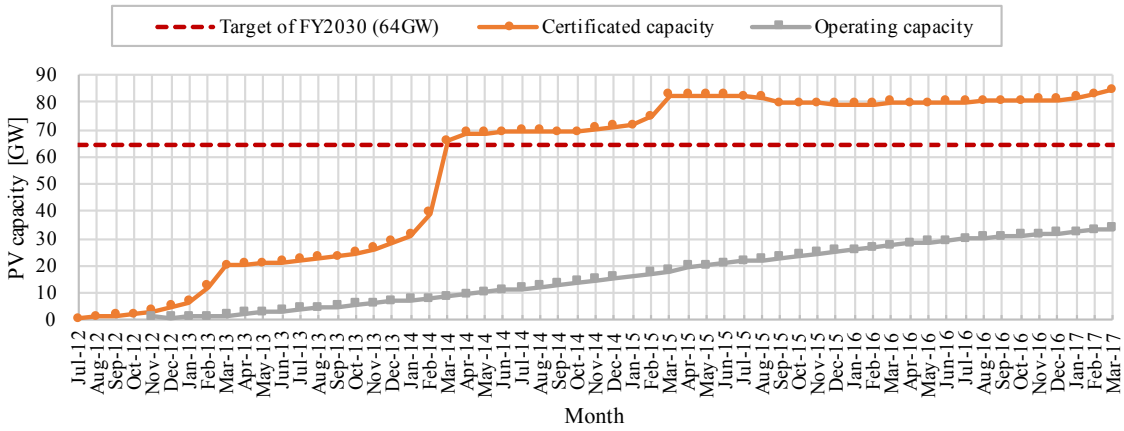

Fig. 1.13 Certificated and operating PV capacity in Japan
(created based on [1-5]).

1.2 Occurrence of PV curtailment in distribution systems

In power systems with a large number of PVs, the PV curtailment, which is a part of the power loss, is carried out to 1) maintain the power supply-demand when PV output peaks and electricity consumption decreases in the power system [1-6], and 2) avoid overvoltage from the prescribed voltage range in the DS [1-7]. Let $t = 1, \dots, T$ be the time in a day where T is the total time, $\boldsymbol{p} = (p_t; t \in \{1, \dots, T\})$ be the sequence of the PV output, the PV curtailment is given as

$$\boldsymbol{x} = \boldsymbol{p}^* - \boldsymbol{p}, \tag{1.1}$$

where $\boldsymbol{p}^*$ is the original PV output (before curtailment) and $\boldsymbol{p}$ is the realized PV output (after curtailment).

In the former issue, the PV is curtailed according to the obliged generation limit $\bar{p}$ provided by the utility and the realized PV output in time t is described as

$$p_t = \begin{cases} p_t^* & \text{if} \quad p_t^* \leq \bar{p} \\ \bar{p} & \text{if} \quad p_t^* > \bar{p}. \end{cases} \tag{1.2}$$

Note that obliged generation limit $\bar{p}$ is determined to coordinate the supply-demand balance among multiple DSs.

On the other hand, in the latter issue, the PV is curtailed according to the voltage at the connecting point of PV to the grid. In distribution systems (DSs), where the PV is mainly connected to, the voltage shall be maintained within the prescribed range. In Japan, this is regulated by the electric utility industry law where the voltage at the customers' receiving end shall be maintained within 101±6 [V] or 202±20 [V]. An overvoltage above these values would break the electrical appliances and a lower voltage violation would degrade their performance. In the conventional DSs without PVs the voltage typically decreases along the distribution line, so that the conventional DSs are planned and operated to maintain their regulated voltage. On the other hand, in the DS with PVs, the PVs supply the generated power to the households and the surplus PV output is fed and sold to the grid (Fig. 1.14). The reverse power flow

from the surplus PV output increase the voltage in the DS. The voltage rise may cause an overvoltage because the conventional DSs are not planned and operated to deal with the voltage rise. As a result, the active power of the PV output is curtailed by the PV inverter to avoid overvoltage. Therefore, the PV curtailment occurs and the expected generation amount could not be obtained [1-7]. An example of the PV curtailment mechanism to avoid overvoltage can be described as following:

$$p_t = \begin{cases} p_t^* & \text{if} \quad v_t^{\mathrm{pv}} \leq v_{\mathrm{th}} \\ p_t^* - a \cdot \left(v_t^{\mathrm{pv}} - v_{\mathrm{s}}\right) & \text{if} \quad v_t^{\mathrm{pv}} > v_{\mathrm{th}}, \end{cases} \tag{1.3}$$

where v_t^{pv} is the voltage at connecting point of the PV to the DSs at time t, v_{th} is the threshold of the voltage to start and end the PV curtailment, and a is a conversion coefficient that means the speed of the PV curtailment.

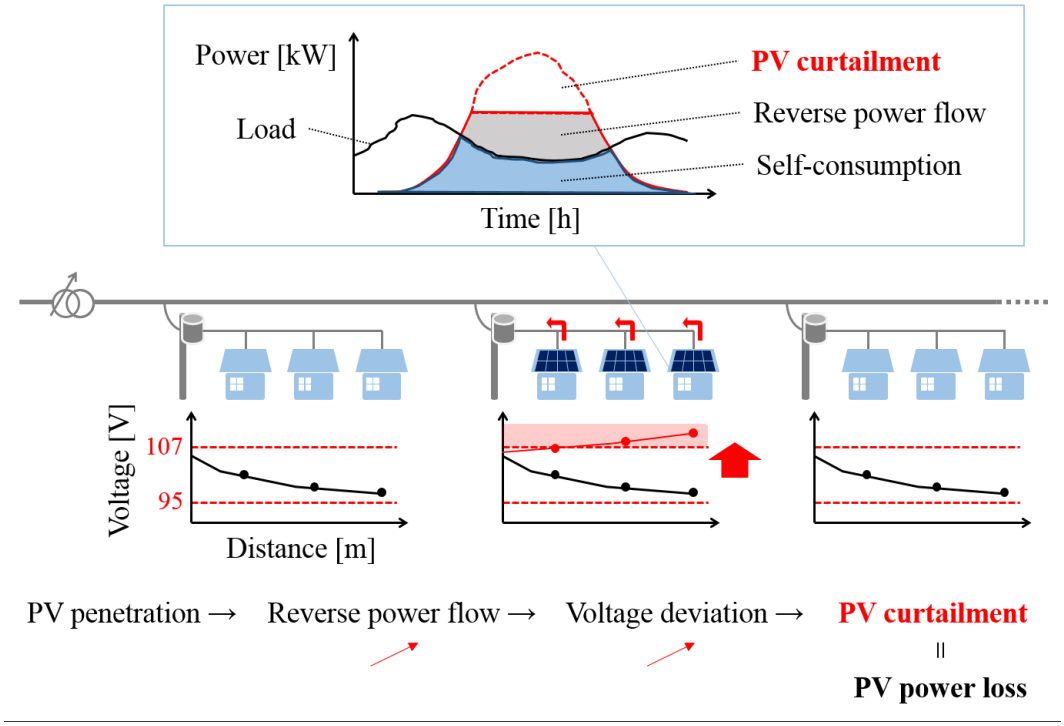

Fig. 1.14 PV penetration, voltage rise, PV curtailment.

1.3 Supply and demand side energy management for reducing PV curtailment

To achieve the 2°C goal mentioned in 1.1, not only an increase in the PV capacity but also the maximum utilization of the PV generation is important so that a reduction of the PV curtailment is essential. While many energy management schemes to reduce the PV curtailment have been proposed, the required energy management schemes depend on the characteristics of the target DSs and the expansion of the devices related to these schemes. In addition, they are various and will change depending on the target periods of practical use. To recognize the energy management schemes that have been proposed for reducing the PV curtailment and their remaining issues, they are classified in terms of the range affected by their control and the time-period of expected practical use (Fig. 1.15).

This section presents these conventional energy management schemes primarily divided into two parts, supply and demand side energy management schemes, and specifies their remaining issues.

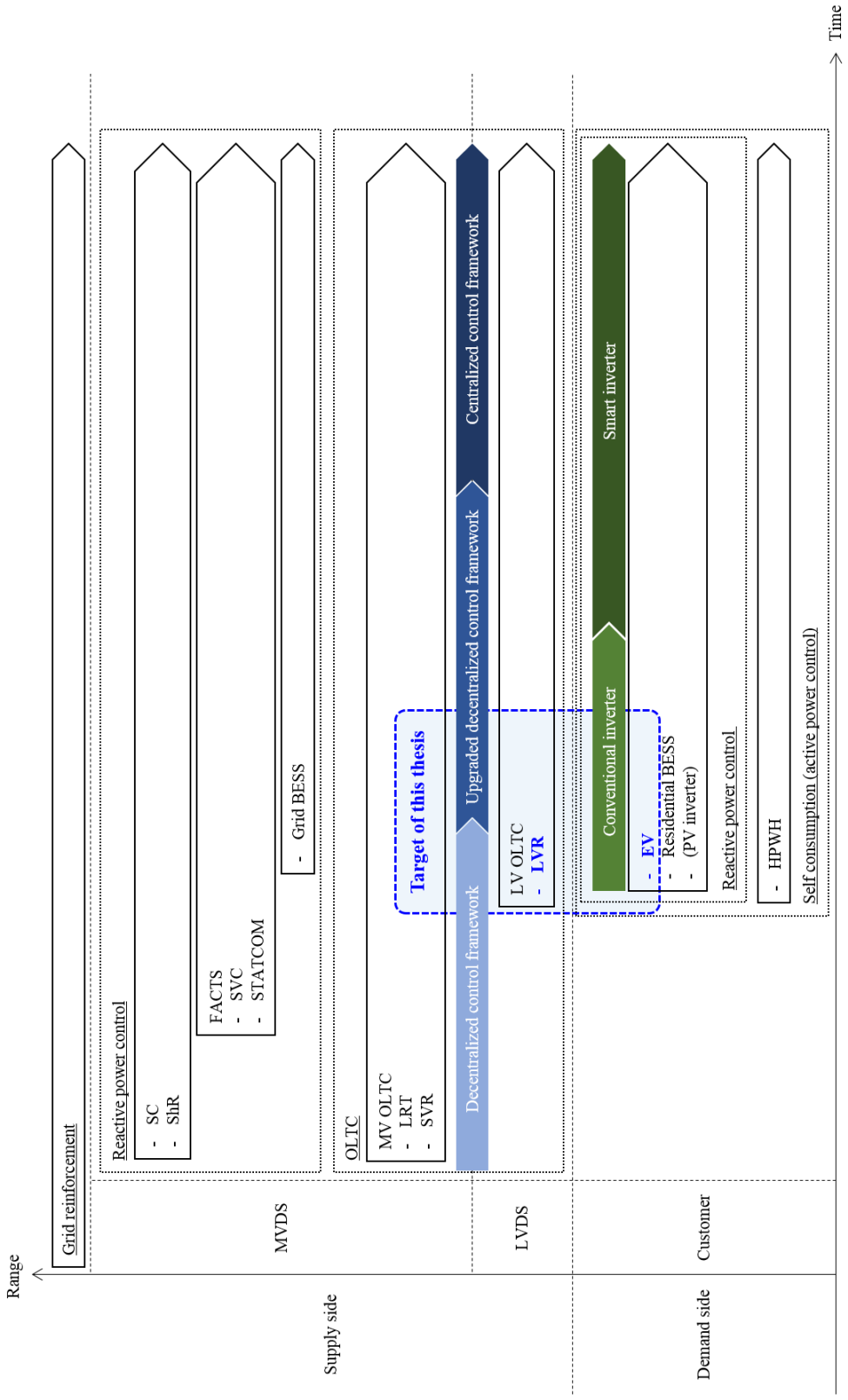

Fig. 1.15 Classification of energy management schemes in supply and demand side for maximum utilization of PV generation.

1.3.1 Supply side energy management: voltage control in distribution systems

(a) Development of voltage control devices

In supply side energy management, the PV curtailment can be reduced to maintain the voltage within the prescribed range. To maintain this voltage, voltage should be increased when it is too low and reduced when it is too high. Many schemes have been proposed to maintain the voltage in the DSs [1-8]. The simplest scheme is grid reinforcement [1-9]–[1-11], for example, distribution line improvement by replacing the line with a cable that reduces the impedance of the line, interconnecting the line to smooth out differences in parallel distribution lines, and separation of low-voltage distribution systems (LVDSs) to shorten the distribution line. However, the grid reinforcement tends to require a high investment and construction might be difficult for some locations. Other schemes are used in order to postpone this high investment until it gets definitely necessary.

Reactive power control is another scheme to control the voltage in the DSs. The voltage decreases when the lagging reactive power is injected into the grid and the voltage increases when the lagging reactive power is absorbed from the grid. There are various devices that can adjust the reactive power injection to control the voltage in the DSs. A shunt capacitor (SC) bank and shunt reactor (ShR) bank are the traditional devices and adjust the amount of reactive power discretely by varying the amount of connected capacitors and reactors to the grid [1-13]–[1-16]. Additionally, the flexible alternative current transmission system (FACTS) devices based on power electronics such as a static synchronous compensator (STATCOM), which is called a static var compensator (SVC) in Japan, are utilized for voltage control [1-10], [1-15]–[1-19]. The FACTS devices can continuously adjust the reactive power injection and flexibly regulate the voltage in the DSs. In recent years, the battery energy storage system (BESS) for the grid has got a lot of attention and its introduction to the grid has begun and there are quite a few example of installation [1-20]. Although most of introduced BESSs are utilized for adjusting the supply-demand balance, they can be mostly located in the DSs and utilized also for voltage control. The BESS can control the voltage by continuously adjusting not only active power injection but also reactive power injection [1-21]–[1-23]. The flexibility for the voltage control of a BESS is equal to or higher than the FACTS, while both devices require a high capital cost.

On-load tap changers (OLTCs) are widely used for voltage control in the DSs. The OLTCs are basically autotransformers with many taps in the series winding. They adjust the tap position, that is the transformer ratio, and discretely control the voltage. In ordinary OLTCs, the voltage varies approximately by 1–2.5% of the nominal voltage per one tap and the full voltage control range is approximately 10–20%. The basic tap changing mechanism of OLTCs are shown in Fig. 1.16. The OLTCs automatically change the tap based on the internally sensed voltage and current. The tap is changed when the deviation of the sensing value from the target value exceeds a specific value. The mechanism includes a time delay, which is the waiting time when the sensing value exceeds the dead band and when the tap change is operated. The time delay is provided to avoid over frequent tap

changing that leads to a shorter lifespan due to machine wear. In the traditional DSs, medium-voltage (MV) OLTCs such as a load ratio control transformer (LRT), which is located in the distribution substation, and a step voltage regulator, which is located in the middle of a long-distance distribution feeder, are mainly used for voltage control [1-24]–[1-26]. In addition, recently a thyristor type step voltage regulator (TVR), which is not affected by machine wear due to frequent tap changes, has developed to deal with the frequent voltage fluctuation [1-27]. These MV OLTCs are designed to maintain the voltage within a specific range in the medium-voltage distribution system (MVDS), which includes many LVDSs, so that the voltage in all LVDSs is varied when the MV OLTC changes the tap position. However, the penetration of a large number of PVs causes a local voltage rise around the PV connected point. This voltage increases in some LVDSs due to the reverse power flow from the PV while decreasing in the other LVDSs. This is a complicated situation for the MV OLTC to maintain for the voltage in all LVDSs because they cannot control the voltage in a specific LVDS. As a solution to this local voltage violation, low-voltage (LV) OLTCs have been studied [1-28]–[1-34]. There are two types of LV OLTCs; one type is installed in the middle of the LV distribution feeder and the other is installed in place of a traditional pole transformer. We call this latter option a **low-voltage regulator (LVR)** (Fig. 1.17). The LVR is a pole transformer with an auto tap changer and can control the voltage in each LVDS [1-35] so that the local voltage violation in the specific LVDS can be avoided (Fig. 1.18). The cost superiority of the LVR to the traditional grid reinforcement is suggested in [1-34] and some voltage control schemes have been proposed [1-29]–[1-31], [1-33]. The point of LVR operation requires considering the MV OLTCs behavior. This is because in the radial DSs, the voltage in the control area of the LVR is affected by the tap changing of MV OLTCs located upstream of the LVR. **However, the voltage control scheme that includes the determination of deployment and the voltage control parameters of the LVR considering the voltage control of the MV OLTCs has not been proposed**.

(b) Development of voltage control frameworks

On the other hand, upgrades to the voltage control frameworks are progressing as well as improvements of the voltage control devices. Traditional voltage control frameworks of OLTCs are to decentralize the control method based on program control methods called a 90 relay method and a line drop compensator (LDC) method [1-36]–[1-39]. The decentralized control framework adjusts the tap position of the OLTCs on the basis of the predetermined control parameters and sensing measurement, which are set prior to factory shipment. However, in the DS with PV, the control parameters that can avoid the voltage violation difference due to the weather such as limited generation during a cloudy day. This requires updating the control parameters corresponding to the PV generation.

Therefore, studies with the upgraded decentralized framework have begun [1-40]–[1-42]. In the upgraded decentralized control framework, the control parameters can be updated from the outside through communication (Fig. 1.19). Since the assumed frequency is updated once every few hours, an enhanced communication infrastructure should not be required. To sequentially and appropriately

update the control parameters depending on PV generation, they should be determined on the basis of reliable power forecasting. In such a mechanism, the immediacy to determine the control parameters is important. **However, in the LVR operation, a method for rapidly determining the voltage control parameters has not been proposed**.

As a further upgrade, centralized voltage control frameworks has been studied [1-26], [1-43], [1-44]. The centralized frameworks control the voltage on the basis of a real-time measurement in the sensors located in middle of the distribution feeders acquired thorough the enhanced communication infrastructure. Thus, implementation of the centralized framework requires a large investment and take longer time to develop the infrastructure that the other framework. In addition, communication fault countermeasures are essential and must be considered.

As mentioned above, the solution to reduce the overvoltage and PV curtailment is urgently required and the investment cost should be reduced. Therefore, in this thesis, the utilization of the LVR, which is easy to deploy and competitively low cost, is focused on as a supply side energy management. Additionally, the distributed and upgraded distributed control frameworks, which would not take long time to construct the required infrastructure, of the LVR are addressed.

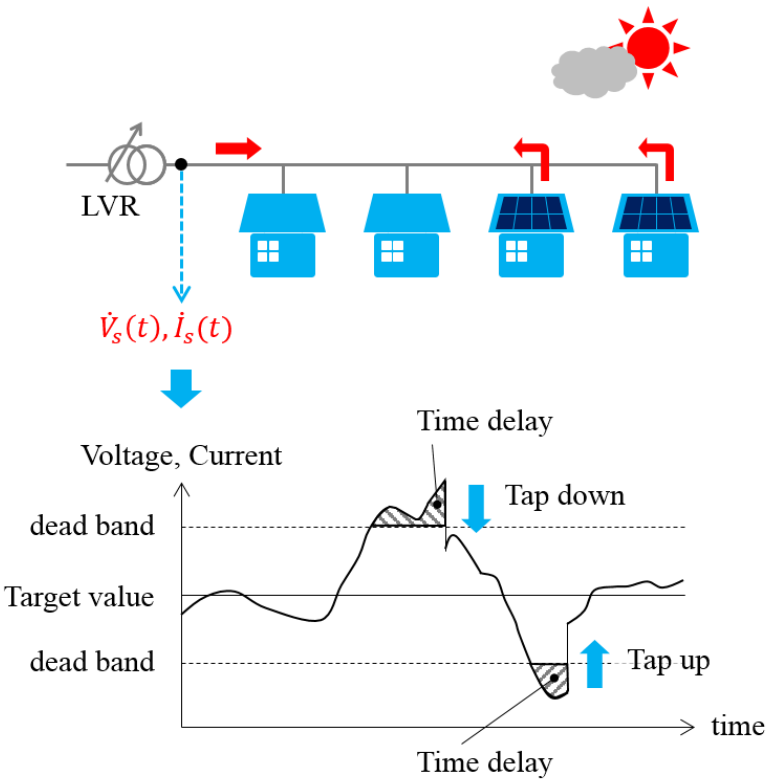

Fig. 1.16 Tap control of the OLTC based on the target value, dead band, and time delay.

Fig. 1.17 Low-voltage regulator (LVR)

(created based on [1-35]).

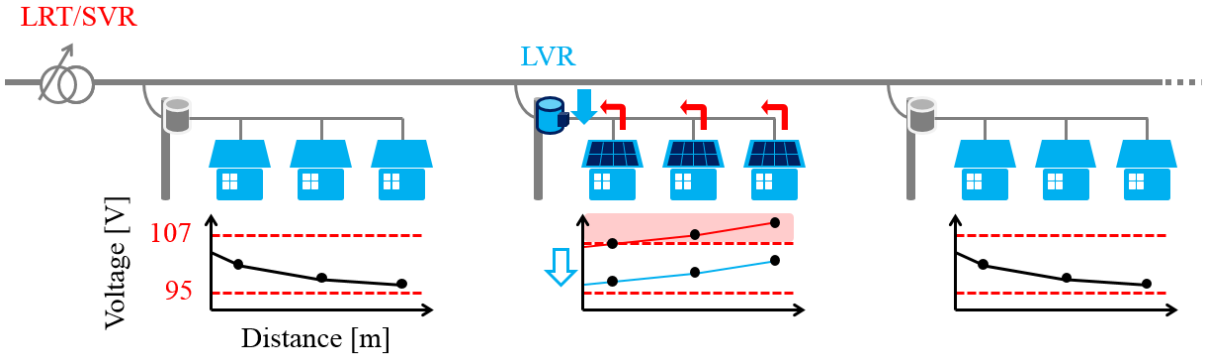

Fig. 1.18 Voltage control by LVR.

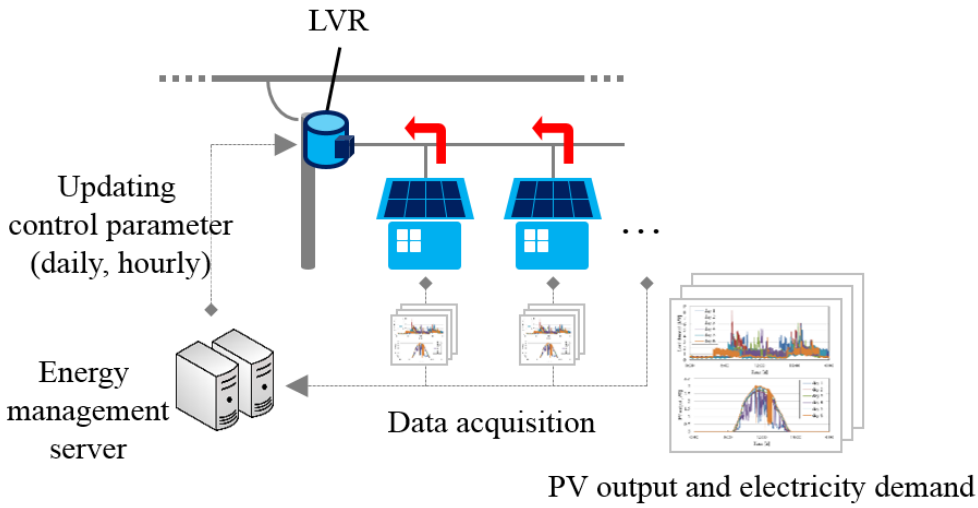

Fig. 1.19 Image of upgraded decentralized voltage control framework.

1.3.2 Demand side energy management: self-consumption of PV output with customers

In demand side energy management, the PV curtailment can be reduced by increasing the self-consumption of PV generation. The increase in the self-consumption of PV generation reduces the reverse power flow to the grid, so that the voltage rise is mitigated and the voltage margin from the prescribed limit, which is the constraint of the PV curtailment, increases (Fig. 1.20). To adjust the self-consumption of the PV, controllable electricity loads such as an electric vehicle (EV), residential BESS, and heat pump water heater (HPWH) are easily utilized by shifting their operation periods. In Japan, the government set a policy to achieve net-zero energy houses (ZEHs) by 2030 for the average newly constructed house [1-45]. To achieve the ZEHs, maximum utilization of PV generation is essential. Therefore, these controllable loads should be deployed in households to flexibly utilize electricity from the PV. Particularly in terms of an EV, regulations on the sale of gasoline and diesel cars have been announced in specific countries (Table 1.1) and car companies also announced shifting to electrified car development (Table 1.2). Therefore, the increase in EVs is strongly expected in many countries. Additionally, the literature in [1-46] mentioned the EV is parked for more than 95% of a day, so that it is rational to utilize the EV for the energy management. There are many studies of demand side load management for voltage control and reducing the PV curtailment using EVs, residential BESSs, and HPWHs. Although the effective load management on the demand side can reduce the PV curtailment and result in the reduction and postponement of investment for voltage control on the supply side, the important point on the demand side of the management is not to lower the convenience of the customers and equitably share in the benefit accordingly with customer contribution. Energy management using the EVs has particularly affected the former point because the EVs are fundamentally installed for driving. **However, the demand side energy management scheme to reduce the PV curtailment using EVs that secures the autonomy of contributing to the energy management and the equity of benefits according to the customers' contribution has not been proposed.**

On the other hand, inverters implemented in the PV system, BESS, and EV charger have the active and reactive power control function. They can be utilized for the voltage control in the grid as well as the demand side energy management [1-47]–[1-49]. Moreover, smart inverters, which have a communication function and are flexibly set the control parameters from the outside, are started to be discussed for regulation, voltage control function, and operation methodologies. The spread of the smart inverter will take time, but it will contribute to the voltage control to help maximum utilization of PV generation in the near future.

In terms of the demand side management, the EV is considered the most likely device to be introduced worldwide and competitively in near future than the other demand side devices. Therefore, this thesis focuses on the EV management scheme as a demand side energy management for reducing the PV curtailment.

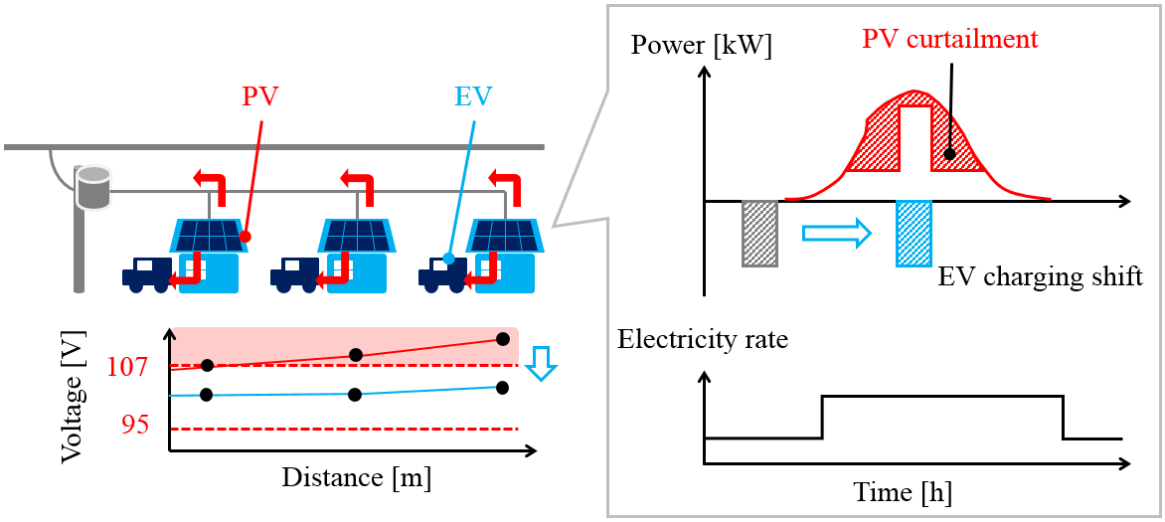

Fig. 1.20 Schematic image of increasing self-consumption of PV generation.

Table 1.1 World movement toward car electrification (created based on [1-50]–[1-54]).

Country	Announcement
Britain	Bans sales of new gasoline and diesel cars by 2040.
France	Plans to end sales of gas and diesel cars by 2040.
India	Promotes to sell only electric cars by 2030.
China	Introduced regulations obliging car companies to manufacture and sell 10% new energy vehicles in 2019.
Norway	Should alter all new passenger cars and vans sold in 2025 to the zero-emission vehicles.

Table 1.2 Trend of car companies toward electrification (created based on [1-55]–[1-59]).

Car company	Announcement
BMW	By 2025, they expect electrified vehicles to account for between 15-25% of sales.
Volvo cars	All launched cars from 2019 will have an electric motor.
Daimler	Plans for more than ten different all-electric vehicles by 2022.
Volkswagen	More than 30 purely battery-powered electric vehicles will be launched by 2025.
TOYOTA	Established a new company for joint technology development including electric vehicles with Mazda and Denso. The capital is 10 million yen.

1.4 Research purpose and construction of this thesis

As mentioned above, a large number of PVs will be installed in the LVDSs and the reverse power flow from the PV generation will locally raise the voltage in the LVDSs around the connected points of the PVs. This results in the occurrence of PV curtailment to avoid voltage violation from the prescribed range. The reduction of PV curtailment caused by the local voltage rise is an important issue to achieve the international 2°C goal. Energy management schemes on both the supply and demand side, which are the voltage control in the DS to maintain the voltage by using the LVR within the prescribed range and the EV charging management by customers to adjust the self-consumption of the PV output, are required to reduce this PV curtailment. Although such energy management schemes have been proposed, some issues remain in the LVDS. In this research, we propose energy management schemes for maximum utilization of PV generation in the LVDS using the LVR on the supply side and using EVs on the demand side. In chapters 2 to 4, supply and demand side energy management schemes are proposed and the effectiveness of these schemes are evaluated. Chapter 5 gives the conclusions and future work.

1.4.1 Distributed and coordinated voltage control of multiple on-load tap changers

In supply side energy management, voltage control using the LVR enables one to solve the local voltage violation that results in the PV curtailment. The LVR is located on the pole transformer where the MV (6.6 [kV]) is transformed to LV (100/200 [V]). Locating the LVRs in the radially spreading DSs, the control areas of the LVRs, whose voltage is affected by the voltage control of the LVRs, is included in the control area of MV OLTCSs. Therefore, to determine the appropriate location and control parameters of LVRs the tap operation behavior of the MV OLTCs, which are located at the root from the LVRs, should be considered.

Chapter 2 presents a distributed and coordinated voltage control scheme that appropriately determines the location and the control parameters of LVRs. In the proposed scheme, the control areas of each MV OLTC is defined not to overlap and the control parameters are determined in order from the MV OLTCs located at the upper stream. The LVRs are deployed in the LVDSs where the MV OLTCs cannot avoid the voltage violation. Moreover, the control parameters of LVRs that cannot disturb the voltage violation with the default control parameters are appropriately determined. The effectiveness of the proposed coordinated voltage control scheme is evaluated based on a Japanese DS model and actual measurement in terms of the number of customers with voltage violation. In addition, the characteristics of the LVDSs that the LVR should be deployed are specified.

1.4.2 Rapid determination for voltage control parameters of LVR using classifiers

In the LVDSs with PVs, the control parameters of the LVR that can avoid voltage violation are varied depending on the weather. To appropriately manage the complex voltage fluctuation, an upgraded voltage control scheme operates to determine and update the appropriate control parameters in a short period, i.e., every few hours, on the basis of the required reliable power forecast. In such an upgraded scheme, a large sum of computational time is required because candidates of the appropriate control parameters are exhaustively evaluated to achieve the robust voltage control against the error included in the power forecasting. Therefore, to implement this upgraded scheme in the operation of the LVR, a reduction of the computation time is needed to meet the sequential update of control parameters.

As an upgraded energy management scheme on the supply side to reduce the local voltage violation, an alternative method for rapidly determining the voltage control parameters of the LVR using classifiers is proposed in **chapter 3**. The proposed determination method learns offline the classifiers that distinguish the appropriateness of the control parameters to the forecasted power profiles. In addition, it narrows the candidates of the appropriate control parameters by using the composed classifiers and precisely evaluates the narrowed candidates of the control parameters by a power flow calculation (PFC). The proposed method is validated by a numerical simulation based on the LVDS model and actual data of power measurement in terms of the computation time and the voltage control performance.

1.4.3 EV charging management

In demand side energy management, the amount of curtailed PV output can be reduced by shifting the EV charging period to increase the self-consumption of PV output. The effective EV charging shift contributes to the reduction of investment for voltage control in the supply side as well as the residential operational cost of customers. In such an EV charging scheme, not only reducing the PV curtailment and residential operation cost but also the equity of customers' benefits and autonomy of contributing to the load shift to increase the self-consumption of the PV output should be secured to ensure customer participation. The equity of customers' benefit means that the benefit should be coordinated depending on the contribution of customers. The autonomy of contributing to the load shift means that the customers should optionally decide to participate in the EV charging shift based on a comparison of the benefits received by contributing to the EV charging shift and utilizing the EV for driving.

In **Chapter 4**, we proposed an EV charging management scheme based on the auction mechanism to reduce the PV curtailment and the residential operation cost in the LVDS with securing the equity of the benefits and autonomy of contributing to the EV charging shift. The introduction of an auction mechanism coordinates the amount of benefits to secure their equity through collecting and distributing the incentive. In addition, it allows customers to secure autonomy to optionally decide whether they

will contribute to the EV charging shift considering the benefits of EV utilization schemes. The effectiveness of our proposed EV charging scheme based on the auction mechanism is evaluated by the numerical simulation using the actual Japanese DS model and power measurement from the view point of the amount of PV curtailment and the residential operation cost.

References

[1-1] *World Energy Outlook 2015*. International Energy Agency, 2015.

[1-2] "The Paris Agreement - main page," *the United Nations/Framework Convention on Climate Change*. [Online]. Available: http://unfccc.int/paris_agreement/items/9485.php. [Accessed: 16-Oct-2017].

[1-3] "Related materials of Long-term energy outlook (in Japanese)," *Ministry of Economy, Trade and Industry/Agency for Natural Resources and Energy*, 2015. [Online]. Available: http://www.enecho.meti.go.jp/committee/council/basic_policy_subcommittee/mitoshi/011/pdf/011_07.pdf. [Accessed: 11-Feb-2017].

[1-4] "Long-term energy outlook (in Japanese)," *Ministry of Economy, Trade and Industry*, 2015. [Online]. Available: http://www.meti.go.jp/press/2015/07/20150716004/20150716004_2.pdf. [Accessed: 18-Oct-2017].

[1-5] "Information disclosure website of feed-in tariff scheme (in Japanese)," *Ministry of Economy, Trade and Industry/Agency for Natural Resources and Energy*. [Online]. Available: http://www.enecho.meti.go.jp/category/saving_and_new/saiene/statistics/index.html. [Accessed: 16-Oct-2017].

[1-6] T. Masuta, J. Gari da Silva, Fonseca, H. Ootake, and A. Murata, "Application of battery energy storage system to power system operation for reduction in PV curtailment based on few-hours-ahead PV forecast," in *2016 IEEE International Conference on Power System Technology (POWERCON)*, 2016, pp. 1–6.

[1-7] Y. Ueda, K. Kurokawa, T. Tanabe, K. Kitamura, and H. Sugihara, "Analysis Results of Output Power Loss Due to the Grid Voltage Rise in Grid-Connected Photovoltaic Power Generation Systems," *IEEE Trans. Ind. Electron.*, vol. 55, no. 7, pp. 2744–2751, Jul. 2008.

[1-8] V. A. Evangelopoulos, P. S. Georgilakis, and N. D. Hatziargyriou, "Optimal operation of smart distribution networks: A review of models, methods and future research," *Electr. Power Syst. Res.*, vol. 140, pp. 95–106, 2016.

[1-9] R. Niemi and P. D. Lund, "Alternative ways for voltage control in smart grids with distributed electricity generation," *Int. J. Energy Res.*, vol. 36, no. 10, pp. 1032–1043, Aug. 2012.

[1-10] T. Kondo, J. Baba, and A. Yokoyama, "Voltage control of distribution network with a large penetration of photovoltaic generation using FACTS devices," *Electr. Eng. Japan*, vol. 165, no. 3, pp. 16–28, Nov. 2008.

[1-11] S. Killinger, W. Biener, G. Gust, and B. Wille-Haussmann, "Impact of the nominal and real peak power of PV systems on grid reinforcement," in *2016 IEEE PES Innovative Smart Grid Technologies Conference Europe (ISGT-Europe)*, 2016, pp. 1–6.

[1-12] W. Biener, K. Dallmer-Zerbe, B. Krug, G. Gust, and B. Wille-Haussmann, "Automated distribution grid planning considering Smart Grid and conventional grid reinforcement technologies," *ETG Congr. 2015 - Die Energiewende*, pp. 456–461, 2015.

[1-13] J. J. Grainger and S. Civanlar, "Volt/Var Control on Distribution Systems with Lateral Branches Using Shunt Capacitors and Voltage Regulators Part I: The Overall Problem," *IEEE Trans. Power Appar. Syst.*, vol. PAS-104, no. 11, pp. 3278–3283, Nov. 1985.

[1-14] M. Aredes, J. Hafner, and K. Heumann, "Three-phase four-wire shunt active filter control strategies," *IEEE Trans. Power Electron.*, vol. 12, no. 2, pp. 311–318, Mar. 1997.

[1-15] A. Sode-Yome and N. Mithulananthan, "Comparison of Shunt Capacitor, SVC and STATCOM in Static Voltage Stability Margin Enhancement," *Int. J. Electr. Eng. Educ.*, vol. 41, no. 2, pp. 158–171, Apr. 2004.

[1-16] T. Senjyu, Y. Miyazato, A. Yona, N. Urasaki, and T. Funabashi, "Optimal distribution voltage control and coordination with distributed generation," *IEEE Trans. Power Deliv.*, vol. 23, no. 2, pp. 1236–1242, Apr. 2008.

[1-17] P. Rao, M. L. Crow, and Z. Yang, "STATCOM control for power system voltage control applications," *IEEE Trans. Power Deliv.*, vol. 15, no. 4, pp. 1311–1317, 2000.

[1-18] V. Salehi, S. Afsharnia, and S. Kahrobaee, "Improvement of Voltage Stability in Wind Farm Connection to distribution Network Using FACTS Devices," in *IECON 2006 - 32nd Annual Conference on IEEE Industrial Electronics*, 2006, pp. 4242–4247.

[1-19] N. Takahashi and Y. Hayashi, "Centralized voltage control method using plural D-STATCOM with controllable dead band in distribution system with renewable energy," in *2012 3rd IEEE PES Innovative Smart Grid Technologies Europe (ISGT Europe)*, 2012, pp. 1–5.

[1-20] "Tesla Powerpack to Enable Large Scale Sustainable Energy to South Australia | Tesla." [Online]. Available: https://www.tesla.com/blog/tesla-powerpack-enable-large-scale-sustainable-energy-south-australia. [Accessed: 18-Oct-2017].

[1-21] C. A. Hill, M. C. Such, D. Chen, J. Gonzalez, and W. M. Grady, "Battery Energy Storage for Enabling Integration of Distributed Solar Power Generation," *IEEE Trans. Smart Grid*, vol. 3, no. 2, pp. 850–857, Jun. 2012.

[1-22] M. Zeraati, M. E. H. Golshan, and J. M. Guerrero, "Distributed control of battery energy storage systems for voltage regulation in distribution networks with high PV penetration," *IEEE Trans. Smart Grid*, vol. PP, no. 99, pp. 1–1, 2016.

[1-23] P. Fortenbacher, J. L. Mathieu, and G. Andersson, "Modeling and Optimal Operation of Distributed Battery Storage in Low Voltage Grids," *IEEE Trans. Power Syst.*, vol. 32, no. 6, pp. 4340–4350, Nov. 2017.

[1-24] Y. P. Agalgaonkar, B. C. Pal, and R. A. Jabr, "Distribution Voltage Control Considering the Impact of PV Generation on Tap Changers and Autonomous Regulators," *IEEE Trans. Power Syst.*, vol. 29, no. 1, pp. 182–192, Jan. 2014.

[1-25] S. N. Salih and P. Chen, "On Coordinated Control of OLTC and Reactive Power Compensation for Voltage Regulation in Distribution Systems With Wind Power," *IEEE Trans. Power Syst.*, vol. 31, no. 5, pp. 4026–4035, Sep. 2016.

[1-26] M. Abdelkhalek Azzouz, H. E. Farag, and E. F. El-Saadany, "Real-Time Fuzzy Voltage Regulation for Distribution Networks Incorporating High Penetration of Renewable Sources," *IEEE Syst. J.*, vol. 11, no. 3, pp. 1702–1711, Sep. 2017.

[1-27] Y. Sasaki, T. Yoshida, N. Seki, T. Watanabe, and Y. Saitoh, "High Speed TVR for Power Distribution Lines and its Test Results," *IEEJ Trans. Power Energy*, vol. 123, no. 9, pp. 1105–1111, 2003.

[1-28] M. Nijhuis, M. Gibescu, and J. F. G. Cobben, "Incorporation of on-load tap changer transformers in low-voltage network planning," in *2016 IEEE PES Innovative Smart Grid Technologies Conference Europe (ISGT-Europe)*, 2016, pp. 1–6.

[1-29] K. N. Bangash, M. E. A. Farrag, and A. H. Osman, "Smart Control of on Load Tap Changer deployed in Low Voltage Distribution Network," in *2015 4th International Conference on Electric Power and Energy Conversion Systems (EPECS)*, 2015, pp. 1–6.

[1-30] C. Long, A. T. Procopiou, L. F. Ochoa, G. Bryson, and D. Randles, "Performance of OLTC-based control strategies for LV networks with photovoltaics," in *2015 IEEE Power & Energy Society General Meeting*, 2015, pp. 1–5.

[1-31] A. T. Procopiou and L. F. Ochoa, "Voltage control in PV-rich LV networks without remote monitoring," *IEEE Trans. Power Syst.*, pp. 1–1, 2016.

[1-32] N. Efkarpidis, T. De Rybel, and J. Driesen, "Optimal placement and sizing of active in-line voltage regulators in flemish LV distribution grids," *IEEE Trans. Ind. Appl.*, vol. 52, no. 6, pp. 4577–4584, 2016.

[1-33] C. Long and L. F. Ochoa, "Voltage control of PV-rich LV networks: OLTC-fitted transformer and capacitor banks," *IEEE Trans. Power Syst.*, vol. 31, no. 5, pp. 4016–4025, Sep. 2016.

[1-34] A. Navarro-Espinosa and L. F. Ochoa, "Increasing the PV hosting capacity of LV networks: OLTC-fitted transformers vs. reinforcements," in *2015 IEEE Power & Energy Society Innovative Smart Grid Technologies Conference (ISGT)*, 2015, pp. 1–5.

[1-35] M. Tsuji, M. Iwata, A. Kurosawa, and S. Watanabe, "Development of pole transformer with auto tap changer (in Japanese)," *Tak. Rev.*, vol. 57, no. 1, pp. 1–6, 2012.

[1-36] Ruey-Hsun Liang and Chen-Kuo Cheng, "Dispatch of main transformer ULTC and capacitors in a distribution system," *IEEE Trans. Power Deliv.*, vol. 16, no. 4, pp. 625–630, 2001.

[1-37] Y. Hayashi, J. Matsuki, R. Suzuki, and E. Muto, "Determination Method for Optimal Sending Voltage Profile in Distribution System with Distributed Generators," *IEEJ Trans. Power Energy*, vol. 125, no. 9, pp. 846–854, 2005.

[1-38] S. Yoshizawa, Y. Yamamoto, Y. Hayashi, S. Sasaki, T. Shigeto, and H. Nomura, "Dynamic updating method of optimal control parameters of multiple advanced SVRs in a single feeder," *IEEJ Trans. Power Energy*, vol. 135, no. 9, pp. 550–558, Sep. 2015.

[1-39] C. Gao and M. A. Redfern, "Automatic compensation voltage control strategy for on-load tap changer transformers with distributed generations," in *2011 International Conference on Advanced Power System Automation and Protection*, 2011, pp. 737–741.

[1-40] S. Kawano, S. Yoshizawa, Y. Fujimoto, and Y. Hayashi, "Maximum PV Penetration Capacity Evaluation of a Novel Method for Determining LDC Control Parameters of Step Voltage Regulators," *Int. J. Electr. Energy*, vol. 3, no. 1, 2015.

[1-41] S. Kawano, S. Yoshizawa, Y. Fujimoto, and Y. Hayashi, "OLTC and multiple SVRs in distribution system by using database," in *2015 5th International Youth Conference on Energy (IYCE)*, 2015, pp. 1–6.

[1-42] S. Kawano, S. Yoshizawa, Y. Fujimoto, and Y. Hayashi, "The basic study for development of a method for determining the LDC parameters of LRT and SVR using PV output forecasting," in *2015 IEEE Power & Energy Society Innovative Smart Grid Technologies Conference (ISGT)*, 2015, pp. 1–5.

[1-43] T. Udagawa, H. Yasuhiro, N. Takahashi, Y. Matsuura, T. Morita, and M. Minami, "Evaluation of Voltage Control Effect for Data Acquisition Period Length from SCADA with IT Switches," *J. Int. Counc. Electr. Eng.*, vol. 3, no. 2, pp. 146–152, Apr. 2013.

[1-44] S. Akagi *et al.*, "Upgrading the voltage control method based on the photovoltaic penetration rate," *IEEE Trans. Smart Grid*, vol. PP, no. 99, pp. 1–1, 2017.

[1-45] "Definition of ZEH and future measures proposed by the ZEH Roadmap Examination Committee," *Energy Efficiency and Conservation Division/Agency for Natural Resources and Energy/Ministry, Trade and Industry*, 2015. [Online]. Available: http://www.enecho.meti.go.jp/category/saving_and_new/saving/zeh_report/pdf/report_160212_en.pdf. [Accessed: 31-Aug-2017].

[1-46] E. Matallanas *et al.*, "Neural network controller for Active Demand-Side Management with PV energy in the residential sector," *Appl. Energy*, vol. 91, no. 1, pp. 90–97, Mar. 2012.

[1-47] B. Bletterie, S. Kadam, R. Bolgaryn, and A. Zegers, "Voltage Control with PV Inverters in Low Voltage Networks—In Depth Analysis of Different Concepts and Parameterization Criteria," *IEEE Trans. Power Syst.*, vol. 32, no. 1, pp. 177–185, Jan. 2017.

[1-48] P. Monica and M. Kowsalya, "Control strategies of parallel operated inverters in renewable energy application: A review," *Renew. Sustain. Energy Rev.*, vol. 65, pp. 885–901, 2016.

[1-49] C.-C. Yeh *et al.*, "Mitigation of Voltage Variation by REMS for Distribution Feeders," *IEEE Trans. Ind. Appl.*, vol. 53, no. 2, pp. 901–907, Mar. 2017.

[1-50] “Britain to Ban New Diesel and Gas Cars by 2040 - The New York Times.” [Online]. Available: https://www.nytimes.com/2017/07/26/world/europe/uk-diesel-petrol-emissions.html. [Accessed: 24-Oct-2017].

[1-51] “France Plans to End Sales of Gas and Diesel Cars by 2040 - The New York Times.” [Online]. Available: https://www.nytimes.com/2017/07/06/business/energy-environment/france-cars-ban-gas-diesel.html. [Accessed: 24-Oct-2017].

[1-52] “India to sell only electric cars by 2030 - Jun. 3, 2017.” [Online]. Available: http://money.cnn.com/2017/06/03/technology/future/india-electric-cars/index.html. [Accessed: 24-Oct-2017].

[1-53] “China Gives Automakers More Time in World’s Biggest EV Plan - Bloomberg.” [Online]. Available: https://www.bloomberg.com/news/articles/2017-09-28/china-to-start-new-energy-vehicle-production-quota-from-2019. [Accessed: 24-Oct-2017].

[1-54] “These countries want to ditch gas and diesel cars - Jul. 26, 2017.” [Online]. Available: http://money.cnn.com/2017/07/26/autos/countries-that-are-banning-gas-cars-for-electric/index.html. [Accessed: 24-Oct-2017].

[1-55] “BMW Group announces next step in electrification.” [Online]. Available: https://www.press.bmwgroup.com/global/article/detail/T0273122EN/bmw-group-announces-next-step-in-electrification-strategy?language=en. [Accessed: 24-Oct-2017].

[1-56] “Volvo Cars to go all electric - Volvo Car Group Global Media Newsroom.” [Online]. Available: https://www.media.volvocars.com/global/en-gb/media/pressreleases/210058/volvo-cars-to-go-all-electric. [Accessed: 24-Oct-2017].

[1-57] “Plans for more than ten different all-electric vehicles by 2022: All systems are go - Daimler Global Media Site.” [Online]. Available: http://media.daimler.com/marsMediaSite/en/instance/ko/Plans-for-more-than-ten-different-all-electric-vehicles-by-2022-All-systems-are-go.xhtml?oid=29779739. [Accessed: 24-Oct-2017].

[1-58] “New Group strategy adopted: Volkswagen Group to become a world-leading provider of sustainable mobility - volkswagen-media-services.com.” [Online]. Available: https://www.volkswagen-media-services.com/en/detailpage/-/detail/New-Group-strategy-adopted-Volkswagen-Group-to-become-a-world-leading-provider-of-sustainable-mobility/view/3681833/7a5bbec13158edd433c6630f5ac445da. [Accessed: 24-Oct-2017].

[1-59] “Mazda, Denso, and Toyota Sign Joint Technology Development Contract for Electric Vehicles | TOYOTA Global Newsroom.” [Online]. Available: http://newsroom.toyota.co.jp/en/detail/18840443/. [Accessed: 24-Oct-2017].

Chapter 2
Coordinated voltage control scheme of multiple OLTCs

2.1 Introduction to this chapter

Some voltage control schemes for supply sides have been proposed to avoid voltage violation when PVs are introduced in DSs. In this regard, some coordinated methods on the SC and LRT have been suggested [2-1]–[2-3]. A real-time centralized voltage control method by supervisory control and data acquisition (SCADA) system was proposed [2-4]. Optimal control in the DS with LRT, SVR, SC, ShR, and SVC has been researched by different groups [2-5], [2-6] and their solutions involved the introduction of a communication infrastructure in the power system with a controller that determines the operation of a large number of candidates by using a genetic algorithm (GA). Subsequently, decentralized control methods for micro-grids were reviewed [2-7], and coordinated control for enhanced voltage harmonics was discussed [2-8]. A voltage control scheme that determines the parameters of multiple SVRs in one feeder by using a combination of a greedy algorithm and tabu search was also reported [2-9]. Optimal decentralized control was achieved by developing a multi-agent system to appropriately control multiple SVRs [2-10], [2-11]. A voltage control method using an LVR in the LVDN was evaluated [2-11]. Although these studies focused on the voltage control to maintain the voltage in MVDSs, the voltage condition in all LVDSs should be evaluated and the local voltage violation should be addressed because the PV penetration causes the local voltage rise in LVDSs. On the other hand, a voltage control scheme that focuses on the LVDS can be effective in resolving this problem [2-12]–[2-16]. Voltage control using the LV OLTC, i.e., LVR, which is more cost-effective than the grid reinforcement when the PV penetration increases [2-17], has been studies as a solution to the local voltage violation in the LVDS. There are some studies on voltage control using the LVR [2-18]–[2-23], such as distributed and centralized voltage control methods and determination of installation location. These studies described the improvement of voltage condition in the LVDS by using the LVR without considering the impact of voltage control devices locate upstream from the LVR. Since the MV OLTCs is commonly deployed in the conventional DSs, a newly deployed LVR will affected by the voltage control of them. Thus, the voltage control scheme of the LVR should be studied with the consideration of voltage control of MV OLTCs, which are located in upstream from the LVR. Although the voltage control performance of the LVR is assessed in [2-24] considering the impact of MV OLTCs, the control method is based on the sensor data and requires a rich communication network. In addition, the installation location of the LVR is not discussed.

Therefore, in this chapter, we propose a coordinated voltage control scheme in DSs by implementing various OLTCs: an LRT, SVRs, and LVRs. The proposed scheme is capable of determining the installation location of the LVRs as well as the control parameters of the OLTCs by considering the behavior of the other OLTCs. We validated the proposed method by carrying out numerical simulations

based on an actual DS model in Japan. In the simulation, we varied the penetration ratio of PV to evaluate the capability of our scheme to control various kinds of voltage fluctuations caused by PVs.

2.2 Decentralized voltage control methods of OLTCs in DSs

In conventional DSs, MV OLTCs, such as, LRT and SVR are widely deployed to maintain the voltage within a prescribed range. The MV OLTCs simultaneously control the voltage in multiple LVDSs. However, a local voltage violation caused by the penetration of the PV makes it difficult for the MV OLTCs to maintain the voltage across all LVDSs. This is because the local voltage violation may arise in an area smaller than that for which the MV OLTC were designed to control. To solve the local voltage violations, the LVR, which is an LV OLTC, is expected to compensate for the limitations of the MV OLTCs by independent control.

Voltage control of an OLTC consists of adjusting a tap position to achieve the desired profile. In most control frameworks, each OLTC monitors its secondary voltage and current to dynamically control the tap (Fig. 2.1). Let $\dot{\boldsymbol{v}}_t$ and $\boldsymbol{i}_t$ be the monitored secondary voltage and current of the target OLTC at time t. These values are used for calculating the cumulative difference from the target value. Let $D_t^{\mathrm{u}}(\boldsymbol{\gamma})$ and $D_t^{\mathrm{l}}(\boldsymbol{\gamma})$ be the cumulative differences between the monitored values and the target values. The tap position of the OLTC s_t at time $t \in \{1, \ldots, T\}$ is found according to the following:

$$s_t = \begin{cases} s_{t-1} - 1, & \text{if } D_t^{\mathrm{u}}(\boldsymbol{\gamma}) > \delta \text{ and } s_t \neq s^{\mathrm{l}}, \\ s_{t-1} + 1, & \text{if } D_t^{\mathrm{l}}(\boldsymbol{\gamma}) > \delta \text{ and } s_t \neq s^{\mathrm{u}}, \\ s_{t-1}, & \text{otherwise}, \end{cases} \tag{2.1}$$

where $\boldsymbol{\gamma}$ are the parameters of the voltage control, δ is the given threshold, and s^{u} and s^{l} are the upper and lower limits of the tap positions. The methods for calculating the cumulative differences $D_t^{\mathrm{u}}(\boldsymbol{\gamma})$ and $D_t^{\mathrm{l}}(\boldsymbol{\gamma})$ differ depending on the control framework. In the remainder of this section, we describe the voltage control frameworks that we adopted for implementing the LRT, SVR, and LVR.

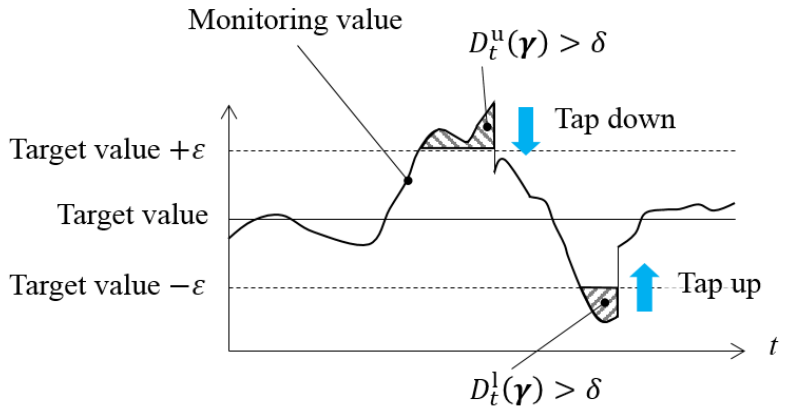

Fig. 2.1 Schematic image of voltage control using OLTCs.

2.2.1 Voltage control framework for LRT

An LRT is located at a distribution substation of an MVDS and is required to appropriately regulate the tap position to maintain the voltage in multiple feeders. Let $\boldsymbol{\gamma}^{\mathrm{lrt}} = \{v^{\mathrm{lrt}}, z^{\mathrm{lrt}}\}$ be the parameter set of a control framework implemented in the LRT, and let ε be the dead band. The controller finds the cumulative difference $D_t^{\mathrm{u}}(\boldsymbol{\gamma}^{\mathrm{lrt}})$ and $D_t^{\mathrm{l}}(\boldsymbol{\gamma}^{\mathrm{lrt}})$ as follows:

$$D_t^{\mathrm{u}}(\boldsymbol{\gamma}^{\mathrm{lrt}}) = \max\{0, \quad D_{t-1}^{\mathrm{u}}(\boldsymbol{\gamma}^{\mathrm{lrt}}) + |\dot{\boldsymbol{v}}_t| - z^{\mathrm{lrt}}|\boldsymbol{i}_t| - v^{\mathrm{lrt}} - \varepsilon\}, \tag{2.2}$$

$$D_t^{\mathrm{l}}(\boldsymbol{\gamma}^{\mathrm{lrt}}) = \max\{0, \quad D_{t-1}^{\mathrm{l}}(\boldsymbol{\gamma}^{\mathrm{lrt}}) + z^{\mathrm{lrt}}|\boldsymbol{i}_t| + v^{\mathrm{lrt}} - \varepsilon - |\dot{\boldsymbol{v}}_t|\}. \tag{2.3}$$

2.2.2 Voltage control framework for SVR and LVR

A voltage control framework based on the LDC method is implemented in the SVR and LVR. Let $\boldsymbol{\gamma}^{\mathrm{ldc}} = \{v^{\mathrm{ldc}}, l\}$ be a parameter set of the LDC method. The voltage v_t^{ref} is an arbitrary voltage reference point on the secondary side of each OLTC estimated in the LDC method by:

$$v_t^{\mathrm{ref}}(l) = |\dot{\boldsymbol{v}}_t - l\dot{\boldsymbol{z}}\boldsymbol{i}_t|, \tag{2.4}$$

where l is the line length between the OLTC and the voltage reference point at time t, and $\dot{\boldsymbol{z}}$ is the unit line impedance. Then, the OLTC derives the cumulative differences between the estimated voltage v_t^{ref} and target voltage v^{ldc}, $D_t^{\mathrm{u}}(\boldsymbol{\gamma}^{\mathrm{ldc}})$ and $D_t^{\mathrm{l}}(\boldsymbol{\gamma}^{\mathrm{ldc}})$, according to the following equations:

$$D_t^{\mathrm{u}}(\boldsymbol{\gamma}^{\mathrm{ldc}}) = \max\{0, D_{t-1}^{\mathrm{u}}(\boldsymbol{\gamma}^{\mathrm{ldc}}) + v_t^{\mathrm{ref}}(l) - v^{\mathrm{ldc}} - \varepsilon\}, \tag{2.5}$$

$$D_t^{\mathrm{l}}(\boldsymbol{\gamma}^{\mathrm{ldc}}) = \max\{0, D_{t-1}^{\mathrm{l}}(\boldsymbol{\gamma}^{\mathrm{ldc}}) + v^{\mathrm{ldc}} - \varepsilon - v_t^{\mathrm{ref}}(l)\}. \tag{2.6}$$

2.3 Coordinated voltage control scheme of OLTCs

The OLTC controls the voltage according to the framework outlined in Section 2.2 based on the parameters $\boldsymbol{\gamma}^{\mathrm{lrt}}$ and $\boldsymbol{\gamma}^{\mathrm{ldc}}$. These parameters must be designed to coordinate action. In a DS with multiple OLTCs, appropriate voltage control actions may not occur because a downstream OLTC will be influenced by the tap operation of the upstream OLTC. In a decentralized control framework, each OLTC is independently operated; thus, interference among the tap operations is more likely.

We propose a scheme of coordinated voltage control for multiple OLTC types (i.e., an LRT, SVRs, and LVRs) to avoid interference. Our design is composed of three parts: 1) determining the control parameters of the MV OLTCs (i.e., LRT and SVRs), 2) locations of the LVRs, and 3) control parameters of some of the LVRs.

The voltage control design first determines appropriate control parameters for the LRT and SVRs to maximize their local voltage control performance. This process can mitigate most of the voltage fluctuations in DSs with PVs but may be insufficient in some LVDSs. In addition, it contributes to suppressing the installation cost by reducing the number of LVRs, which are considered in the next step.

Assume that the DS is divided into specific areas, each of which is controlled by an MV OLTC. Each MV OLTC manages a zone from the point of its location to that of the next downstream MV

OLTC (Fig. 2.2). The control parameters of each MV OLTC are determined in the order of upstream to downstream to maintain the voltage of LV consumers in their control areas. Therefore, the control parameters of a downstream MV OLTC can be determined by considering the influence of the voltage control of the upstream MV OLTC/s. Next, LVRs are introduced in areas where the MV OLTCs cannot prevent excessive voltage violations. All the LVRs are initially given identical default control parameters to minimize complexity.

Once the LVRs—for which the default control parameters are used—have been introduced, appropriate control parameters are determined for the LVRs in those LVDSs where voltage violations occur. The control parameters of the LVRs are determined on the basis of power flow calculation (PFC) that can confirm the behavior of the MV OLTCs during voltage control. The LVRs using the control parameters determined in this way should control the voltage in coordination with the MV OLTCs.

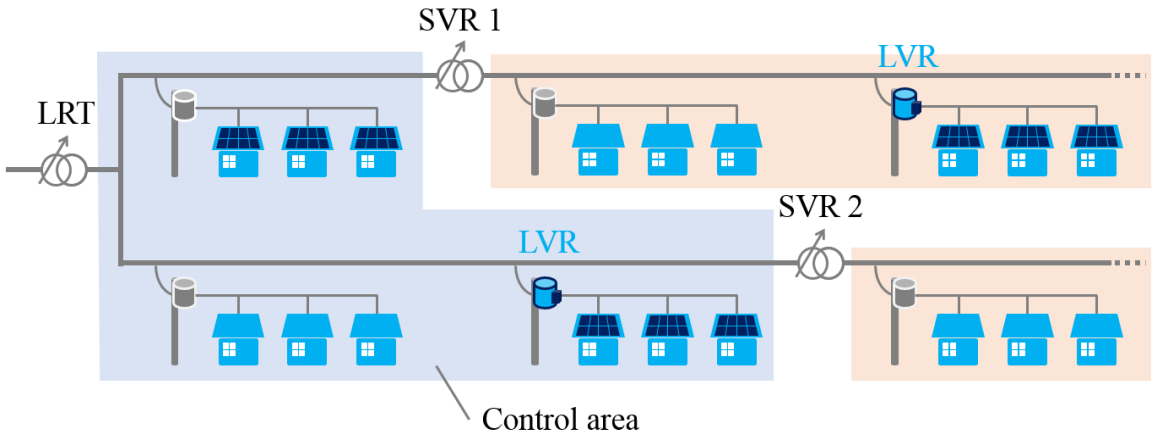

Fig. 2.2 MVDS example showing the control areas of each MV OLTC.

2.3.1 Determination of control parameters for the LRT

The LRT must maintain the voltage in multiple feeders. The secondary voltage $\dot{\boldsymbol{v}}_t$ and current $\boldsymbol{i}_t$ should include characteristics of the total power fluctuation in multiple feeders; thus, the control parameters of an LRT $\boldsymbol{\gamma}^{\mathrm{lrt}} = \{v^{\mathrm{lrt}}, z^{\mathrm{lrt}}\}$ are determined as follows on the basis of the maximum and minimum of $|\dot{\boldsymbol{v}}_t|$ and $|\boldsymbol{i}_t|$(Fig. 2.3):

$$z^{\mathrm{lrt}} = \frac{v_{\max} - v_{\min}}{i_{\max} - i_{\min}}, \tag{2.7}$$

$$v^{\mathrm{lrt}} = \frac{v_{\max} + v_{\min} - z^{\mathrm{lrt}}(i_{\max} + i_{\min})}{2}, \tag{2.8}$$

where

$$\begin{cases} v_{\max} = \max\limits_t |\dot{\boldsymbol{v}}_t| \\ v_{\min} = \min\limits_t |\dot{\boldsymbol{v}}_t| \\ i_{\max} = \max\limits_t |\boldsymbol{i}_t| \\ i_{\min} = \mathrm{mix}\limits_t |\boldsymbol{i}_t| \end{cases}. \tag{2.9}$$

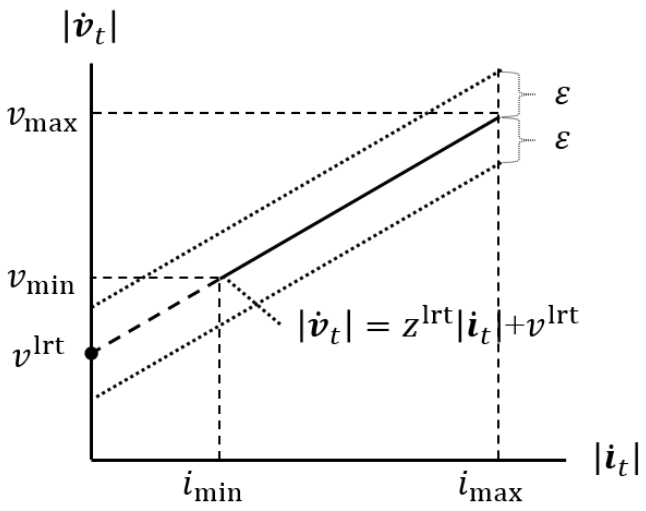

Fig. 2.3 Graphic illustration showing the determination of the LRT parameters [2-25] © 2016 IEEE.

2.3.2 Determination of control parameters for SVR and LVR

The control parameters of the LDC method implemented in the SVRs and LVRs are $\boldsymbol{\gamma}^{\mathrm{ldc}} = \{v^{\mathrm{ldc}}, l\}$. Let v_t^j be the voltage at the LV receiving end j at time t, and let $\mathcal{J}$ be the set of LV receiving ends. We also let v^{u} and v^{l} are the upper and lower acceptable voltage limits. The appropriate LDC control parameter set $\boldsymbol{\gamma}_q^{\mathrm{ldc}}$ is determined to minimize the voltage difference, which is the one between the voltage at the LV receiving ends v_t^j and the central voltage of the acceptable voltage limits in the LDVS, and the number of tap operations using a suitable weight coefficient $\alpha > 0$:

$$\boldsymbol{\gamma}_q^{\mathrm{ldc}} = \underset{\boldsymbol{\gamma}^{\mathrm{ldc}}}{\operatorname{argmin}} \left\{ \max_{j \in \mathcal{J}, t} \left| v_t^j\left(\boldsymbol{\gamma}^{\mathrm{ldc}} | \boldsymbol{\gamma}_1, \ldots, \boldsymbol{\gamma}_n\right) - \frac{v^{\mathrm{u}} - v^{\mathrm{l}}}{2} \right| + \alpha \sum_{t=1}^{\mathrm{T}} \left| s_{t-1}\left(\boldsymbol{\gamma}^{\mathrm{ldc}} | \boldsymbol{\gamma}_1, \ldots, \boldsymbol{\gamma}_n\right) - s_t\left(\boldsymbol{\gamma}^{\mathrm{ldc}} | \boldsymbol{\gamma}_1, \ldots, \boldsymbol{\gamma}_n\right) \right| \right\}, \tag{2.10}$$

where $\boldsymbol{\gamma}_n$ and n are the parameter set and number of the OLTCs located upstream of the target OLTC. The above minimization problem can be solved by evaluating the values derived by the PFC on all control parameter set candidates, $l \in \mathcal{L}$ and $v^{\mathrm{ldc}} \in \mathcal{V}$.

2.4 Numerical simulation

The validity of our coordinated voltage control scheme was verified by carrying out a voltage control simulation using the DS model shown in Fig. 2.4 [2-26], which also explains the fixed tap ratio of pole transformers. This model was built on the basis of actual Japanese DSs and has two distribution feeders that include both MV and LV DSs. The DS model has five MV OLTCs, i.e., an LRT is located at the distribution substation, and four SVRs are deployed in the middle of the feeders. Feeder 1 (F1) simulates an industrial area with an 18.4-km main line, three SVRs, 20 MV consumers, 60 low-voltage distribution systems (LVDSs), and 551 LV consumers. Feeder 2 (F2) simulates a residential area with a 10.5-km main line, an SVR, 14 MV consumers, 48 LVDSs, and 479 LV consumers.

We conducted the numerical case studies on the basis of the load and PV profiles of MV and LV consumers. Fig. 2.5(a) shows the MV load profiles in each feeder created from actual measurements. Fig. 2.5(b) shows the set of the load and PV profiles for an LV consumer with a time step of 10 s. The different real-world profiles were individually used for each LV consumer. The PVs were introduced by the LV consumers at the end of each feeder to validate our scheme in different voltage distributions. Their penetration ratios varied (0, 25, 50, 75, 100%). Table 2.1 outlines our experimental setup, including several dominant parameters. The total number of LV consumers and PV introduction areas in each MV node are shown in Fig. 2.6. In this simulation, we evaluate the controls under the following conditions:

- MV OLTCs only (conventional scheme, case 1)
- MV OLTCs and LVRs with default control parameters (case 2)
- MV OLTCs and LVRs with coordinated control parameters (proposed scheme, case 2)

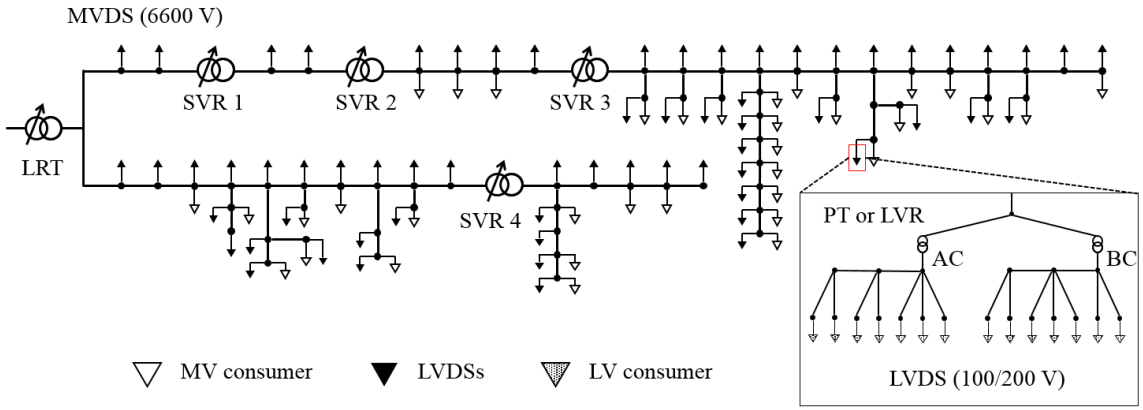

Fig. 2.4 Distribution system model that includes both MV and LV distribution systems.

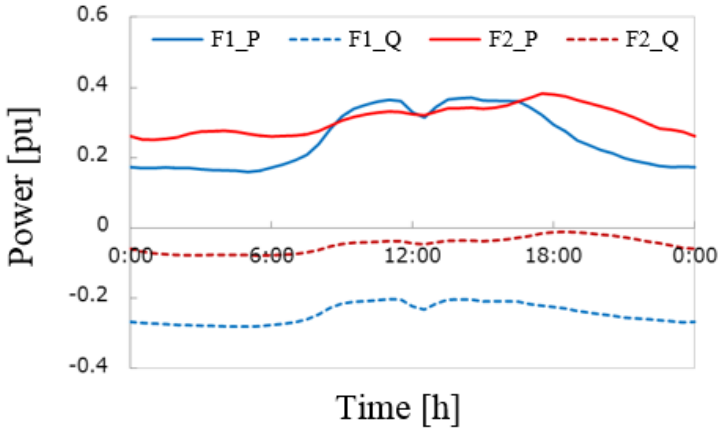

(a) Load profiles in MV consumers

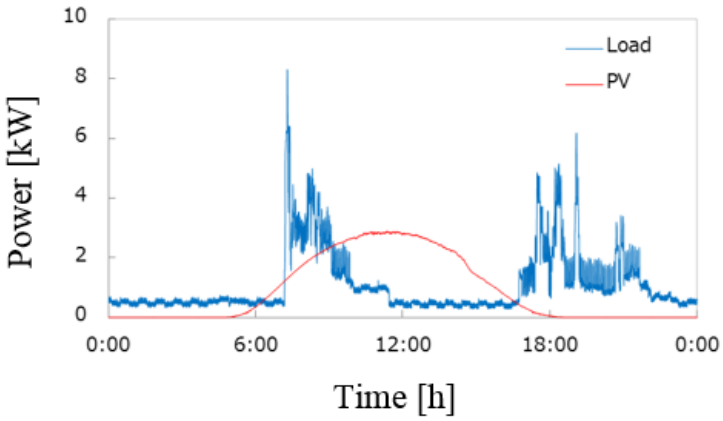

(b) Load and PV profiles in as LV consumer

Fig. 2.5 Profiles used in the simulation [2-25] © 2016 IEEE.

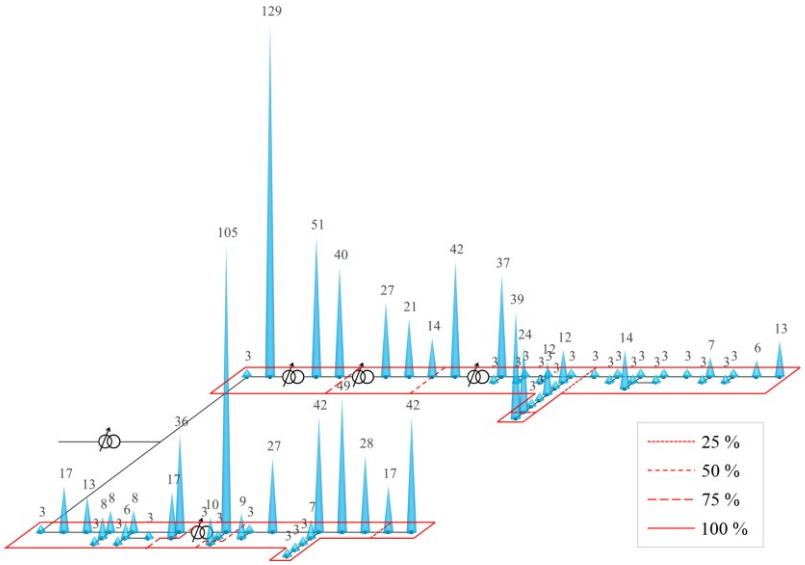

Fig. 2.6 Number of LV consumers and PV introduction area in each MV node.

Table 2.1 Simulation setup.

DS model	Appropriate voltage range in LVDS	95–107 [V]
LRT parameters	Tap position	{1, 2, ..., 21}
	Tap width	60 [V]
	Dead band	1 [%]
SVR parameters	Tap position	{1, 2, ..., 9}
	Tap width	100 [V]
	Dead band	1.5 [%]
	Candidates for l_τ	SVR 1: {0.5, 1.0, ..., 4.0} [km]
		SVR 2: {0.5, 1.0, ..., 4.5} [km]
		SVR 3: {0.5, 1.0, ..., 3.5} [km]
		SVR 4: {0.5, 1.0, ..., 4.5} [km]
	Candidates for v_t^{ref}	{95, 95.5, ..., 107}*6600/105 [V]
LVR parameters	Tap position	{1, 2, ..., 5}
	Tap width	2.38 [V]
	Dead band	1.5 [%]
	Candidates for l_τ	{0.01, 0.02, ..., 0.18} [km]
	Candidates for v_t^{ref}	{95, 95.5, ..., 107} [V]

Fig. 2.7 shows the number of LV consumers with voltage violations for all cases. Table 2.2 presents the number of LVRs introduced in the LVDSs in which the MV OLTCs cannot prevent voltage violations. These results show that the MV OLTCs can maintain the voltage within the prescribed range when the PV introduction ratio is 0%. Thus, the conventional voltage control scheme was found to be suitable for cases without PV introduction. These results also indicate that there was no voltage violation in F2 for all cases. Therefore, the following discussion focuses on the results obtained for F1 hereafter. Fig. 2.7 shows that the introduction of LVRs significantly reduces voltage violations, which is further reduced by the coordinated voltage control scheme.

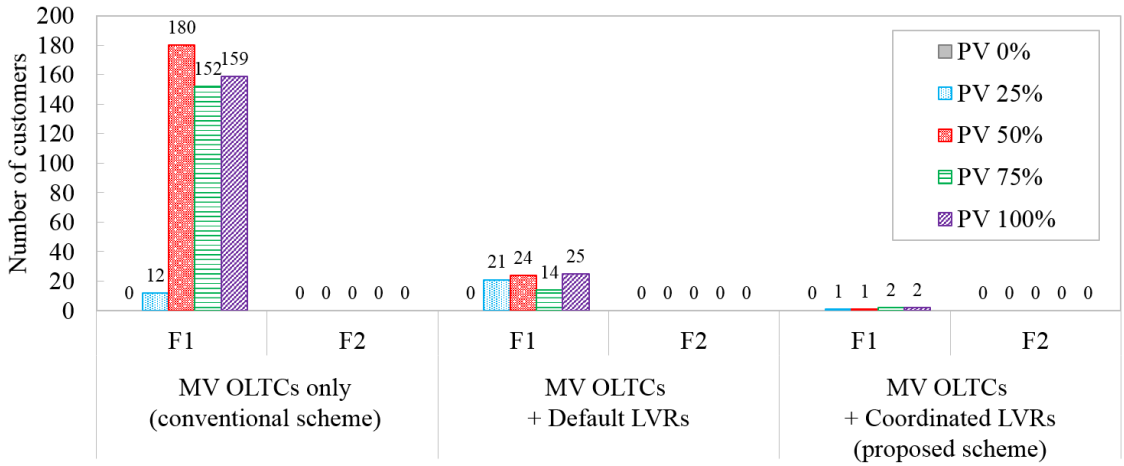

Fig. 2.7 Number of LV consumers with voltage violation [2-25] © 2016 IEEE.

Table 2.2 Number of LVRs [2-25] © 2016 IEEE.

PV penetration	0%	25%	50%	75%	100%
Number of LVRs	0	4	20	15	15

The number of houses with voltage violation in each MV node of line F1 is shown in Figs. 2.8-2.10. Figs. 2.8(a)-(d) indicate that there are three major reasons for voltage violation in the conventional scheme: boundaries of fixed tap ratio of PTs, boundaries of PV introduction, and a large number of houses.

Figs. 2.8(b)-(d) show that there are many houses with voltage violation in the MV nodes located on the primary side of SVR1 and between SVR2 and SVR3. These areas include a boundary of the fixed tap ratio of PTs. Voltage control in these areas is difficult for legacy LTCs because the difference in the voltage trend in each LVDN in an area controlled by an LTC becomes much larger than in other areas.

Figs. 2.8(b), (c) show the harmful effect of boundaries of PV introduction. Fig. 2.8(b) shows that there is a boundary of PV introduction in an area between SVR2 and SVR3 where many voltage violations occur. This is why the number of voltage violations of PV 50% is the highest of all in case 1 (Fig. 2.7). Voltage control is complicated for LTCs that have both LVDSs with and without PV in their control area. It particularly occurs during the daytime because the voltage will rise in the LVDSs with PV despite the voltage dropping in the LVDSs without PV. Moreover, the PV introduction area of the F2 in Fig. 2.4 shows that the boundaries of PV introduction on 50% and 75% are in a control area of the LRT. Figs. 2.7(a), (b) shows that voltage violation on the primary side of SVR1 sharply increases when the introduction ratio of PV increases from 25% to 50%. These results suggest that the boundary of PV introduction in F2 affects the voltage violation on the primary side of SVR1. Voltage control of the LRT becomes difficult when the introduction ratio of PV increases from 25% to 50% because the

voltage will rise at the end of control area of the LRT in F2 despite the voltage dropping in the other area controlled by the LRT.

Voltage violation cannot be prevented in the MV node at the vertical end of F1 as shown in Figs. 2.8(a)-(d). This section of F1 contains an LVDN with 29 houses, which is the largest of all, in the MV node. It is complicated to maintain the voltage within the prescribed range because the amount by which the voltage rises and drops from the PT to the end of the LVDN increases.

Figs. 2.9(a)-(d) show that the introduction of LVRs with default parameters solves the voltage violation problem in all LVDNs except for the area with the 29 houses. This result illustrates that the LVRs introduced at appropriate locations effectively compensate for the performance of the LRT and SVRs and mitigate the voltage violation based on the boundaries of the fixed tap ratio of PTs and the boundaries of PV introduction. However, the number of occurrences of voltage violation increases in the LVDN with 29 houses because the default parameters are not suitable regarding coordination with the LRT and SVRs.

Figs. 2.10(a)-(d) show that the proposed scheme succeeds in achieving a further reduction in the number of houses with voltage violation compared to case 2. The coordinated scheme also mitigates the voltage violation caused by the large number of houses in addition to the other reasons. This is why the coordinated control parameters of the LVR are determined considering the influence of the other LTCs. Moreover, the proposed scheme is shown to appropriately compensate for the shortcomings of the legacy LTCs, and can prevent the various kinds of voltage violation.

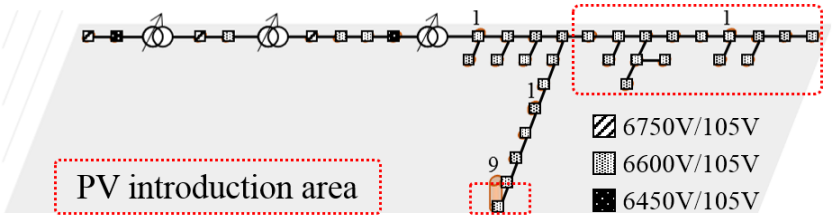

(a) PV penetration ratio 25%

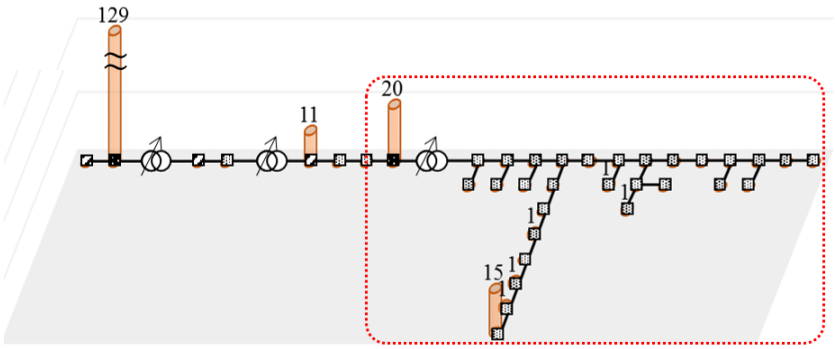

(b) PV penetration ratio 50%

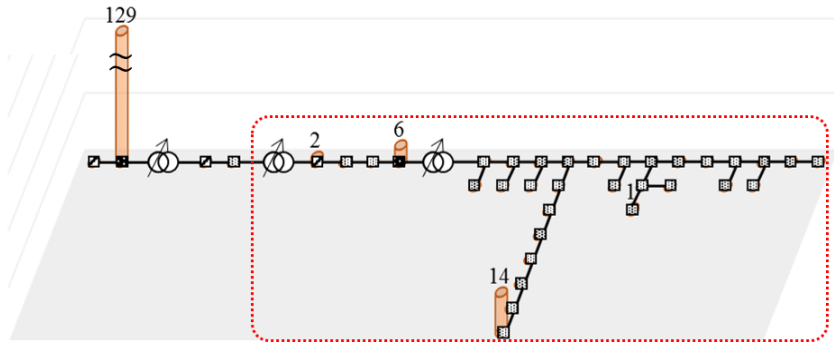

(c) PV penetration ratio 75%

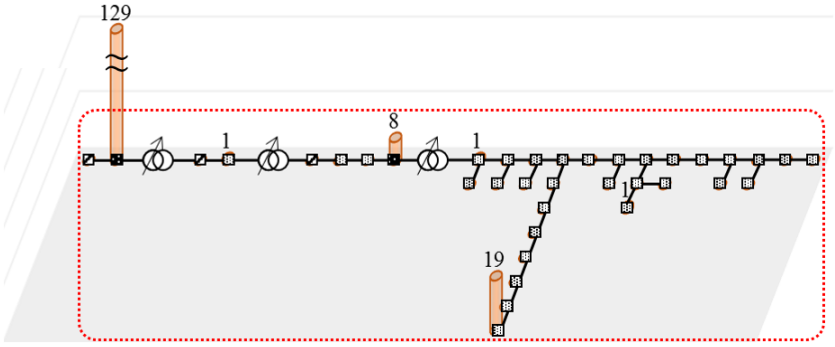

(d) PV penetration ratio 100%s

Fig. 2.8 Number of houses with voltage violation in each MV node of line F1 (case 1, conventional scheme) [2-25] © 2016 IEEE.

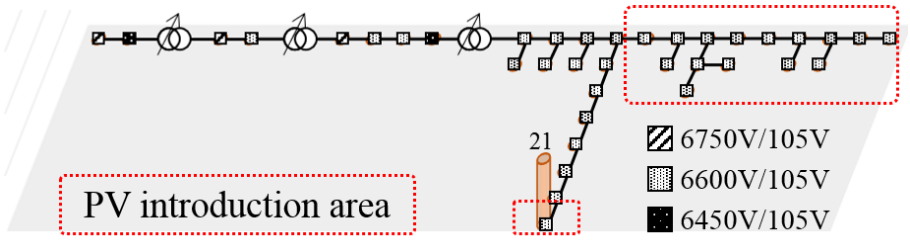

(a) PV penetration ratio 25%

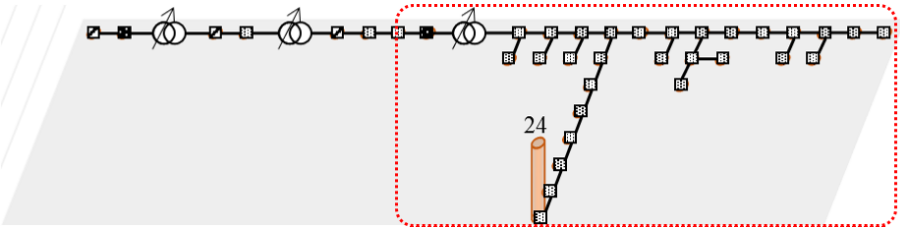

(b) PV penetration ratio 50%

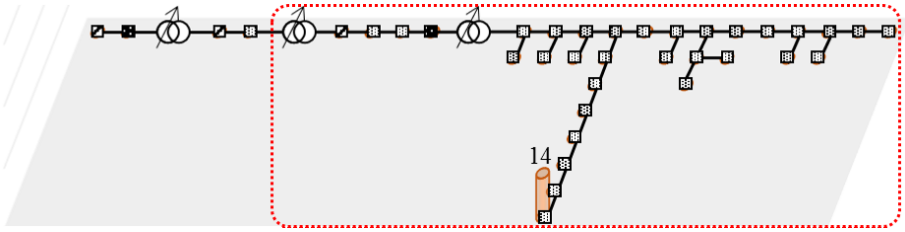

(c) PV penetration ratio 75%

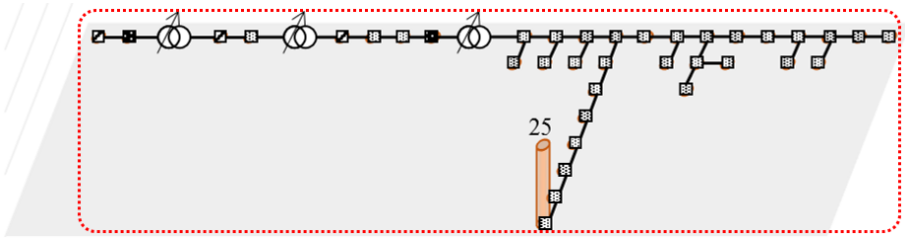

(d) PV penetration ratio 100%

Fig. 2.9 Number of houses with voltage violation in each MV node of line F1 (case 2) [2-25] © 2016 IEEE.

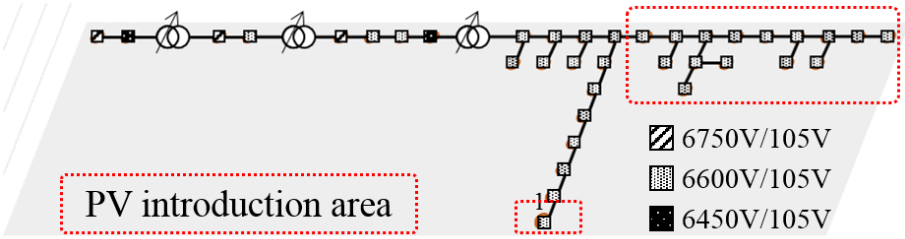

(a) PV penetration ratio 25%

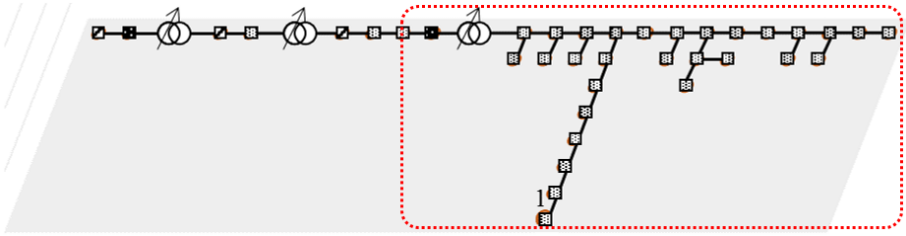

(b) PV penetration ratio 50%

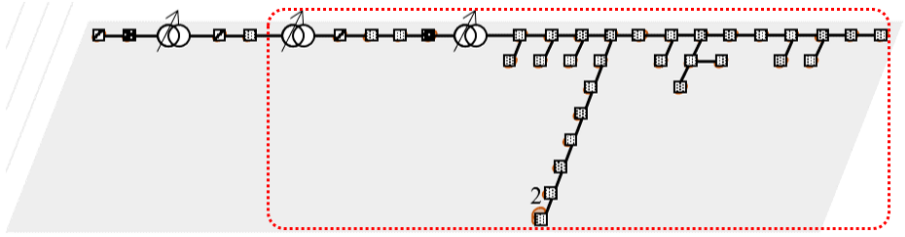

(c) PV penetration ratio 75%

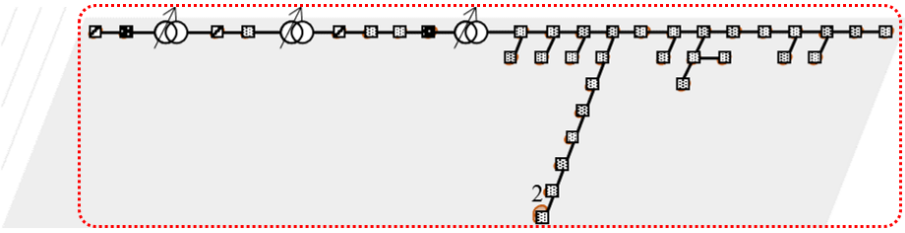

(d) PV penetration ratio 100%

Fig. 2.10 Number of houses with voltage violation in each MV node of line F1 (case 3, proposed scheme) [2-25] © 2016 IEEE.

2.5 Summary of this chapter

In this chapter, we proposed a coordinated voltage control scheme for multiple kinds of OLTCs. The proposed scheme appropriately determined the installation location of LVRs and the control parameters of each OLTC by considering the influence of the other OLTCs on the voltage control. We performed a numerical simulation using a DS model. The proposed scheme succeeded in preventing almost all occurrences of voltage violation. The proposed scheme is capable of responding to additional kinds of voltage violation, which cannot be solved by the conventional method, such as those caused by boundaries on the fixed tap of PTs, boundaries of PV introduction, and a large number of houses. Moreover, the improvement on the voltage control performance of LVR is expected corresponding to various voltage fluctuations that varies depending on the weather condition.

References

[2-1] Z. Gu and D. T. Rizy, "Neural networks for combined control of capacitor banks and voltage regulators in distribution systems," *IEEE Trans. Power Deliv.*, vol. 11, no. 4, pp. 1921–1928, 1996.

[2-2] Ruey-Hsun Liang and Chen-Kuo Cheng, "Dispatch of main transformer ULTC and capacitors in a distribution system," *IEEE Trans. Power Deliv.*, vol. 16, no. 4, pp. 625–630, 2001.

[2-3] R. H. Liang and Y. S. Wang, "Fuzzy-Based Reactive Power and Voltage Control in a Distribution System," *IEEE Power Eng. Rev.*, vol. 22, no. 12, pp. 64–64, Dec. 2002.

[2-4] A. Kulmala, A. Mutanen, A. Koto, S. Repo, and P. Jarventausta, "Demonstrating coordinated voltage control in a real distribution network," in *2012 3rd IEEE PES Innovative Smart Grid Technologies Europe (ISGT Europe)*, 2012, pp. 1–8.

[2-5] T. Senjyu, Y. Miyazato, A. Yona, N. Urasaki, and T. Funabashi, "Optimal control of distribution voltage with coordination of distribution installations," in *2007 IEEE Power Engineering Society General Meeting*, 2007, pp. 1–7.

[2-6] T. Senjyu, Y. Miyazato, A. Yona, N. Urasaki, and T. Funabashi, "Optimal distribution voltage control and coordination with distributed generation," *IEEE Trans. Power Deliv.*, vol. 23, no. 2, pp. 1236–1242, Apr. 2008.

[2-7] J. M. Guerrero, M. Chandorkar, T.-L. Lee, and P. C. Loh, "Advanced control architectures for intelligent microgrids—part I: decentralized and hierarchical control," *IEEE Trans. Ind. Electron.*, vol. 60, no. 4, pp. 1254–1262, Apr. 2013.

[2-8] J. M. Guerrero, P. C. Loh, T.-L. Lee, and M. Chandorkar, "Advanced control architectures for intelligent microgrids—part II: power quality, energy storage, and AC/DC microgrids," *IEEE Trans. Ind. Electron.*, vol. 60, no. 4, pp. 1263–1270, Apr. 2013.

[2-9] S. Yoshizawa, Y. Yamamoto, Y. Hayashi, S. Sasaki, T. Shigeto, and H. Nomura, "Dynamic updating method of optimal control parameters of multiple advanced SVRs in a single feeder," *IEEJ Trans. Power Energy*, vol. 135, no. 9, pp. 550–558, Sep. 2015.

[2-10] Y. Zoka, N. Yorino, M. Watanabe, and T. Kurushima, "An optimal decentralized control for voltage control devices by means of a multi-agent system," in *2014 Power Systems Computation Conference*, 2014, pp. 1–8.

[2-11] N. Yorino, Y. Zoka, M. Watanabe, and T. Kurushima, "An optimal autonomous decentralized control method for voltage control devices by using a multi-agent system," *IEEE Trans. Power Syst.*, vol. 30, no. 5, pp. 2225–2233, Sep. 2015.

[2-12] M. M. Haque and P. Wolfs, "A review of high PV penetrations in LV distribution networks: Present status, impacts and mitigation measures," *Renew. Sustain. Energy Rev.*, vol. 62, pp. 1195–1208, 2016.

[2-13] A. Navarro-Espinosa and L. F. Ochoa, "Probabilistic impact assessment of low carbon technologies in LV distribution systems," *IEEE Transactions on Power Systems*, vol. 31, no. 3, IEEE, pp. 2192–2203, May-2015.

[2-14] M. Nijhuis, M. Gibescu, and S. Cobben, "Risk-based framework for the planning of low-voltage networks incorporating severe uncertainty," *IET Gener. Transm. Distrib.*, vol. 11, no. 2, pp. 419–426, Jan. 2017.

[2-15] M. Nijhuis, M. Gibescu, and S. Cobben, "Clustering of low voltage feeders form a network planning perspective," *23 rd Int. Conf. Electr. Distrib.*, vol. Paper 0680, no. June, 2015.

[2-16] V. Rigoni, L. F. Ochoa, G. Chicco, A. Navarro-Espinosa, and T. Gozel, "Representative residential LV feeders: A case study for the North West of England," *IEEE Trans. Power Syst.*, vol. 31, no. 1, pp. 348–360, Jan. 2016.

[2-17] A. Navarro-Espinosa and L. F. Ochoa, "Increasing the PV hosting capacity of LV networks: OLTC-fitted transformers vs. reinforcements," in *2015 IEEE Power & Energy Society Innovative Smart Grid Technologies Conference (ISGT)*, 2015, pp. 1–5.

[2-18] N. Efkarpidis, T. De Rybel, and J. Driesen, "Optimal placement and sizing of active in-line voltage regulators in flemish LV distribution grids," *IEEE Trans. Ind. Appl.*, vol. 52, no. 6, pp. 4577–4584, 2016.

[2-19] M. Nijhuis, M. Gibescu, and J. F. G. Cobben, "Incorporation of on-load tap changer transformers in low-voltage network planning," in *2016 IEEE PES Innovative Smart Grid Technologies Conference Europe (ISGT-Europe)*, 2016, pp. 1–6.

[2-20] C. Long, A. T. Procopiou, L. F. Ochoa, G. Bryson, and D. Randles, "Performance of OLTC-based control strategies for LV networks with photovoltaics," in *2015 IEEE Power & Energy Society General Meeting*, 2015, pp. 1–5.

[2-21] A. T. Procopiou and L. F. Ochoa, "Voltage control in PV-rich LV networks without remote monitoring," *IEEE Trans. Power Syst.*, pp. 1–1, 2016.

[2-22] N. Takahashi, H. Kikusato, J. Yoshinaga, Y. Hayashi, S. Kusagawa, and N. Motegi, "Dynamic voltage control method and optimization for LVR in distribution system with PV systems," in *ISGT 2014*, 2014, pp. 1–4.

[2-23] C. Long and L. F. Ochoa, "Voltage control of PV-rich LV networks: OLTC-fitted transformer and capacitor banks," *IEEE Trans. Power Syst.*, vol. 31, no. 5, pp. 4016–4025, Sep. 2016.

[2-24] K. N. Bangash, M. E. A. Farrag, and A. H. Osman, "Smart Control of on Load Tap Changer deployed in Low Voltage Distribution Network," in *2015 4th International Conference on Electric Power and Energy Conversion Systems (EPECS)*, 2015, pp. 1–6.

[2-25] H. Kikusato *et al.*, "Coordinated voltage control of load tap changers in distribution networks with photovoltaic system," *IEEE PES Innov. Smart Grid Technol. Eur.*, 2016.

[2-26] "[Y. Hayashi], 'Development of distributed cooperative EMS methodologies for multiple scenarios by using versatile demonstration platform,' CREST." [Online]. Available: https://www.jst.go.jp/kisoken/crest/en/project/36/36_05.html. [Accessed: 28-Feb-2017].

Chapter 3
Method for rapidly determining voltage control parameters of LVR using classifiers

3.1 Introduction to this chapter

The LVR controls the voltage in situations where the uncertain fluctuation of PV output significantly affects the DSs. To handle the uncertainty, various forecasting methods for PV output and electricity load have been proposed [3-1]–[3-3]. In addition, various model predictive control scheme has been introduced in the supply side energy management [3-4]–[3-9]. Particularly, in [3-9], an upgraded voltage management scheme, which consists of forecast, operational plan, and control, has been studied. This scheme updates the voltage control parameters in a short period corresponding to the sequentially forecasted power profile. The updated control parameters should be determined within the limited time between end of forecasting phased and start of control phase. Therefore, to apply such model predictive control to the LVR operation, the voltage control parameters should be rapidly determined to meet for every updating.

In this chapter, we apply the upgraded voltage management scheme in [3-9] and propose a method for rapidly and accurately determining the control parameters of LDC method for the LVR as a part of an upgraded voltage management scheme. In the proposed method, solution candidates of the appropriate LDC parameters are selected with low computational cost by using classifiers that learns the relation between power series data and the appropriateness of LDC parameters. We performed numerical simulations to evaluate the validity from the viewpoints of computational time and classification accuracy for determination of the LDC parameters, and verified the voltage control performance of the proposed method.

3.2 Upgraded voltage management scheme using LVR

We apply the voltage management in [3-9] to the LVR to appropriately adjust the tap position to respond to the fluctuating PV output and electricity load. A scheme of the voltage management is shown in Fig. 3.1, which is composed of the following three phases:

- prediction, in which the future fluctuation of the load demand and PV output are estimated,
- operational plan, in which the appropriate control parameters are derived on the basis of the prediction results,
- control, in which the voltage is automatically controlled on the basis of the derived control parameters.

According to this scheme, we proposed the method for determining control parameters required for appropriate voltage control of the LVR. The important objective on the LVR operation is to satisfy the following requirements:

- adjusting the tap position that can stabilize the voltage within an prescribed range,
- avoiding extra tap changes in terms of the equipment life,
- deriving the control parameters quickly to reflect the reliable prediction results, which are slightly ahead, for control (shortening of the operation phase).

The main purpose of the LVR operation is to automatically adjust the tap position to maintain the voltage at all receiving ends ($\forall j \in \mathcal{J}$) in the LVDS. Although some control methods that satisfy this purpose are available, the LDC method described in 2.2.2 is implemented in the LVR. Equations (2.1), (2.4)–(2.6) indicate that a parameter set of the LDC method $\boldsymbol{\gamma}^{\mathrm{ldc}} = \{v^{\mathrm{ldc}}, l\}$ must be set properly to achieve an appropriate tap change. In the next section, a framework how to evaluate and determine the LDC parameter set $\boldsymbol{\gamma}^{\mathrm{ldc}} = \{v^{\mathrm{ldc}}, l\}$.

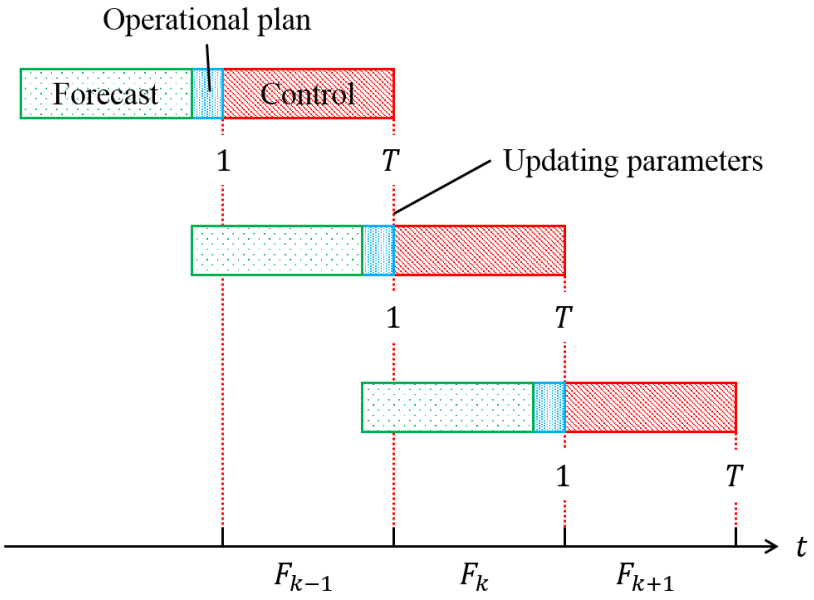

Fig. 3.1 Schematic image of the upgraded voltage management scheme, which consists of forecast, operational plan, and control.

3.3 Determination of LDC parameters for LVR

This section presents the method for determining the appropriate parameter set according to the voltage management scheme described in section 3.2. The appropriate parameter set is determined in each control phase F_k composed of $t = 1, \dots, T$ on the basis of the forecasted profile of PV output and electricity demand. Here, under the constraint condition that the voltage v_t^j at every LV receiving end $(\forall j \in \mathcal{J})$ is always maintained within the prescribed range, we define such parameter set as the appropriate parameter set that minimizes the number of LVR tap changes in order to extend the operation life, and maximize the voltage margin from the upper and lower limit in order to correspond to the uncertainty of forecasting. Regarding to the evaluation of maximizing the voltage margin, the highest and lowest voltage of all receiving ends and time steps are evaluated in order to focus on the worst point voltage closest to the limits. In the voltage management scheme in section 3.2, since the appropriateness of the parameter set depends on the initial tap value $s_{t=1}$, the appropriate parameter sets to all tap values $s \in \{1, \dots, P\}$ should be prepared by the beginning of the control phase F_k. The parameter set is finalized from the prepared parameter set corresponding to the tap value at the beginning of control phase F_k. Such parameter set $\boldsymbol{\gamma}_q^{\mathrm{ldc}}$ on each tap value can be achieved by considering the following problem at a suitable weight coefficient $\alpha > 0$:

For each tap value $s \in \{1, \dots, P\}$,

$$\boldsymbol{\gamma}_q^{\mathrm{ldc}} = \underset{\boldsymbol{\gamma}^{\mathrm{ldc}}}{\operatorname{argmin}} \left\{ \sum_{t=1}^{\mathrm{T}} \left| s_{t-1}\left(\boldsymbol{\gamma}^{\mathrm{ldc}}\right) - s_t\left(\boldsymbol{\gamma}^{\mathrm{ldc}}\right) \right| + \frac{\alpha}{\min\limits_{j \in \mathcal{J}, t} \left(v_t^j\left(\boldsymbol{\gamma}^{\mathrm{ldc}}\right) - v^{\mathrm{l}} \right) + \min\limits_{j \in \mathcal{J}, t} \left(v^{\mathrm{u}} - v_t^j\left(\boldsymbol{\gamma}^{\mathrm{ldc}}\right) \right)} \right\}, \tag{3.1}$$

$$\text{subject to } v^{\mathrm{l}} \le v_t^j\left(\boldsymbol{\gamma}^{\mathrm{ldc}}\right) \le v^{\mathrm{u}} \qquad (\forall j \in \mathcal{J}, t = 1, \cdots, T).$$

In this study, $\mathcal{L}$ and $\mathcal{V}$, which consist of a finite number of elements, are solved as the candidates of the above optimization problem.

The above framework can only be evaluated when the forecasted PV output and electricity load at $t = 1, \cdots, T$ are obtained. The PFC, whose scale and complexity vary with the power system configuration, is also required to evaluate the objective function. Therefore, the practical issue is how to solve the minimization problem in (3.1). Let $|\mathcal{L}|$ and $|\mathcal{V}|$ be the numbers of parameters in search ranges, $P \times |\mathcal{L}| \times |\mathcal{V}|$ times PFC is required. However, in the scheme introduced in 3.2, the parameter set must be determined online during the operational plan phase; between end of the forecasting phase and beginning of the control phase, so that the scalability to the size of LVDS and immediacy of optimization process are significant. In the next section, we propose a method that uses classifiers that learn the appropriateness of the parameters for a given forecasted PV output and electricity load from the previous data to instantly derive either an optimized or a suboptimized solution for such problems.

The proposed method combines the PFC [3-10], whose evaluation accuracy is high though calculation time is not fast, and the classifiers [3-11], [3-12], whose evaluation accuracy is not high though calculation time is rapid, to achieve the rapid and accurate determination of parameters (Fig. 3.4).

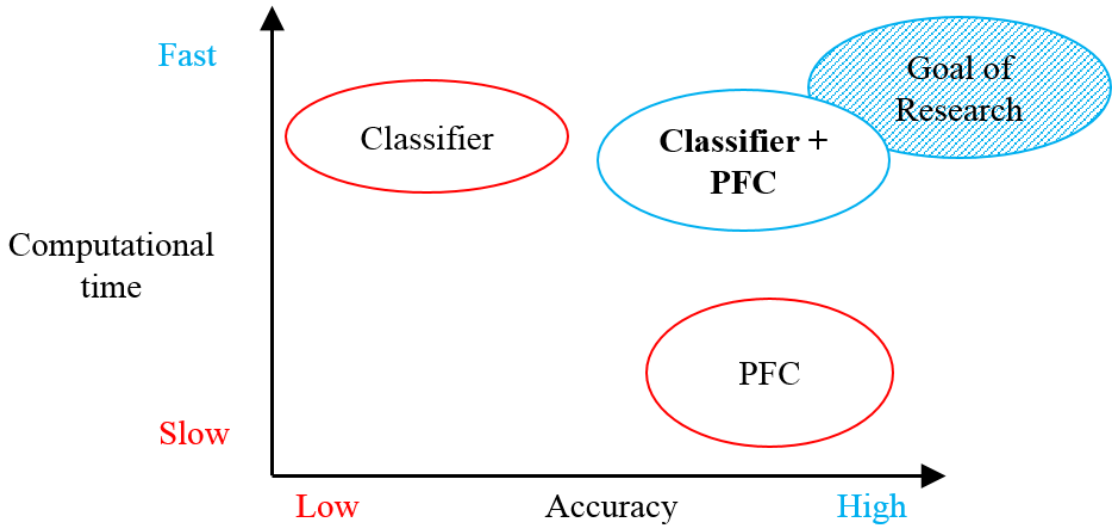

Fig. 3.2 Comparison of conventional and proposed method for determining LDC parameter set.

3.4 Method for determining LDC parameters using classifiers

A method for rapidly and accurately determining the appropriate parameter set is proposed in this section. The proposed method rapidly narrows the candidate of the appropriate parameters on the basis of the classification probability derived by classifiers. In addition, it strictly evaluates the narrowed parameters candidates by the PFC (Fig. 3.2).

The narrowing by the classifier is divided into two processes, learning and classifying. First, the classifier is learned offline in advance to determine whether the parameter set $\boldsymbol{\gamma}^{\mathrm{ldc}}$ is appropriate to the past-accumulated data of the PV output and electricity load. Let $J = |\mathcal{J}|$ be the number of customers in the LVDS, the input for classification is the $J \times T$ -dimensional time series data $\boldsymbol{x} = (x_{1,1}, \dots, x_{1,T}, x_{2,1}, \dots, x_{J,T})$, which consists of a power balance (PV output – electricity load) of J customers in the LVDS at each time $t = 1, \dots, T$. When the N -input data $\{\boldsymbol{x}^n = (x_{1,1}^n, \dots, x_{1,T}^n, x_{2,1}^n, \dots, x_{J,T}^n); n = 1, \dots, N\}$ are applied to each parameter set $\boldsymbol{\gamma}^{\mathrm{ldc}}$ for learning process, the following classification function $G_{\boldsymbol{\gamma}^{\mathrm{ldc}}}$ and classification probability are built in each parameter set:

For each tap value $s \in \{1, \dots, P\}$,

$$G_{\boldsymbol{\gamma}^{\mathrm{ldc}}}: \boldsymbol{x} \to y_{\boldsymbol{\gamma}^{\mathrm{ldc}}} \in \{-1, 1\}, \tag{3.2}$$

$$P_{\boldsymbol{\gamma}^{\mathrm{ldc}}}\left(y_{\boldsymbol{\gamma}^{\mathrm{ldc}}} = 1 | \boldsymbol{x}\right) \in [0, 1]. \tag{3.3}$$

where $y_{\boldsymbol{\gamma}^{\mathrm{ldc}}}$ is an output of the classification that becomes 1 when (3.1) is solved and the parameter set $\boldsymbol{\gamma}^{\mathrm{ldc}}$ is optimal and it becomes -1 in other cases. In this study, we focus on support vector machine

(SVM) [3-13], random forest (RF) [3-14], and a combination method of SVM and RF, although some typical approaches for building a binary classification function based on the accumulated data are available [3-15], [3-16].

The basic concept of each method is presented below. Additionally, we apply these methods to narrow the choice of resolution candidates by majority vote to improve the accuracy of the classification because the use of only one method cannot always achieve highly accurate classification. In 3.4.1–3.4.3, we explain methods for classifying the parameter set and deriving the classification probability in each approach when the input data aggregate $\{\boldsymbol{x}^n\}$ and the corresponding output data aggregate $\left\{y^n_{\boldsymbol{\gamma}^{\mathrm{ldc}}} \in \{-1,1\}; n = 1, \dots, N\right\}$.

After the narrowing, in online operation phase, the appropriateness of each parameter set to the forecasted power profile $\boldsymbol{x}$ is evaluated on the basis of the classification function $G_{\boldsymbol{\gamma}^{\mathrm{ldc}}}$ that has learned the relation past-accumulated power data and the appropriateness of parameter set. Since the appropriateness of parameter set to the past data has been learned offline, the appropriateness of parameter set to the forecasted data can be classified without carrying out the PFC. In addition, this results in the rapid classification without depending on the size of LVDSs. Then, following the flowchart in Fig. 3.3, the parameter sets whose classification probability $P_{\boldsymbol{\gamma}^{\mathrm{ldc}}}$ is included in the Cth highest are precisely evaluated in terms of the optimization problem (3.1). The parameter sets that minimize the objective function is finally selected in each initial tap. The narrowing based on the classification probability can significantly reduce the number of PFCs and accurately determine parameter sets.

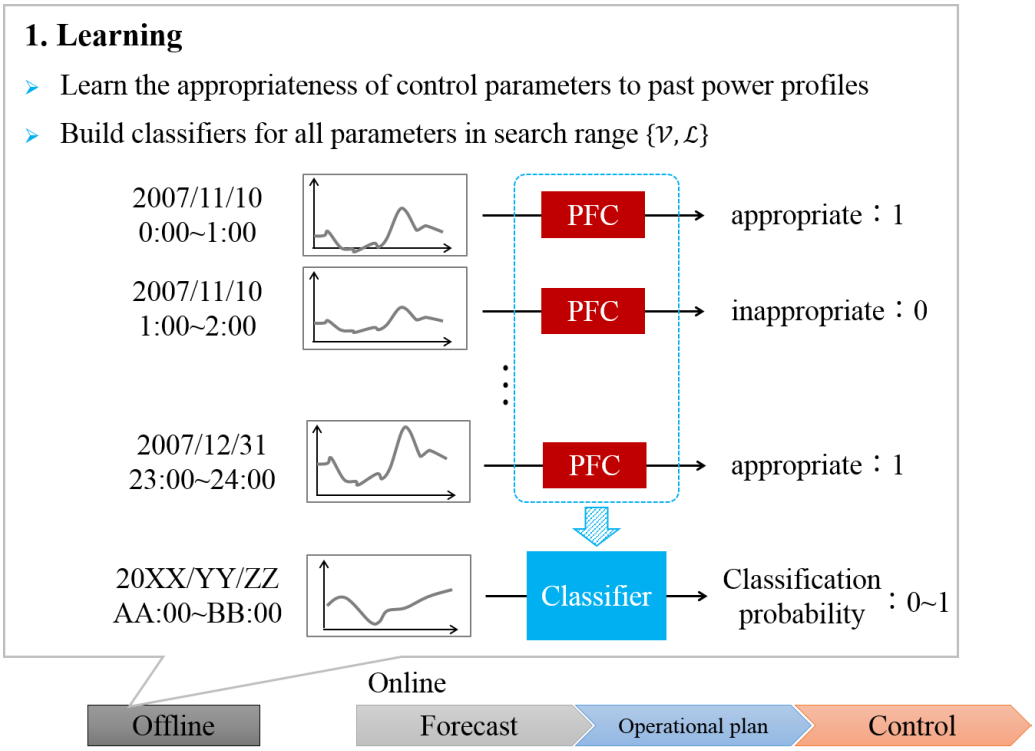

(a) Learning

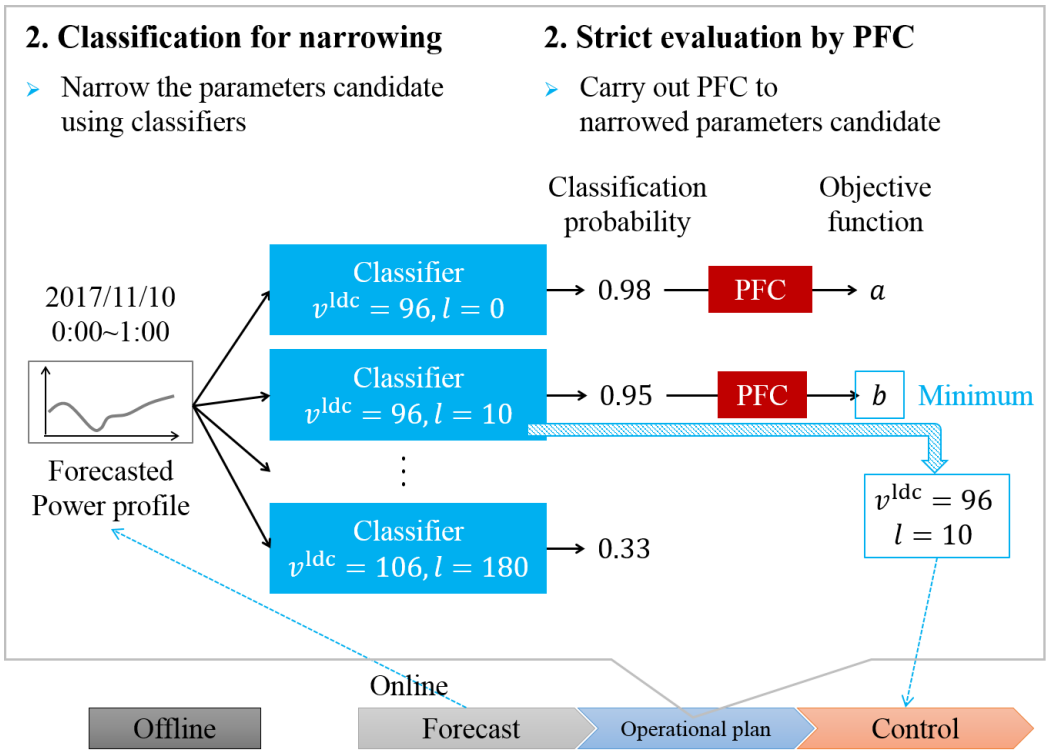

(b) Classification and strict evaluation

Fig. 3.3 Schematic image of proposed method based on classification.

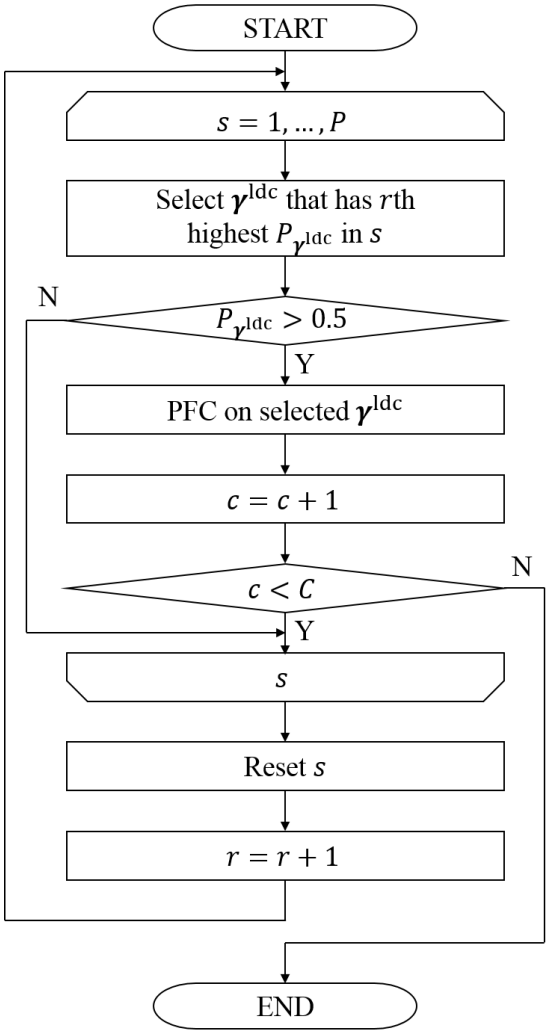

Fig. 3.4 Flowchart of PFC after narrowing solution candidates by the classifier [3-17].

3.4.1 Support vector machine

An SVM is known as a typical approach to no-linear binary classification problems. In this study, the formulation of the following classification function is presented (Fig. 3.4):

$$G_{\boldsymbol{\gamma}^{\mathrm{ldc}}}(\boldsymbol{x}) = h\left(f_{\boldsymbol{\gamma}^{\mathrm{ldc}}}(\boldsymbol{x})\right), \tag{3.4}$$

where $h(\cdot)$ and $f_{\boldsymbol{\gamma}^{\mathrm{ldc}}}(\boldsymbol{x})$ is shown as following functions:

$$h(z) = \begin{cases} -1 & \text{if } z \leq 0 \\ 1 & \text{if } z > 0, \end{cases} \tag{3.5}$$

$$f_{\boldsymbol{\gamma}^{\mathrm{ldc}}}(\boldsymbol{x}) = \sum_{n} \hat{a}_n K(\boldsymbol{x}, \boldsymbol{x}^{\boldsymbol{n}}) + \hat{b}. \tag{3.6}$$

$K(\boldsymbol{x}, \boldsymbol{x}^{n})$ is a function called ad kernel used to describe the similarity in the dimensions where the nonlinear conversion between the two $J \times T$-dimensional vectors $\boldsymbol{x}$ and $\boldsymbol{x}^{n}$ is performed. In this study, the following Gaussian kernel is used:

$$K(\boldsymbol{x}, \boldsymbol{x}') = \exp\left(-\frac{\|\boldsymbol{x} - \boldsymbol{x}'\|_2^2}{\sigma^2}\right). \tag{3.7}$$

In addition, $\{\hat{a}_n; n = 1, \cdots, N\}$ and $\hat{b}$ in (3.6) are described as a solution for the following optimization problem:

$$\begin{aligned}\left\{\{\hat{a}_n\}, \hat{b}\right\} = \underset{\{\hat{a}_n\}, \hat{b}}{\operatorname{argmin}} \frac{1}{2}\sum_{nn'} a_n a_{n'} K\left(\boldsymbol{x}^n, \boldsymbol{x}^{n'}\right) \\ + c\sum_n \max\left\{1 - y^n_{\boldsymbol{\gamma}^{\mathrm{ldc}}}\left(\sum_{n'} a_{n'} K\left(\boldsymbol{x}^{n'}, \boldsymbol{x}^n\right) + b\right), 0\right\}.\end{aligned} \tag{3.8}$$

The classification probability is defined as the following sigmoid function:

$$P_{\boldsymbol{\gamma}^{\mathrm{ldc}}}\left(y_{\boldsymbol{\gamma}^{\mathrm{ldc}}} = 1 | \boldsymbol{x}\right) = \frac{1}{1 + \exp\left(A f_{\boldsymbol{\gamma}^{\mathrm{ldc}}}(\boldsymbol{x}) + B\right)}. \tag{3.9}$$

When the output of the classification is given as $f^n_{\boldsymbol{\gamma}^{\mathrm{ldc}}} = f_{\boldsymbol{\gamma}^{\mathrm{ldc}}}(\boldsymbol{x}^n)$ and the target probability is given as

$$q^n_{\boldsymbol{\gamma}^{\mathrm{ldc}}} = \frac{y^n_{\boldsymbol{\gamma}^{\mathrm{ldc}}} + 1}{2}, \tag{3.10}$$

The parameters A and B are determined to solve the following optimization problem on the basis of learning data set $\left\{\left(f^n_{\boldsymbol{\gamma}^{\mathrm{ldc}}}, q^n_{\boldsymbol{\gamma}^{\mathrm{ldc}}}\right); n = 1, \ldots, N\right\}$:

$$\min -\sum_n \left\{q^n_{\boldsymbol{\gamma}^{\mathrm{ldc}}} \log\left(p^n_{\boldsymbol{\gamma}^{\mathrm{ldc}}}\right) + \left(1 - q^n_{\boldsymbol{\gamma}^{\mathrm{ldc}}}\right) \log\left(1 - p^n_{\boldsymbol{\gamma}^{\mathrm{ldc}}}\right)\right\}, \tag{3.11}$$

where

$$p^n_{\boldsymbol{\gamma}^{\mathrm{ldc}}} = \frac{1}{1 + \exp\left(A f^n_{\boldsymbol{\gamma}^{\mathrm{ldc}}}(\boldsymbol{x}) + B\right)}. \tag{3.12}$$

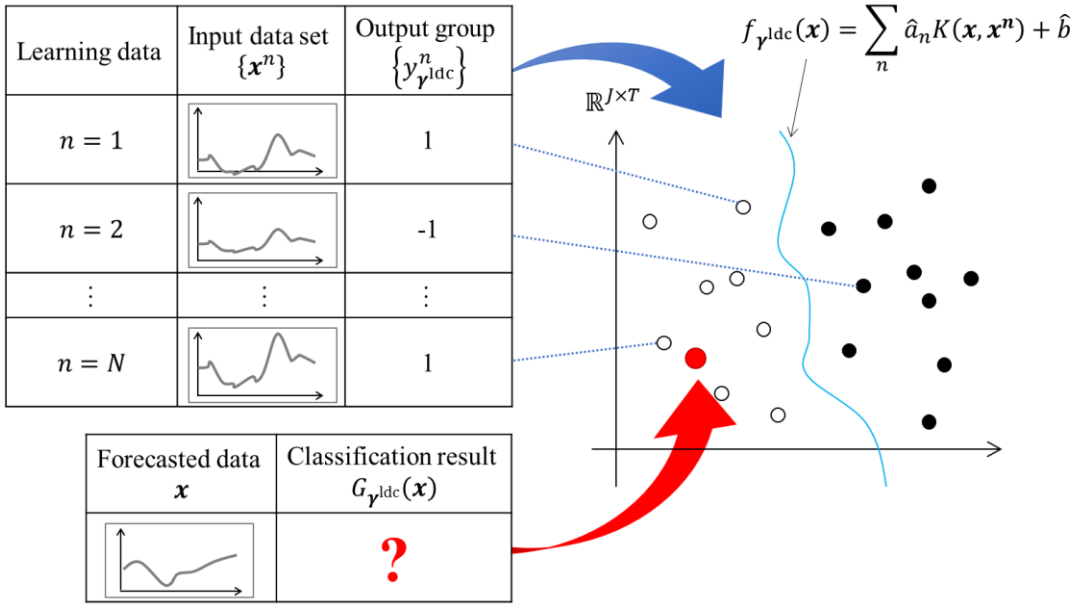

Fig. 3.5 Classification based on SVM.

3.4.2 Random forest

An RF is a type of ensemble learning that generates a plurality of classifiers called a decision tree by choosing the data and dimensions from the set of N $J \times T$-dimensional vector data (Fig. 3.5).

In the decision tree for binary classification, a threshold d is set well when we focus on a certain dimension (j,t) of the input data set $\{\boldsymbol{x}^n\}$. Consequently, the $J \times T$-dimensional feature quantity area of the input $\boldsymbol{X} \in \mathbb{R}^{J\times T}$ is separated into two areas, $\boldsymbol{X}_1 = \{\boldsymbol{X}|x_{j,t} \le d\}$ and $\boldsymbol{X}_2 = \{\boldsymbol{X}|x_{j,t} > d\}$, in order that the corresponding output group $\left\{y^n_{\boldsymbol{\gamma}^{\mathrm{ldc}}}\right\}$ in each area can be preferably separated by 1 or -1. The same process is conducted repetitively for the included input data sets in each area. By replicating this process, a multistep classifier having a tree structure is obtained. The terminations corresponding to the leaves are focused for the new data $\boldsymbol{x}$, and the following classification is performed on the basis of the learning data that belong to the ith leaf that expresses the area $\boldsymbol{X}_i \ni \boldsymbol{x}$, including $\boldsymbol{x}$:

$$\bar{G}_{\boldsymbol{\gamma}^{\mathrm{ldc}}}(\boldsymbol{x}) = h\left(\sum_{\boldsymbol{x}^n \in \boldsymbol{X}_i} y^n_{\boldsymbol{\gamma}^{\mathrm{ldc}}}\right). \tag{3.13}$$

In the RF, the subset initially consists of $N'(< N)$ input–output relationships randomly extracted from N learning data sets. Second, a new data set $\bar{\mathcal{D}} = \left\{\left(\bar{\boldsymbol{x}}^n, y^n_{\boldsymbol{\gamma}^{\mathrm{ldc}}}\right); \bar{\boldsymbol{x}}^n \in \mathbb{R}^S, n = 1, \cdots, N'\right\}$ is created by randomly extracting only $S(< J \times T)$ dimensions from the $J \times T$-dimensional data of each input. In this manner, the randomly created data sets $\{\bar{\mathcal{D}}^m; \mathrm{m} = 1, \cdots, M\}$ are prepared, and discriminations are performed on each data set by the decision trees. The basic approach of the RF is to perform the following final discrimination using the majority vote of the obtained results:

$$G_{\boldsymbol{\gamma}^{\mathrm{ldc}}}(\boldsymbol{x}) = h\left(\sum_m \bar{G}^m_{\boldsymbol{\gamma}^{\mathrm{ldc}}}(\boldsymbol{x})\right), \tag{3.14}$$

where $\bar{G}^m_{\boldsymbol{\gamma}^{\mathrm{ldc}}}$ represents the classifier based on the decision tree in (3.13) learned on the basis of $\bar{\mathcal{D}}^m$. From (3.13) and (3.14), the RF improves the generalization ability using the majority vote on the basis of the results of the various weak classifiers. The various weak classifiers are created to randomly extract different subsets, which consist of different combinations of partial variates and case study sets in the data. Here, the classification probability is defined as the following value:

$$P_{\boldsymbol{\gamma}^{\mathrm{ldc}}}\left(y_{\boldsymbol{\gamma}^{\mathrm{ldc}}} = 1|\boldsymbol{x}\right) = \frac{1}{M}\sum_m \frac{h\left(\bar{G}^m_{\boldsymbol{\gamma}^{\mathrm{ldc}}}(\boldsymbol{x})\right) + 1}{2}. \tag{3.15}$$

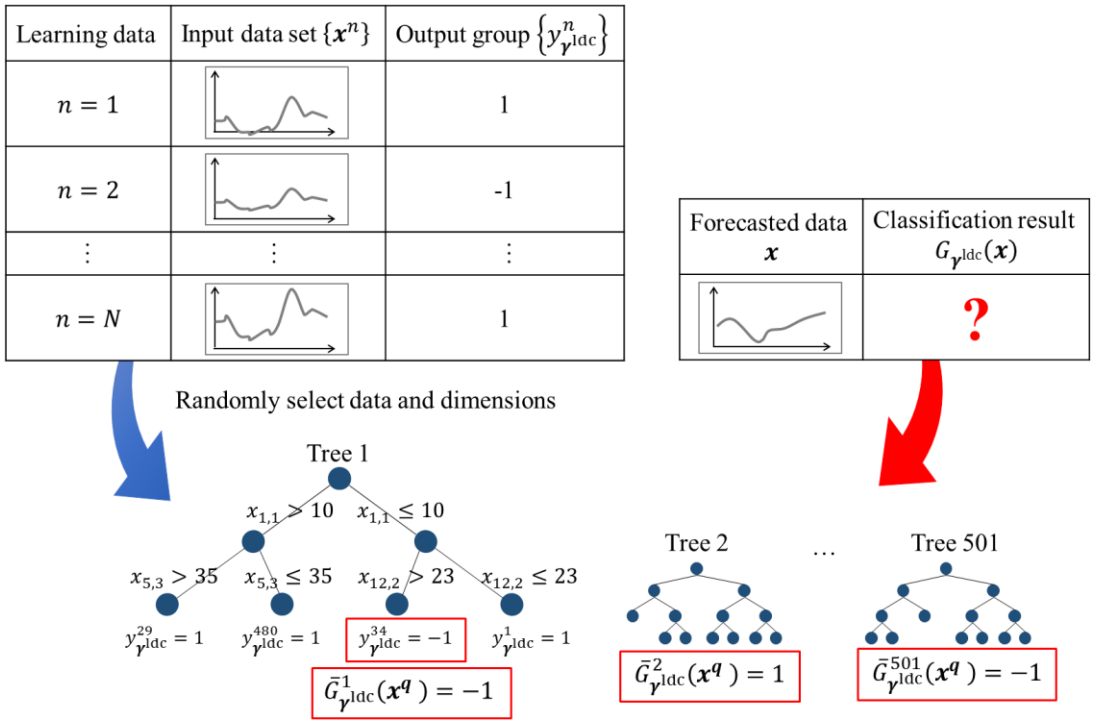

Fig. 3.6 Classification based on RF.

3.4.3 Multiple classifiers

More accurate classification results could be obtained to combine multiple classifiers. Therefore, we suggest the following classification probability combining the classification probabilities of the SVM and RF described in (3.12) and (3.15):

$$P_{\boldsymbol{\gamma}^{\mathrm{ldc}}}\left(y_{\boldsymbol{\gamma}^{\mathrm{ldc}}}=1|\boldsymbol{x}\right)=\begin{cases}\dfrac{P_{\boldsymbol{\gamma}^{\mathrm{ldc}}}^{SVM}+P_{\boldsymbol{\gamma}^{\mathrm{ldc}}}^{RF}}{2} & \text{if } P_{\boldsymbol{\gamma}^{\mathrm{ldc}}}^{SVM}>0.5 \text{ and } P_{\boldsymbol{\gamma}^{\mathrm{ldc}}}^{RF}>0.5\\ 0 & \text{otherwise}\end{cases}, \tag{3.16}$$

where $P_{\boldsymbol{\gamma}^{\mathrm{ldc}}}^{SVM}$ and $P_{\boldsymbol{\gamma}^{\mathrm{ldc}}}^{RF}$ are the classification probabilities based on the SVM and RF.

3.5 Numerical simulation

To verify the validity of the proposed method in terms of the determination accuracy, the computation time required for determining the parameter set, and voltage control performance using the determined parameter set, we carried out numerical simulation using an LVDS model shown in Fig. 3.6, which includes an LVR and 29 LV consumers with PVs. In the simulation, the following methods for determining the parameter set are compared:

- evaluation of the optimization problem by carrying out PFCs of all solution candidates;
- use of the classifiers (SVM, RF, multiple classifiers: SVM+RF) without carrying out a PFC; and
- narrowing of the solution candidates by the classifiers before carrying out a PFC, which is the proposed method.

Table 3.1 lists the simulation setup, including some dominant parameters. A period of control phase is set one hour; the control parameter set is updated every one hour. In addition, we prepared 51-day actual measurement of PV output and electricity load with a time step of 10 s in each 29 house. The example data for two days are shown in Fig. 3.7. 31-day data set is used for evaluation of the methods. 20-day data set is divided into one-hour data and used as a training data for building the classifier $G_{\boldsymbol{\gamma}^{\mathrm{ldc}}}$. The forecasted power profile $\boldsymbol{x}$ used to determine the parameter set does not contain any forecasting errors.

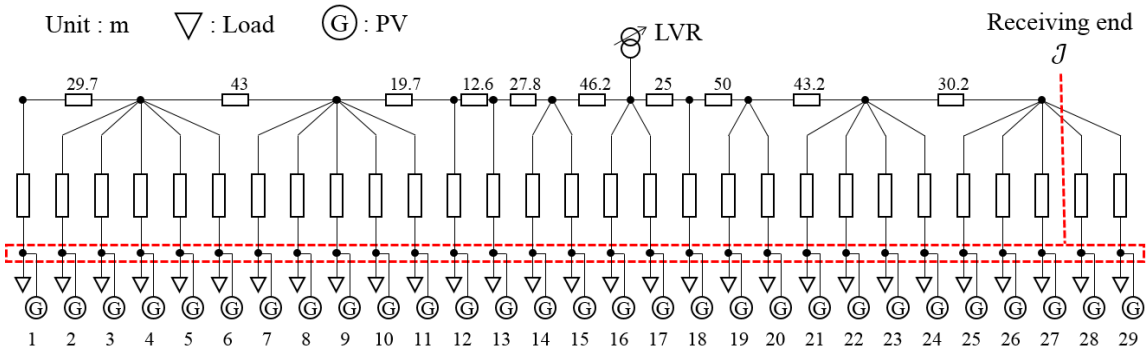

Fig. 3.7 LVDS model with LVR and PVs [3-18].

Table 3.1 Simulation setup.

LVR	Rated capacity	75 kVA
	Rated primary voltage	6.6 kV
	Rated secondary voltage	105 V
	Tap value	s={1, 2, 3, 4, 5}
	(primary voltage)	(6.9, 6.75, 6.6, 6.45, 6.3 kV)
LDC method	Parameters search range	$\mathcal{L}$={0,10, …, 180 m}
		$\mathcal{V}$={96, 97, …, 106 V}
	Dead band	ε=1.5 %
LVDS condition	Impedance of LV main line	0.2526+j0.3485 Ω/km
	Prescribed voltage range	95–107 V
Conversion factor in (3.1)	α=0.01	
Number of PFCs for the proposed method	C=5	

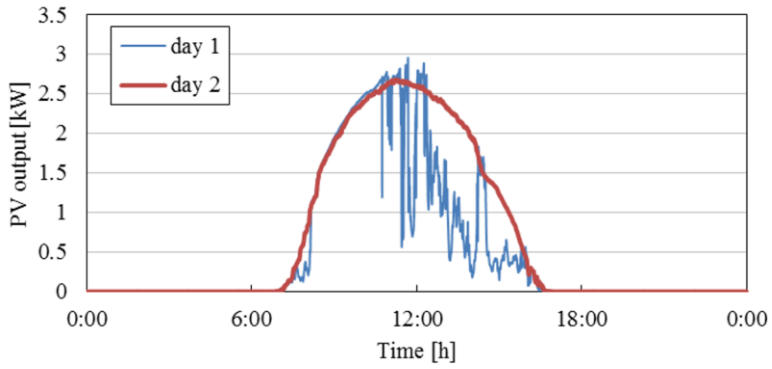

(a) PV output

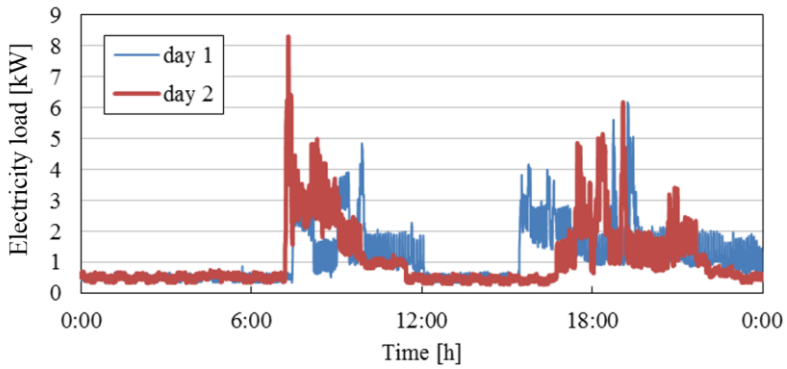

(b) Electricity load

Fig. 3.8 Example power profiles for 2 days [3-17].

Fig. 3.7 shows average accuracy of the parameters determination for 31 days. Let $\{l, v^{\mathrm{ldc}}\}^k$ be the LDC parameters finally used in control phase F_k and $\{\mathcal{L}', \mathcal{V}'\}_{PFC}^k$ be the set of solutions obtained by the PFC, where $\mathcal{L}' \leq \mathcal{L}, \mathcal{V}' \leq \mathcal{V}$, the average accuracy, which evaluates whether the parameters $\{l, v^{\mathrm{ldc}}\}^k$ are included in the set of solutions $\{\mathcal{L}', \mathcal{V}'\}_{PFC}^k$, is described as following:

$$\text{Accuracy} = \left\{ \frac{1}{24} \sum_{k=1}^{24} \delta\left(\{l, v^{\mathrm{ldc}}\}^k, \{\mathcal{L}', \mathcal{V}'\}_{PFC}^k \right), \right. \tag{3.17}$$

where

$$\delta\left(\{l, v^{\mathrm{ldc}}\}^k, \{\mathcal{L}', \mathcal{V}'\}_{PFC}^k \right) = \begin{cases} 1 & \text{if } \{l, v^{\mathrm{ldc}}\}^k \in \{\mathcal{L}', \mathcal{V}'\}_{PFC}^k. \\ 0 & \text{otherwise} \end{cases} \tag{3.18}$$

The result in Fig. 3.7 shows the accuracies of the proposed methods (classifier +PFC) are higher than only using the classifier (SVM, RF, SVM+RF). Further, the accuracy of the proposed methods is always greater than 0.9. The values suggest that exactly evaluating the parameter candidates by the PFC after narrowing the parameter candidates by the classifier can exclude inappropriate parameters that are classified as the appropriate parameters by the classifier. Moreover, the accuracy of SVM+RF+PFC is particularly higher than the others, thereby, it is considered that the classification using multiple classifiers can result in the accurate narrowing in the classification process. In the narrowed areas of parameters candidates, whose classification probabilities is larger than 0.5 ($P_{\boldsymbol{\gamma}^{\mathrm{ldc}}} > 0.5$), on each classifier SVR and RF, $P_{\boldsymbol{\gamma}^{\mathrm{ldc}}}$ gradually decreases toward the boundary of the area. Although there is large difference between the narrowed areas of SVM and RF, the classification probability $P_{\boldsymbol{\gamma}^{\mathrm{ldc}}}$ becomes close to 0.5 around the boundary of narrowed area. Therefore, accurate narrowing is achieved around the boundary by using the multiple classifiers based on (3.16).

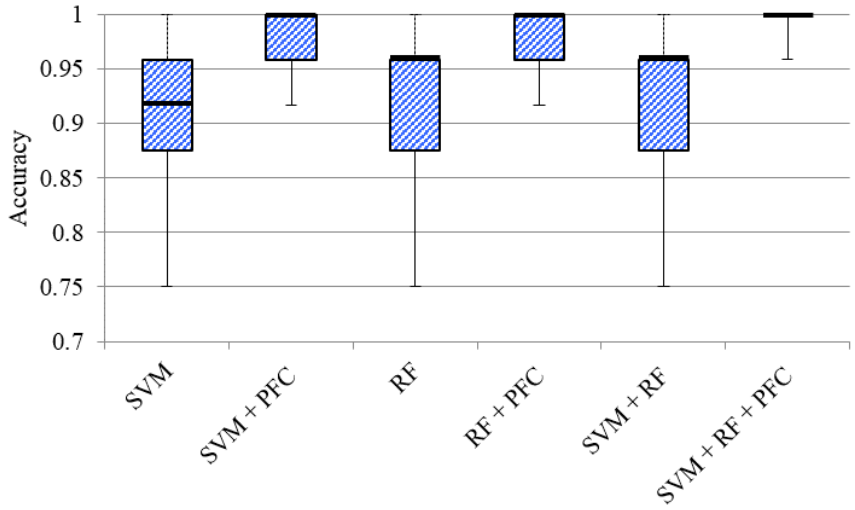

Fig. 3.9 Accuracy of parameters determination [3-17].

Fig. 3.9 shows the relative computation time for determining the appropriate parameter set for every initial tap value. The results suggest that the computation times of using the classifier and classifier +PFC are much shorter than the PFC because the former methods avoid the large number of PFCs requiring a large computational cost. Particularly in RF, the computation time is significantly shorter than the others. Furthermore, we can verify that the increase in computation time due to the several PFCs in the RF+PFC method is not a serious problem.

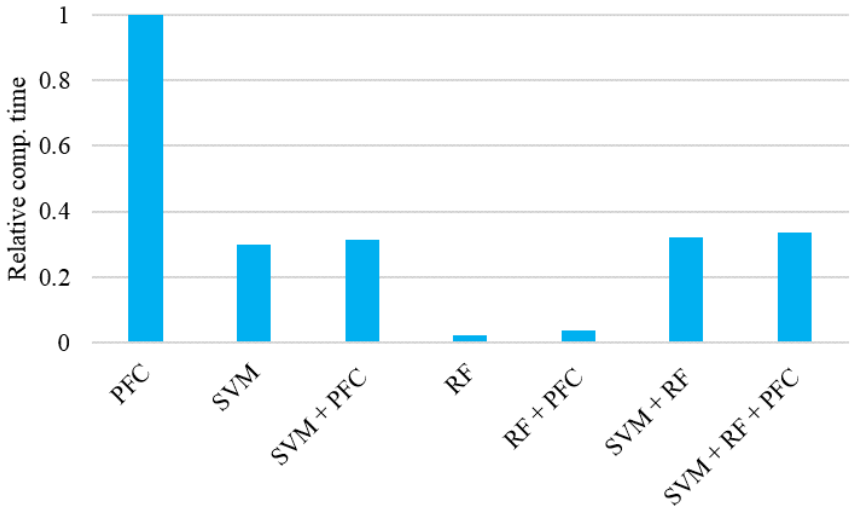

Fig. 3.10 Relative computation time required for determining appropriate parameters [3-17].

Fig. 3.10 shows the number of days in which the voltage is maintained within the prescribed range when voltage control is performed using the parameter set determined by each method. The proposed method (classifier +PFC) can maintain the voltage for 30 days, which is almost equivalent to the PFC method. On the other hand, the number of days that the classifier method can maintain the voltage is much less than the proposed method, and the difference is more notable than that of the accuracy. This result suggests that even one classification error when maintaining the voltage produces a worse voltage control result, although this affects the parameters determination accuracy very little.

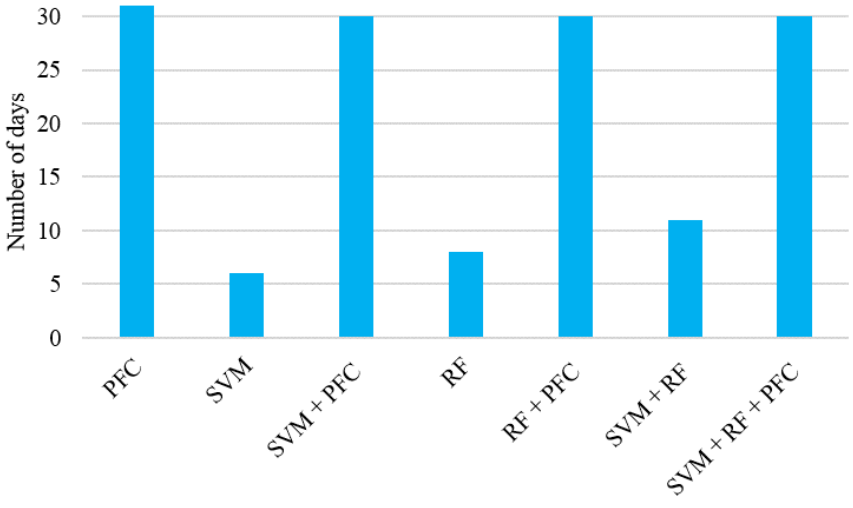

Fig. 3.11 Number of days without voltage violation [3-17].

The number of the average tap changes for 30 days when the proposed methods (classifier +PFC) can maintain the voltage is shown is Fig. 3.11. The proposed methods obtain similar results as the PFC method. From the results above, the proposed method can rapidly and accurately determine the parameters, and the validity of the proposed method is verified.

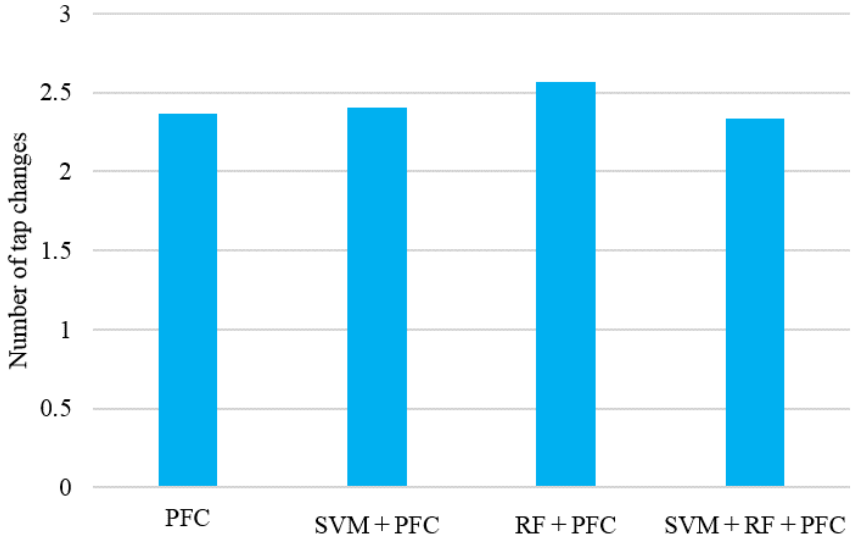

Fig. 3.12 Average number of tap changes for 30 days when four methods maintain the voltage within prescribed range [3-17].

3.6 Summary of this chapter

In this chapter, we proposed a method for rapidly and accurately determining the LDC control parameter set by narrowing the solution candidates using an classifiers before solving the optimization problem. Learning the relationship between the power series data and the control parameters on the basis of the past data and classifying the solution narrowed the solution candidates in the proposed method. As a result, the computational cost for determining the parameters was reduced because the number of PFCs necessary for evaluating the objective function was reduced. By comparing the voltage control results using the proposed method with the method using a PFC that can obtain the optimal solution in terms of the number of the voltage violation days and the number of LVR tap changes, the proposed method achieved equivalent voltage control performance. This work is significant because the rapid determination of the control parameters could lead to an increase in the forecasting accuracy. In addition, high-performance voltage control leads to maximum utilization of PV power.

References

[3-1] C. W. Chow *et al.*, "Intra-hour forecasting with a total sky imager at the UC San Diego solar energy testbed," *Sol. Energy*, vol. 85, no. 11, pp. 2881–2893, 2011.

[3-2] R. Weron, *Modeling and Forecasting Electricity Loads and Prices: A Statistical Approach*. Wiley Finance, 2006.

[3-3] H. T. C. Pedro and C. F. M. Coimbra, "Assessment of forecasting techniques for solar power production with no exogenous inputs," *Sol. Energy*, vol. 86, no. 7, pp. 2017–2028, 2012.

[3-4] L. Jin, R. Kumar, and N. Elia, "Model predictive control-based real-time power system protection schemes," *IEEE Trans. Power Syst.*, vol. 25, no. 2, pp. 988–998, May 2010.

[3-5] B. Houska, H. J. Ferreau, and M. Diehl, "ACADO toolkit-an open-source framework for automatic control and dynamic optimization," *Optim. Control Appl. Methods*, vol. 32, no. 3, pp. 298–312, 2011.

[3-6] R. R. Negenborn and J. M. Maestre, "Distributed model predictive control: an overview and roadmap of future research opportunities," *IEEE Control Syst.*, vol. 34, no. 4, pp. 87–97, Aug. 2014.

[3-7] A. Parisio, E. Rikos, G. Tzamalis, and L. Glielmo, "Use of model predictive control for experimental microgrid optimization," *Appl. Energy*, vol. 115, pp. 37–46, 2014.

[3-8] Y. Hayashi, "Japanese energy management in smart grid after the Great East Japan Earthquake," *IEEJ Trans. Power Energy*, vol. 133, no. 3, pp. 225–228, Mar. 2013.

[3-9] Y. Fujimoto *et al.*, "Distributed energy management for comprehensive utilization of residential photovoltaic outputs," *IEEE Trans. Smart Grid*, pp. 1–13, 2016.

[3-10] H. Kikusato, N. Takahashi, J. Yoshinaga, Y. Hayashi, S. Kusagawa, and N. Motegi, "A method for determining the optimal parameters for LDC in distribution system with PV (in Japanese)," in *National Convention of IEEJ 2013*, 2013, pp. 414–415.

[3-11] H. Kikusato *et al.*, "Method for determining line drop compensator parameters of low voltage regulator using support vector machine," in *ISGT 2014*, 2014, pp. 1–5.

[3-12] Y. Fujimoto *et al.*, "判別器を用いたLVRにおけるLDC制御パラメタの高速導出手法 (in Japanese)," in 計測自動制御学会システム・情報部門学術講演会講演論文集, 2013, vol. 2013, p. ROMBUNNO.SS9-8.

[3-13] J. C. Platt, "Probabilistic outputs for support vector machines and comparisons to regularized kikelihood methods," *Adv. LARGE MARGIN Classif.*, pp. 61–74, 1999.

[3-14] L. Breiman, "Random Forests," *Mach. Learn.*, vol. 45, no. 1, pp. 5–32, 2001.

[3-15] C. M. Bishop, *Pattern recognition and machine learning*. Springer, 2006.

[3-16] K. P. Murphy, *Machine learning : a probabilistic perspective*. MIT Press, 2012.

[3-17] H. Kikusato *et al.*, "Method for rapidly determining line drop compensator parameters of low-voltage regulator using classifiers," *IEEJ Trans. Power Energy*, vol. 135, no. 7, pp. 446–453, Jul. 2015.

[3-18] H. Kikusato *et al.*, "Method for determining line drop compensator control parameters of low-voltage regulator using random forest," *Appl. Mech. Mater.*, vol. 799–800, pp. 1299–1305, Oct. 2015.

Chapter 4
EV charging management using auction mechanism for reducing PV curtailment in LVDSs

4.1 Introduction of this chapter

PV curtailment is carried out to maintain the power supply-demand balance [4-1] when PV output exceeds electricity consumption with minimum thermal power generation in the power system, and to avoid overvoltage from the prescribed voltage upper limit in the DS with intensive PV penetration [4-2]; the former is addressed to coordinate the supply-demand balance among whole grid scale, while the latter can be prevented by mitigating voltage rise in the DS. The reduction of the PV curtailment is an important issue to achieve maximum utilization of the penetrated PV power. It can be an alternative to power sources with high fuel cost in the supply side and can reduce the residential operation cost in demand side. We consider several approaches to mitigate voltage rise in the DS from the viewpoint of both the supply and the demand sides. In the supply side, OLTCs and BESSs are used to control the voltage in the DS. The solution in the supply side would be costly because such voltage control schemes require investment in additional apparatuses and communication network.

On the other hand, in the demand side, voltage rise could be avoided to increase the self-consumption of the PV output by utilizing controllable loads in the households, such as EV, residential BESS, and HPWH. Particularly, EVs are expected to be a core of the promising controllable loads, since they will be penetrated largely owing to the prohibition of selling gasoline and diesel cars proposed in some countries. The controllable loads contribute to increase the self-consumption of the PV output by shifting their electricity consumption to mid-day when the PV output would be curtailed.

Various approaches have been proposed in the supply side to mitigate voltage rise caused by PV penetration and to reduce PV curtailment. Although the simplest solution in the supply side is grid reinforcement, it is more expensive than other schemes such as [4-3], [4-4]. Another possible approach is voltage control scheme using OLTCs [4-5]–[4-8]. Voltage control using MV OLTCs has been improved to implement a centralized control scheme [4-5], which requires an enhanced communication infrastructure. The LV OLTCs are deployed in LVDSs with voltage violation that cannot be avoided by the MV OLTCs [4-6]–[4-8]. Another technique to mitigate the overvoltage problem is the method of voltage control using BESS deployed in the supply side [4-9], [4-10]. The BESS could be used for other objectives as well, such as the coordination of the supply-demand balance [4-9] and cost reduction in EV charging facilities [4-10], as well as voltage control. A main advantage of these approaches is that the supply side can operate the devices only for the most convenient way to achieve its objectives; however, additional investment is required in the supply side.

Another effective approach for mitigation of voltage rise and reduction of PV curtailment are based on utilization of the customers' controllable loads, such as the EV, residential BESS, and HPWH; these

loads contribute to increase the self-consumption of the PV output by shifting their operation time. Such a demand side management scheme can reduce PV curtailment without additional investment (or with minimal investment) in the supply side solutions. In this case, customers' benefits of their contribution in mitigating voltage rise, such as reduction of residential operation cost and acquisition of economic incentive, should be provided. For example, the operation scheme of the HPWH proposed in [4-11] reduces PV curtailment by increasing the self-consumption of the PV output in peak periods. The residential operation cost of customers who carry out the load shift of HPWHs can be reduced because the electricity purchased for the HPWH operation is replaced by the self-consumed PV output that would be curtailed. There also have been proposed several voltage control methods based on the residential BESS [4-12]–[4-14]. Although the voltage violation caused by the PV penetration will be mitigated by these methods, the benefits to the customers for contributing to voltage control was not discussed explicitly. The EV can be utilized for the load shift as well though the EVs are originally introduced for travel. According to the literature [4-15], most EVs are parked almost 95% of a day, so that the EV owner will obtain the benefit by utilizing the EV for load shift when it is connected to the house. When the EV is utilized for load shift to increase the self-consumption of PV output, unlike the other controllable loads, securing the convenience of the customers is an important issue in addition to the economic benefit because the EV is primarily used for travel. In [4-16], the consensus based cooperative control of the EVs has been proposed to mitigate overvoltage. In this scheme, effect of uncertainty in customer's response due to securing the EV utilization for travel was evaluated by considering the variation in the number of connected EVs to the grid during voltage control. However, in these researches, the equity of customers' benefits and autonomy of the load shift for the self-consumption of PV output have not been studied. The equity of customers' benefit implies a philosophy such that the benefit should be coordinated depending on the contribution of each customer; customers who carry out the load shift should receive a larger benefit than those who do not. The autonomy to the load shift similarly implies another philosophy such that the customers should voluntarily decide to participate in the load shift based on a comparison between the benefit of the load shift contribution and that of travel for themselves.

In this chapter, we propose an EV charging management scheme based on an auction mechanism for increasing self-consumption of PV so as to reduce PV curtailment originating from the voltage constraint in the LVDS. The auction mechanism is introduced in order to simultaneously secure the customers' equity of benefit and the autonomy of contributing to the load shift of EV charging from an economic perspective. The proposed scheme allows customers to voluntarily decide whether they will contribute to the load shift considering the benefits of EV utilizations; the valid benefit of the load shift is equitably returned to the contributors by sharing fees collected from the auction participants. Moreover, the scheme proposed in this work does not require an enhanced communication infrastructure, such as real-time communication, among all customers with EVs.

The remainder of this chapter is organized as follows. In Section 4.2, the formulation and the issues of the EV charging shift for reducing PV curtailment and residential operation cost is described. We introduce the proposed EV charging scheme based on the auction mechanism in Section 4.3. Section 4.4 provides the expected bidders' behavior in the auction mechanism preparing for the numerical simulation. The simulation results of the proposed charging shift scheme are shown in Section 4.5. Section 4.6 summarizes this chapter.

4.2 EV charging shift for reducing PV curtailment

In our scheme, EV is assumed to be charged by considering the residential operation cost, regarding purchased and sold electricity, and customer's convenience. To minimize the residential operation cost in a house with a PV and an EV under the present Feed-in Tariff (FIT) Program, the electricity consumption should be avoided when the PV is generating so as to sell surplus PV output to the grid as much as possible. However, considering the grid voltage constraint, the significant reverse power flow caused by surplus PV output leads to voltage rise and PV curtailment resulting in the reduction of expected profit. In this situation, although the supply side utility is required to reinforce the grid to mitigate voltage rise, so that the PVs installed in the target area tend to curtail their output, a customer residing within the target area can contribute to reduce PV curtailment by shifting the charging period of EV to increase the self-consumption of PV output. The reduction of PV curtailment will reduce the residential operational cost of the customers because some purchased electricity is replaced by the curtailed PV output; therefore, the implementation of effective charging shift in the demand side provides benefits to both the demand and supply sides. In this section, we formulate the problem setting of the EV charging shift scheme and discuss issues of a charging shift for reducing PV curtailment and residential operation cost.

4.2.1 Formulation of EV charging shift

Suppose some houses with PVs and EVs are connected to an LVDS where PV curtailment frequently occurs. We introduce a charging shift scheme to reduce PV curtailment and residential operation cost in the target LVDS. Let $t \in \{1, \dots, T\}$ be the time in a day where T is the total time, and $n \in \mathcal{N}$ be an index of a customer in the LVDS where $\mathcal{N}$ is the index set of the customers. We also let $\boldsymbol{p} = (p_{n,t}; n \in \mathcal{N}, t \in \{1, \dots, T\})$ be a sequence of the consequent (after curtailed) PV output in the target houses and $\boldsymbol{p}^*$ be the original (before curtailed) one; then, a sequence of the PV curtailment $\boldsymbol{x}$ in the target houses is given by

$$\boldsymbol{x} = \boldsymbol{p}^* - \boldsymbol{p}. \tag{4.1}$$

Let $\boldsymbol{y} = (y_{n,t}; n \in \mathcal{N}, t \in \{1, \dots, T\})$ and $\boldsymbol{z} = (\boldsymbol{z}_n \in \{\boldsymbol{z}_n^{\mathrm{ori}}, \boldsymbol{z}_n^{\mathrm{sft}}\}; n \in \mathcal{N})$ be electricity consumptions of uncontrollable load and EV in houses where $\boldsymbol{z}_n^{\mathrm{ori}} = \left(z_{n,t}^{\mathrm{ori}}; t \in \{1, \dots, T\}\right)$ and $\boldsymbol{z}_n^{\mathrm{sft}} = \left(z_{n,t}^{\mathrm{sft}}; t \in \{1, \dots, T\}\right)$ indicate the sequences of EV charging electricity consumption determined not considering

PV curtailment and that shifted for reducing PV curtailment, respectively. We also let $\mathcal{W} \subset \mathcal{N}$ be the subset of customers who carry out the charging shift (hereinafter called "shifters"). In the case of $\mathcal{W} = \emptyset$, the sequence of EV charging in all customers becomes $\boldsymbol{z}_n = \boldsymbol{z}_n^{\mathrm{ori}}$ $(\forall n)$ and the total residential operation cost of customers in the LVDS is given by

$$\begin{aligned} C(\boldsymbol{z}) &= \sum_{n\in\mathcal{N}} C_n^{\mathrm{ori}}\big(\boldsymbol{z}(\mathcal{W})\big) \\ &= \sum_{n\in\mathcal{N}}\sum_{t=1}^{T}\Big(c_t^{\mathrm{g}}\big[y_{n,t} + z_{n,t}^{\mathrm{ori}} - p_{n,t}\big(\boldsymbol{z}(\mathcal{W})\big)\big]_+ - c_t^{\mathrm{PV}}\big[p_{n,t}\big(\boldsymbol{z}(\mathcal{W})\big) - y_{n,t} - z_{n,t}^{\mathrm{ori}}\big]_+\Big), \end{aligned} \tag{4.2}$$

where

$$[a]_+ = \begin{cases} a & \text{if} \quad a \geq 0 \\ 0 & \text{otherwise,} \end{cases} \tag{4.3}$$

C_n^{ori} is the residential operation cost of non-shifter $n \notin \mathcal{W}$, who does not carry out the charging shift, and c_t^{g} and c_t^{PV} are the cost conversion coefficients of the purchased and sold electricity at time t, respectively. On the other hand, when customers carry out the charging shift ($\mathcal{W} \neq \emptyset$), the electricity consumption of EV charging of shifters $n \in \mathcal{W}$ is converted from $\boldsymbol{z}_n^{\mathrm{ori}}$ to $\boldsymbol{z}_n^{\mathrm{sft}}$, so that the total residential operation cost in the LVDS is given by

$$C\big(\boldsymbol{z}(\mathcal{W})\big) = \sum_{n\in\mathcal{W}} C_n^{\mathrm{sft}}\big(\boldsymbol{z}(\mathcal{W})\big) + \sum_{n\notin\mathcal{W}} C_n^{\mathrm{ori}}\big(\boldsymbol{z}(\mathcal{W})\big), \tag{4.4}$$

where C_n^{sft} indicates the residential operation cost of shifters $n \in \mathcal{W}$ given by

$$C_n^{\mathrm{sft}}\big(\boldsymbol{z}(\mathcal{W})\big) = \sum_{t=1}^{T}\Big(c_t^{\mathrm{g}}\big[y_{n,t} + z_{n,t}^{\mathrm{sft}} - p_{n,t}\big(\boldsymbol{z}(\mathcal{W})\big)\big]_+ - c_t^{\mathrm{PV}}\big[p_{n,t}\big(\boldsymbol{z}(\mathcal{W})\big) - y_{n,t} - z_{n,t}^{\mathrm{sft}}\big]_+\Big). \tag{4.5}$$

As shown in Eqs. (4.2)–(4.5), the effectiveness of charging shift depends on how to determine the subset of shifters $\mathcal{W}$ and the shifted EV charging profiles $\boldsymbol{z}_n^{\mathrm{sft}}$. The charging shift scheme can be classified into two types from a perspective of how to determine them: distributed and centralized approaches. Both types of charging shift might be executed according to the pre-set schedules given via in-home controllers. In the distributed charging shift approach, each customer autonomously manages individual charging shift; $\mathcal{W}$ and $\boldsymbol{z}_n^{\mathrm{sft}}$ are determined as a result of the customers' decisions. On the other hand, in the centralized charging approach, an aggregator manages the charging shift in the target area; $\mathcal{W}$ and $\boldsymbol{z}_n^{\mathrm{sft}}$ are determined by the aggregator and customers carry out the EV charging shift according to the aggregator's decision. In the next subsection, issues of the EV charging shift are discussed on both types of approach.

4.2.2 Issues of EV charging shift

There are three issues introducing the EV charging shift for reducing the PV curtailment and residential operation cost. The first issue is determination of an appropriate amount of charging shift

based on $\mathcal{W}$ and $\boldsymbol{z}_n^{\mathrm{sft}}$. An inappropriate amount of charging shift would result in an inappropriate amount of self-consumption of PV output; the residential operation cost would be increased when the PV output that could be sold is self-consumed, or the PV output that would be curtailed is not self-consumed. In the distributed approach, it is difficult for each customer to appropriately determine when and how much EV charging should be shifted to reduce PV curtailment and residential operation cost because the voltage varies with the electricity consumption of all houses connected to the same LVDS. PV curtailment in a house increases when the loads in the other houses are light, and decreases when they are heavy. Therefore, customers cannot accurately estimate their expected PV curtailment unless they acquire the behavior of the other customers. On the other hand, in the centralized charging shift approach, an aggregator can manage when and how much charging shift should be carried out considering an appropriate balance in amounts of charging shift and expected PV curtailment in all houses connected to the same LVDS.

The second issue is to secure equity: a philosophy such that the customers' benefit obtained by the charging shift should be coordinated depending on contribution of the customers, i.e., the shifters should receive a larger benefit than the non-shifters. The charging shift carried out by certain customers will reduce PV curtailment not only in their own house but also in other local houses connected in the same LVDS because the increase of self-consumption of PV output by the charging shift reduces the voltage, which is the implicit constraint of PV curtailment, in the entire LVDS. The reduction of voltage depends on the number and location of shifters. Therefore, the consequent PV output $p_{n,t}\big(\boldsymbol{z}(\mathcal{W})\big)$ changes depending on set of shifters $\mathcal{W}$. Equation (4.5) suggests that the residential operation cost of shifters changes depending on the increase of consequent PV output $p_{n,t}$, i.e., reduction of PV curtailment, caused by customer's own and others' charging shift. On the other hand, Eq. (4.2) shows that the residential operation cost of non-shifters changes depending on the increase of consequent PV output $p_{n,t}$ caused by the decrease of voltage due to the others' charging shift. This relationship implies that the total benefit produced by the charging shift carried out by a subset of customers is expressed as the total reduction of PV curtailment in all the customers. However, from the viewpoint of the shifters, the benefit seems only the cost reduction resulting from reducing PV curtailment in shifter's own house; the benefit is lower than the appropriate value of the charging shift, so that non-shifters could obtain the benefit even though they do not contribute to the charging shift (see Fig. 4.1). This inequity on the benefit would have a negative impact on customers' participation in the charging shift. Thus, the value for non-shifters should be appropriately evaluated and returned to shifters. In the distributed charging shift approach, the mechanism for solving the inequity is not included. Meanwhile, the centralized charging shift approach have a potential to equitably share the benefit between the customers mediated by the aggregator.

The third issue is to secure autonomy: another philosophy such that the customers should voluntarily decide to participate in the charging shift based on a comparison between an EV utilization benefit by

the charging shift contribution and that by travel for themselves, because EV is preliminary utilized for travel. In the distributed charging shift approach, since each customer independently decides the participation in the charging shift, the autonomy is secured. However, in the centralized charging shift approach, autonomy is difficult to be secured because it is difficult for the aggregator to compare the individual values of EV utilization. Let $\widehat{\mathcal{W}} \subset \mathcal{N}$ be the set of shifters determined by the aggregator, $\widehat{\mathcal{W}}$ is determined for satisfying the objectives indicated by the aggregator, although the target customers $n \in \widehat{\mathcal{W}}$ will not contribute to the charging shift when the benefit of EV travel is higher for the customer than the value of cost reduction by the charging shift. In order to secure the autonomy and not to neglect the convenience of customers, the centralized approach should include the mechanism that the customers voluntarily participate in the charging shift evaluating the values of EV utilization.

Therefore, the admittable charging shift scheme requires to solve above three issues. i.e., determination of appropriate amount of charging shift, securing equity, and securing autonomy. In the next section, we propose an EV charging shift scheme based on an auction mechanism, which is a hybrid approach of the distributed and centralized ones, to tackle these three issues.

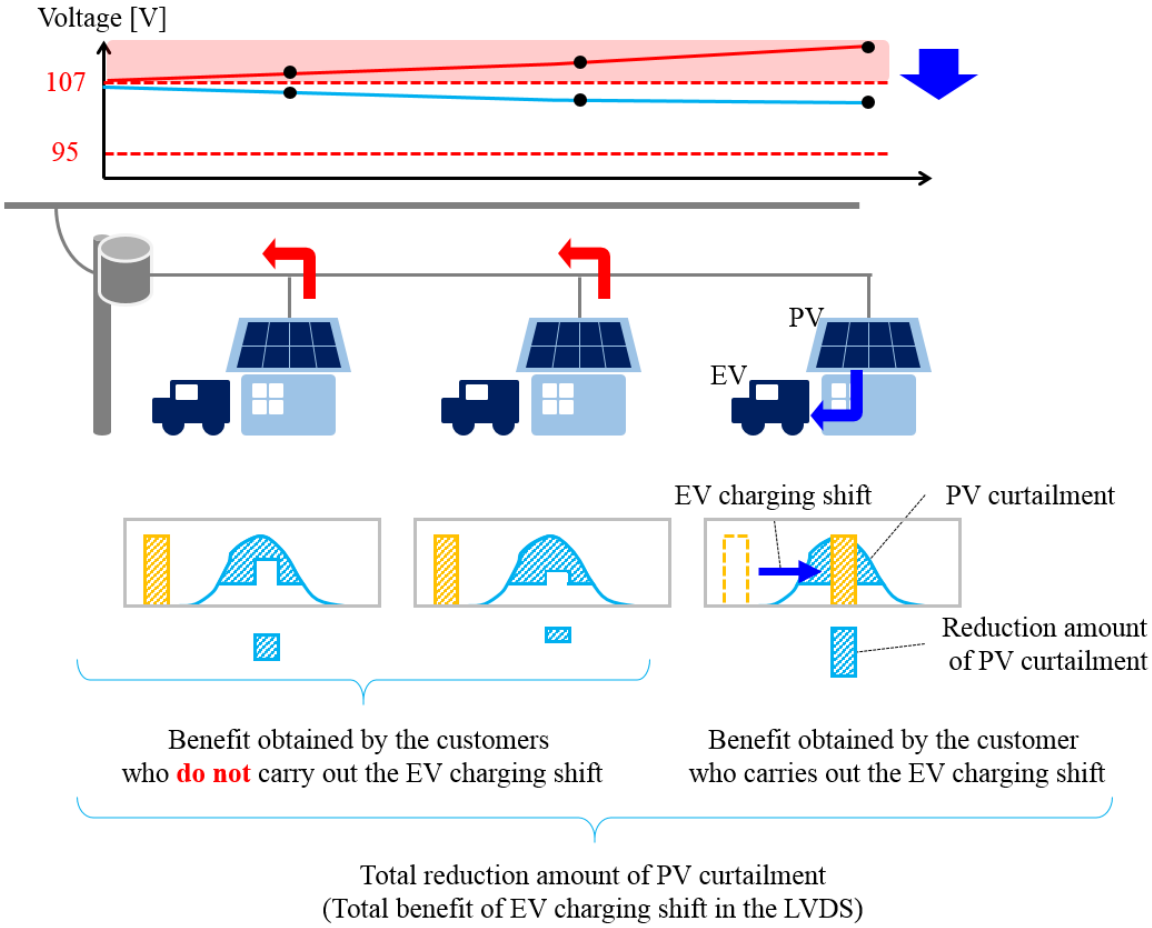

Fig. 4.1 Total benefit produced by the EV charging shift. The benefit obtained by the customer who carries out the EV charging shift is smaller than the total reduction benefit in the LVDS.

4.3 EV charging shift based on auction mechanism

We introduce the second-price sealed-bid auction mechanism [4-17] in the EV charging shift scheme to determine the shifters so as to secure the equity and autonomy in the charging shift as well as an appropriate amount of charging shift. This auction mechanism is known that it is reasonable for the bidders to submit their bids according to the truthful bids for the target value. In the auction mechanism, customers voluntarily determine the bids without knowing the other's bids and compete to obtain the rights to carry out the charging shift. Customers can determine the bids that will not win the auction when they do not want to carry out the charging shift, so that the autonomy is secured. Moreover, the winners of the auction carry out the charging shift and obtain the incentive that is sum of collected price from the other bidders to compensate for the difference between the appropriate total value of charging shift and the benefit resulting from reducing their own PV curtailment, thereby the equity is secured. The detailed procedure of the auction mechanism is explained below.

4.3.1 Determination of participants and number of winners

The aggregator decides to hold the auction for EV charging shift in the next day on the basis of the estimated result of day-ahead PV curtailment, i.e.,

$$\widehat{\boldsymbol{x}} = \widehat{\boldsymbol{p}}^{*} - \widehat{\boldsymbol{p}}, \tag{4.6}$$

because the actual day-ahead sequences in Eq. (4.1) are not available; here, we will use the symbol $\widehat{\cdot}$ to denote forecasted values. We assume that the aggregator owns information of the target LVDS and estimate the day-ahead PV curtailment $\widehat{\boldsymbol{x}}$ on the basis of the numerical simulation that can grasp the voltage in the whole LVDS. The auction for charging shift is held when: 1) PV curtailment would occur in the next day in multiple customers; this gives the following inequality,

$$\sum_{n \in \mathcal{N}} \delta(\widehat{\boldsymbol{x}}_n) \geq 2, \tag{4.7}$$

where

$$\delta(\widehat{\boldsymbol{x}}_n) = \begin{cases} 1 & \text{if} \quad \sum_{t=1}^{T} \widehat{\boldsymbol{x}}_{n,t} > 0 \\ 0 & \text{otherwise} \end{cases}, \tag{4.8}$$

and 2) the expected residential operation cost in the target LVDS would be reduced by carrying out the charging shift, i.e.,

$$C\big(\boldsymbol{z}(\mathcal{W} = \widehat{\mathcal{W}})|\widehat{\boldsymbol{x}}\big) < C(\boldsymbol{z}(\mathcal{W} = \emptyset)|\widehat{\boldsymbol{x}}), \tag{4.9}$$

Then, the aggregator suggests a set of relevant participants $\mathcal{P} = \{n|\delta(\widehat{\boldsymbol{x}}_n) > 0\}$, preferable number of winners, i.e., shifters, $|\widehat{\mathcal{W}}|$, and request of the charging shift $\boldsymbol{z}_n^{\text{sft}}$. Note that the number of shifters for minimizing PV curtailment and that for minimizing the residential operation cost would be different. Since the charging shift in the demand side is not achieved without contribution of customers, the aggregator should consider increasing the benefit to the customers even though a major objective of the

charging shift is to reduce PV curtailment. Here, the preferable number of winners $|\widehat{\mathcal{W}}|$ is derived by a set of winners $\widehat{\mathcal{W}}$ that is determined for minimizing the total residential operation cost in the LVDS under the forecasted PV curtailment $\hat{\boldsymbol{x}}$,

$$\widehat{\mathcal{W}} = \underset{\mathcal{W}\subset\mathcal{P}}{\operatorname{argmin}}\, C(\boldsymbol{z}(\mathcal{W})|\hat{\boldsymbol{x}}). \tag{4.10}$$

Equation (4.10) can be solved through the power flow calculation by evaluating the total residential operation cost described in Eq. (4.4) in terms of all combinations of $\mathcal{W}$ in $\mathcal{P}$. Note that computational cost required for searching minimizer $\widehat{\mathcal{W}}$ is increases exponentially according to the number of participants $|\mathcal{P}|$; therefore, the computational cost for exact minimization of Eq. (4.10) becomes significantly high when $|\mathcal{P}|$ is large. We introduce the following greedy algorithm for searching such a set of winners $\widehat{\mathcal{W}}$.

Algorithm 1 Determination of the set of winners $\widehat{\mathcal{W}}$.

$i = 0, \mathcal{W}^{(0)} = \emptyset, \mathcal{P}^{(0)} = \{n|\delta(\hat{\boldsymbol{x}}_n) > 0\}$

REPEAT

$i = i + 1$

$\hat{n} = \underset{n\in\mathcal{P}^{(i-1)}}{\operatorname{argmin}}\, C\left(\boldsymbol{z}, \mathcal{W}^{(i-1)} \cup \{n\}|\hat{\boldsymbol{x}}\right)$

$\mathcal{W}^{(i)} = \mathcal{W}^{(i-1)} \cup \{\hat{n}\}$

$\mathcal{P}^{(i)} = \mathcal{P}^{(i-1)}\backslash\{\hat{n}\}$

UNTIL $C\left(\boldsymbol{z}, \mathcal{W}^{(i)}|\hat{\boldsymbol{x}}\right) \geq C\left(\boldsymbol{z}, \mathcal{W}^{(i-1)}|\hat{\boldsymbol{x}}\right)$ or $i = \left|\mathcal{P}^{(0)}\right| - 1$

$\widehat{\mathcal{W}} = \mathcal{W}^{(i-1)}$

Note that, since the set of winners $\widehat{\mathcal{W}}$ and participants $\mathcal{P}$ determined by the aggregator are derived on the basis of the forecasted values $\hat{\boldsymbol{x}}$, it is not always equal to the optimal set of winners $\mathcal{W}^{\mathrm{o}}$ and participants $\mathcal{P}^{\mathrm{o}}$ derived on the basis of the consequent values $\boldsymbol{x}$ given by

$$\mathcal{W}^{\mathrm{o}} = \underset{\mathcal{W}\subset\mathcal{P}}{\operatorname{argmin}}\, C(\boldsymbol{z}(\mathcal{W})|\boldsymbol{x}),$$

and $\mathcal{P}^{\mathrm{o}} = \{n|\delta(\boldsymbol{x}_n) > 0\}$.

4.3.2 Determination of winners based on bidding

Assume that a bidder $n \in \mathcal{P}$, who is determined by the aggregator as a participant, submits his/her bid b_n, which is not known by the other bidders. The aggregator determines $|\widehat{\mathcal{W}}|$ winners from the lowest bidders. Let $b_{[|\widehat{\mathcal{W}}|]}$ be the $|\widehat{\mathcal{W}}|$th lowest bid. Then, the final winners are shown as $\mathcal{W}^* = \left\{n|b_n \leq b_{[|\widehat{\mathcal{W}}|]}\right\}$ and the losers are shown as $\left\{n|b_n \geq b_{[|\widehat{\mathcal{W}}|+1]}\right\} = \mathcal{P}\backslash\mathcal{W}^*$. The aggregator collects the price $b_{[|\widehat{\mathcal{W}}|+1]}$ from all the losers and distributes the incentive cost,

$$\frac{\left(|\mathcal{P}| - |\widehat{\mathcal{W}}|\right)b_{[|\widehat{\mathcal{W}}|+1]}}{|\widehat{\mathcal{W}}|},$$

to the winners $n \in \mathcal{W}^*$. Hence, the expected residential operation cost of each customer after carrying out the charging shift based on the auction mechanism is given as

$$C_n\left(\boldsymbol{z}(\mathcal{W}_b^*)\right) = \begin{cases} C_n^{\mathrm{sft}}\left(\boldsymbol{z}(\mathcal{W}_b^*)\right) - \dfrac{\left(|\mathcal{P}| - |\widehat{\mathcal{W}}|\right) b_{[|\widehat{\mathcal{W}}|+1]}}{|\widehat{\mathcal{W}}|} & (n \in \mathcal{W}^*) \\ C_n^{\mathrm{ori}}\left(\boldsymbol{z}(\mathcal{W}_b^*)\right) + b_{[|\widehat{\mathcal{W}}|+1]} & (n \notin \mathcal{W}^*), \end{cases} \tag{4.11}$$

where $\mathcal{W}_b^* = \mathcal{W}^*(\{b_n\})$. In this scheme, the collected price $b_{[|\widehat{\mathcal{W}}|+1]}$ never exceeds any bid of the losers. The bidders will submit their bids by considering the amount of incentive when they win and the benefit of their individual PV curtailment reduction when they lose; the bidders will set their bids high when they want to utilize the EVs for travel and not to contribute to the charging shift. Besides, the aggregator does not need to prepare the additional incentive because the sum of the incentive cost and the collected price is zero. The benefit of the charging shift is produced from the total reduction of the PV curtailment, i.e., the total reduction of the purchased electricity of all customers in the target LVDS. Moreover, the required communication in the proposed scheme is significantly low; therefore, the proposed scheme can be operated without an enhanced communication infrastructure.

4.4 Expected behavior of bidders

Economic rationality is an important factor for the bidders to determine the bids. Although some economical decision policies have been discussed for determination of such bids, here, we assume the minimax strategy for bidders' decision making, which minimizes the possible loss for a worst-case scenario. Fig. 4.2 depicts the schematic image of customer's bid determination based on the minimax strategy. Applying the minimax strategy to our auction mechanism, the individual bid is determined to minimize the possible total cost, which is the sum of the residential operation cost and the incentive or the collected price, for a worst-case winner set that makes the total cost the highest as following:

$$b_n^* = \underset{b_n}{\operatorname{argmin}} \left(\max \left[\max_{\mathcal{W} \ni n} \left\{ C_n^{\mathrm{sft}}\left(\boldsymbol{z}(\mathcal{W})\right) - \frac{\left(|\mathcal{P}| - |\widehat{\mathcal{W}}|\right) b_n}{|\widehat{\mathcal{W}}|} + o_n \right\}, \max_{\mathcal{W} \not\ni n} \left\{ C_n^{\mathrm{ori}}\left(\boldsymbol{z}(\mathcal{W})\right) + b_n \right\} \right] \right), \tag{4.12}$$

where o_n indicates the opportunity cost of EV utilization for travel, which is the conceptual cost that the bidder obtains by selecting the utilization instead of the changing shift. Note that required computational cost for evaluation of all winner sets $\mathcal{W} \subset \mathcal{P}$ is proportional to ${}_{|\mathcal{P}|}\mathrm{C}_{|\widehat{\mathcal{W}}|}$; again, the computational cost for exact determination of bids and winners becomes significantly high when $|\mathcal{P}|$ is large. In our simulation given in the next section, the plausible bids derived from the economic rationality are assumed to be determined according to the following greedy algorithm.

Algorithm 2 Derivation of expected bids $\{b_n^*\}$ based on minimax policy.

$\mathcal{P}^{(0)} = \{n|\delta(\hat{\boldsymbol{x}}_n) > 0\}$

FOR $i = 1$ to $|\hat{\mathcal{W}}|$

$$b_n^* = \underset{b_n}{\operatorname{argmin}}\left\{\max\left[C_n^{\mathrm{sft}}\left(\boldsymbol{z}(\mathcal{W}=\{n\})\right) - \left(|\mathcal{P}^{(i-1)}|-1\right)b_n + o_n,\ \max_{m\in\mathcal{P}^{(i-1)}\setminus\{n\}}\left\{C_n^{\mathrm{ori}}\left(\boldsymbol{z}(\mathcal{W}=\{m\})\right) + b_n\right\}\right]\right\} \tag{4.13}$$

$n^{*(i)} = \underset{n\in\mathcal{P}^{(i-1)}}{\operatorname{argmin}}\, b_n^*$

$\mathcal{P}^{(i)} = \mathcal{P}^{(i-1)}\setminus n^{*(i)}$

FOREND

In algorithm 2, $n^{*(i)}$ denotes the determined winner and $\boldsymbol{n}^* \in \{n^{*(i)}|i = 1, \dots, |\hat{\mathcal{W}}|\}$ is the set of winners. Note that $\mathcal{W}^*$ may not equal to $\hat{\mathcal{W}}$ when the assumption of economic rationality and uniform opportunity cost are violated.

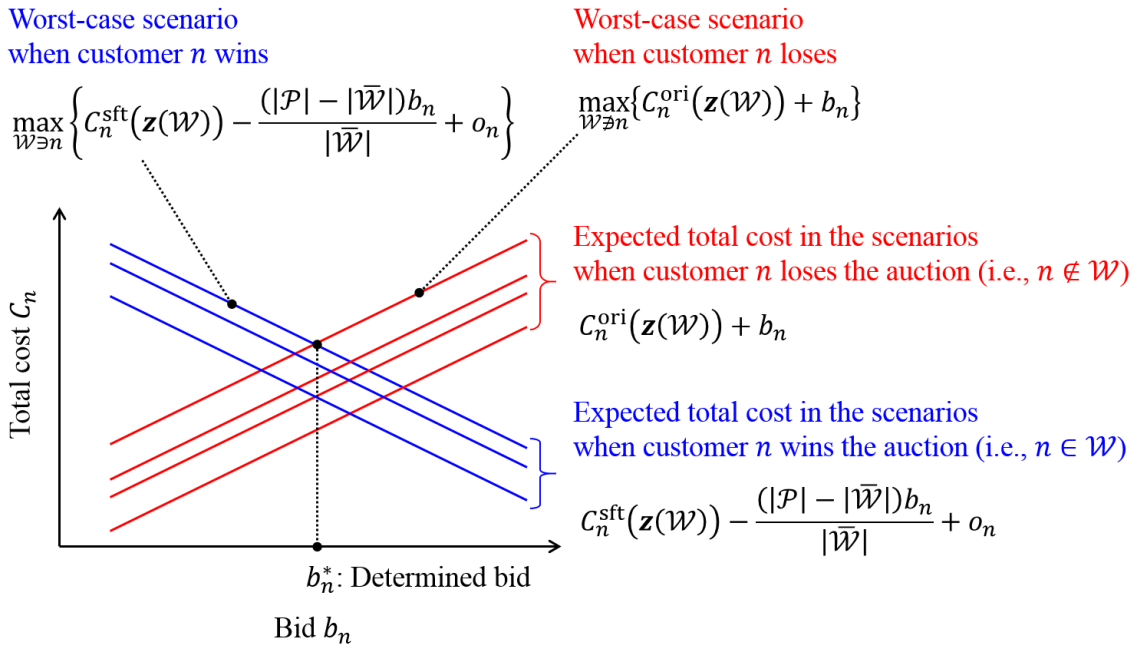

Fig. 4.2 Schematic plot of bid determination based on minimax strategy.

4.5 Simulation

Our proposed EV charging management scheme based on the auction mechanism is expected to achieve the autonomy and equity in the charging shift. To verify the effectiveness of our method in terms of the total residential operation cost, the total amount of PV curtailment, and the difference of the effectiveness caused by uncertainties resulting in difference of the auction results, i.e., difference of $\mathcal{W}^{\mathrm{o}}$, $\hat{\mathcal{W}}$, and $\mathcal{W}^*$, we conducted numerical simulation using a DS model [4-18] based on a 30-day (June 2007) actual measurement of PV output and electricity consumption with a time step of 10 s. This model

simulates an actual DS in Japan and comprises two distribution feeders (industrial area and residential area), which include MV (6.6 kV) and LV (100/200 V) systems (Fig. 4.3). The model has four MV OLTCs operated on the basis of the centralized voltage control method [4-5], and includes 35 MV customers, 91 LVDSs, and 812 LV customers. The residential PV systems are installed in 90% of the LV customers, the situation suggests the condition that the total PV curtailment in the DS is significantly large. The load shift based on the auction mechanism is implemented in the LVDS #10 which includes 14 LV customers with a PV and an EV. Table 4.1 shows the simulation setup, including some dominant parameters. Table 4.2 presents the electricity rate for calculating the residential operation cost, which is based on an actual time-of-use (TOU) menu provided by the Tokyo Electric Power Company Energy Partner, Inc.

In this simulation, we assessed the effectiveness of the charging shift based on the auction mechanism in the LVDS #10. We assumed that all LV customers charge their EVs 4 kWh (2 kW x 2 hours) in a day. The all winners of the auction charge their EVs at 11:00–13:00 when PV curtailment frequently occurs, while others charge their EVs at 2:00–4:00 when the purchasing price of the TOU menu is low. To assess the uncertainties included in the auction results, we compared the following seven cases (see also Table 4.3).

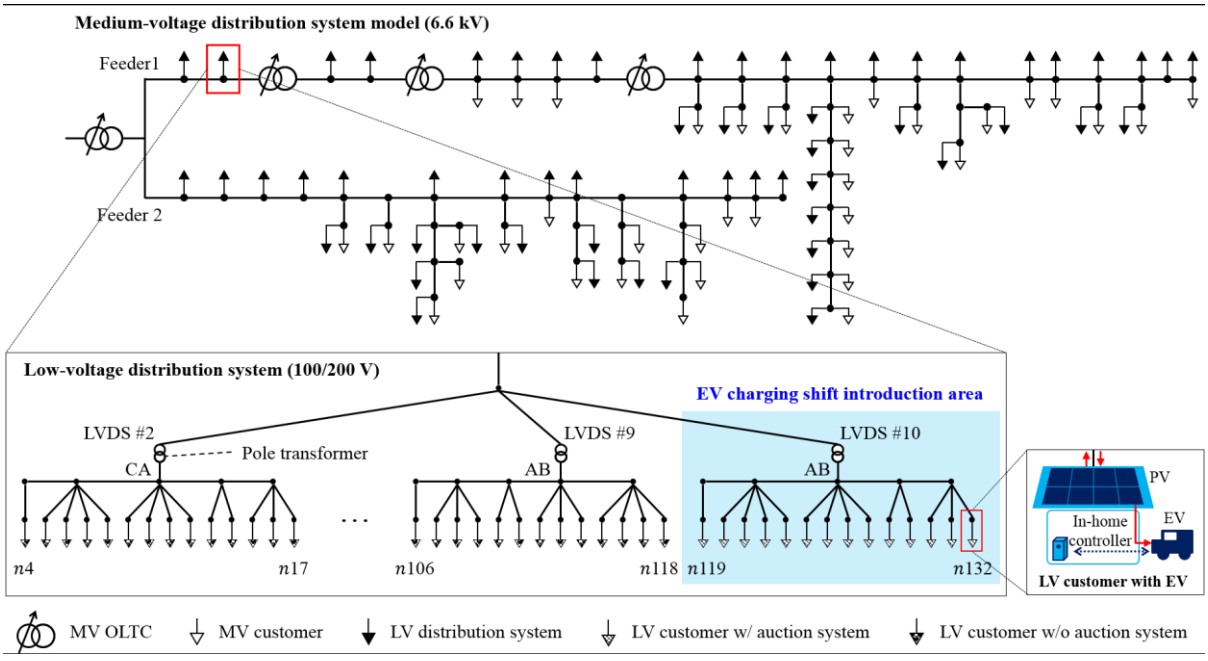

Fig. 4.3 Simulation model.

Table 4.1 Simulation setup.

Distribution system model	Line length	Feeder 1: 18.4 km Feeder 2: 7.48 km
	Load capacity	Feeder 1: 2220 kW Feeder 2: 2113 kW
	Appropriate voltage range	95–107 V
Spec of PV inverters	Curtailment starting voltage	107 V
	Curtailment ending voltage	106.5 V
	Speed of curtailment	0.02 kW/s

Table 4.2 Electricity rate.

Purchasing price (TOU pricing)	7:00–23:00	32.14 JPY/kWh
	23:00–7:00	20.74 JPY/kWh
Selling price (Feed-in tariff)		30.00 JPY/kWh

Table 4.3 Simulation cases.

	Auction mechanism	Consideration of uncertainties in auction mechanism			EV charging period
		Forecasting error	Opportunity cost	Economic rationality	
Case 1	w/o	-	-	-	Random
Case 2	w/o	-	-	-	2:00–4:00
Case 3	w/	w/o	w/o	w/o	Winners: 11:00–13:00, Others: 2:00–4:00
Case 4	w/	w/	w/o	w/o	
Case 5	w/	w/o	w/	w/o	
Case 6	w/	w/o	w/o	w/	
Case 7	w/	w/	w/	w/	

- Case 1: customers do not carry out the charging shift based on the auction mechanism and all customers charge their EVs at random arbitrary time.
- Case 2: customers do not carry out the charging shift based on the auction mechanism and all customers charge their EVs at 2:00–4:00 to reduce residential operation cost.

- Case 3: customers carry out the charging shift based on the auction mechanism in the ideal condition; there is no forecasting error on PV curtailment; the bidders decide their bids with economic rationality under the common opportunity cost o_n for all customers, i.e., $\mathcal{P} = \mathcal{P}^{\mathrm{o}}$, $\mathcal{W}^* = \mathcal{W}^{\mathrm{o}} = \widehat{\mathcal{W}}$.
- Case 4: customers carry out the charging shift based on the auction mechanism under the condition that the aggregator estimates the forthcoming PV curtailment on the basis of the forecast of PV output [4-19], [4-20] and electricity consumption [4-21]; note that forecasting error affects the number of participants $\mathcal{P}$ and winners $|\widehat{\mathcal{W}}|$ suggested by the aggregator, so that $\mathcal{P}$ and $\widehat{\mathcal{W}}$ would be different from the ideal ones $\mathcal{P}^{\mathrm{o}}$ and $\mathcal{W}^{\mathrm{o}}$, respectively. Namely, this case assumes that $\mathcal{W}^* = \widehat{\mathcal{W}}$ holds, but $\mathcal{P} = \mathcal{P}^{\mathrm{o}}$ and $\widehat{\mathcal{W}} = \mathcal{W}^{\mathrm{o}}$ may not.
- Case 5: customers carry out the charging shift based on the auction mechanism under the condition that the opportunity cost o_n is individually given at random; customers whose opportunity cost of EV travel is high increases their bids in order not to win the auction and avoid carrying out the charging shift, therefore the final winners $\mathcal{W}^*$ would be different from the ideal condition. Namely, this case assumes that $\mathcal{P} = \mathcal{P}^{\mathrm{o}}$ and $\widehat{\mathcal{W}} = \mathcal{W}^{\mathrm{o}}$ hold, but $\mathcal{W}^* = \mathcal{W}^{\mathrm{o}}$ may not.
- Case 6: customers carry out the charging shift based on the auction mechanism under the condition that the customers determine their bids without economic rationality; they randomly determine their bids, so that the determined winners $\mathcal{W}^*$ would be different from the ideal condition. Namely, this case assumes that $\mathcal{P} = \mathcal{P}^{\mathrm{o}}$ and $\widehat{\mathcal{W}} = \mathcal{W}^{\mathrm{o}}$ hold, but $\mathcal{W}^* = \mathcal{W}^{\mathrm{o}}$ may not.
- Case 7: customers carry out the charging shift based on the auction mechanism on the condition of all uncertainties considered in Cases 4–6. Namely, this case assumes that $\mathcal{P} = \mathcal{P}^{\mathrm{o}}$, $\mathcal{W}^* = \mathcal{W}^{\mathrm{o}}$, and $\widehat{\mathcal{W}} = \mathcal{W}^{\mathrm{o}}$ may not hold.

Fig. 4.4 shows the simulation results on the total amount of the residential operation cost (Fig. 4.4(a)) and PV curtailment (Fig. 4.4(b)) in the LVDS #10 for 30 days. The results of Cases 4–6 indicate the average values of 100 times simulations. The residential operation cost of Case 1 is 2.17 times higher than that of Case 2, although the amount of PV curtailment of Case 1 is smaller than that of Case 2. This result suggests that. If the individual EVs are charged at a random arbitrary time, the residential operation cost can be large. If all EVs are charged at the same period (2:00–4:00) in which the TOU pricing is low, the residential operation cost is significantly reduced. This result also implies that customers should charge the EVs at night to reduce the residential operation cost when there is no aggregator to coordinate charging shift in the LVDS. However, the residential operation cost in Case 2 seems to be further reduced by effectively reducing PV curtailment. On the other hand, the introduction of our proposed charging shift based on the auction mechanism in the ideal condition (Case 3) achieves 20.1% reduction in the residential operational cost and 45.1% reduction in the amount of PV curtailment

compared with Case 2. The figures also show that Cases 4–7 reduce the residential operation cost by 18.8%, 12.2%, 8.2%, and 6.2%, respectively, and PV curtailment by 45.1%, 28.4%, 32.3%, and 22.2%, respectively, compared with Case 2 (w/o the charging shift scheme), although the reduction ratio is smaller than in Case 3. These results suggest that the proposed charging shift scheme can effectively reduce the residential operation cost and the amount of PV curtailment, even by considering the effects of uncertainties involved in forecast methods and human behaviors that result in the auction result. Note that the residential operation cost and the PV curtailment of Case 4 are lower than those of Cases 5 and 6. This result suggests that the negative effect caused by the forecasting error of the PV curtailment is smaller than the other uncertainties. A comparison between the results of Case 5 and Case 6 shows that the residential operation cost of Case 5 is lower than that of Case 6, while the amount of PV curtailment of Case 5 is larger than that of Case 6. These results imply that the reduction of the residential operation cost becomes higher when the customers determine the bids with economic rationality, and the reduction of the PV curtailment becomes larger when the proposed scheme is introduced in the LVDS whose customers' opportunity costs are the same and relatively low.

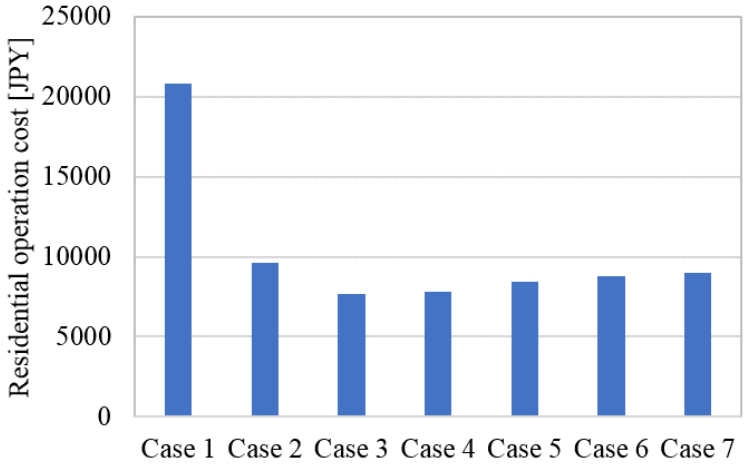

(a) Total amount of residential operation cost in the LVDS #10

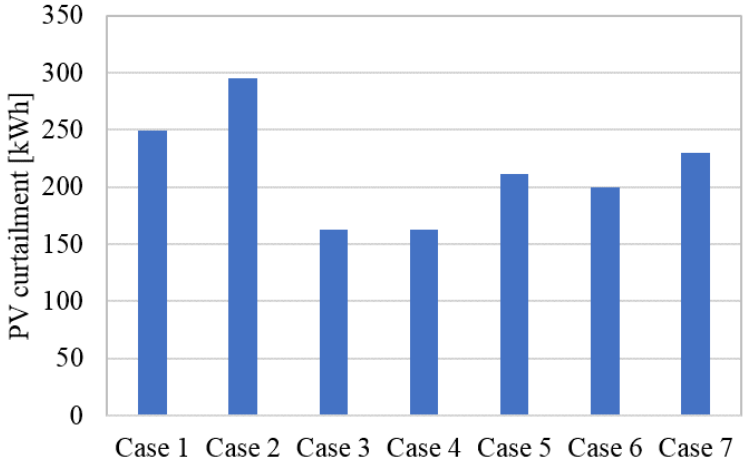

(b) Total amount of PV curtailment in the LVDS #10

Fig. 4.4 Simulation results.

Fig. 5.5 shows the total residential operation cost (Fig. 5.5(a)) and the total amount of PV curtailment (Fig. 5.5(b)) in a day for Cases 1–3 and 7 under various number of shifters (number of winners on the auction mechanism). In Case 3, the residential operation cost declines until the number of winners increases to four and then increases, although the amount of PV curtailment is monotonically reduced when the number of winners increases. It is notable that the residential operation cost of Cases 3 and 7 becomes higher than that of Case 2 when more than ten (Case 3) or eight (Case 7) customers carry out the charging shift. However, in the proposed scheme, the aggregator can determine the number of shifters to reduce the residential operation cost on the basis of the forecasted amount of day-ahead PV curtailment. Since the sensitivity of the operational cost to the optimal number of winners is low, there seems to have little impact of the estimation error of number of winners due to the PV forecast error in the proposed scheme.

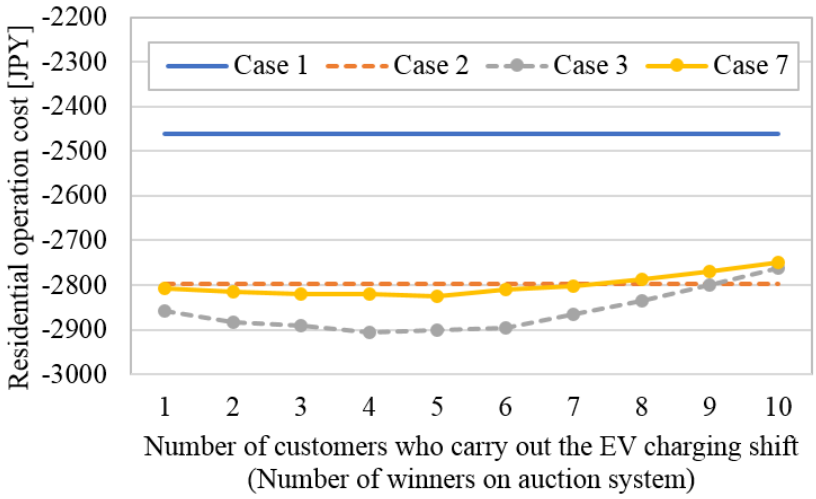

(a) Residential operation cost in the LVDS #10

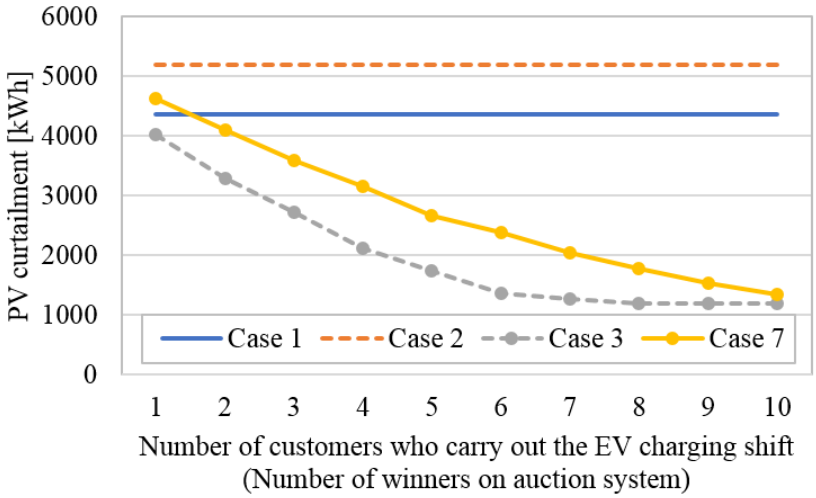

(b) PV curtailment in the LVDS #10

Fig. 4.5 Total residential operation cost and total amount of PV curtailment under various number of shifters (number of winners on the auction system).

Fig. 4.6 shows the total amount of PV curtailment in the LVDS with the charging shift and in the other LVDSs. The result indicates that the introduction of the proposed scheme reduces PV curtailment not only in the LVDS where the scheme is introduced but also in the other LVDSs. This can be interpreted as follows; the reduction of the reverse power flow by the charging shift in the LVDS slightly reduced the voltage in LVDSs, so that the PV generation in the LVDSs were increased.

The simulation results suggest that our proposed scheme contributes to achieve a robust reduction of the residential operation cost and PV curtailment even under uncertainties without an enhanced communication network, while securing the autonomy and equity on the charging shift.

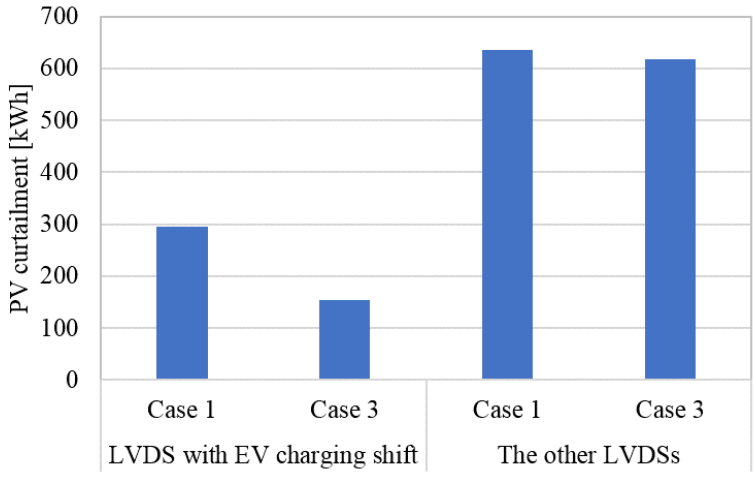

Fig. 4.6 Total amount of PV curtailment in the LVDS and in the other LVDSs.

4.6 Summary of this chapter

In this study, we proposed the EV charging management scheme based on the auction mechanism to reduce PV curtailment caused by voltage rise in the DS. The proposed scheme reduces PV curtailment by increasing the self-consumption of PV output, and lowers the voltage by shifting the charging period of EVs, while securing the equity of customers' benefit and the autonomy of contributing to the charging shift. The introduction of the auction mechanism allowed EV owners to participate in the load shift of EV charging voluntarily by comparing the benefits of using EV for carrying out load shift and for travel. In this scheme, customers who contribute to the charging shift can obtain not only the benefit from reducing PV curtailment in their own houses but also the benefit of the incentive of contributing to reduce PV curtailment in other houses. Besides, the proposed scheme can be implemented without an enhanced communication network. The effectiveness of the proposed scheme was evaluated using a DS simulation model and actual measurements of power profiles in terms of the residential operation cost and PV curtailment. The simulation results demonstrated that our proposed scheme is expected to achieve a reduction in the residential operation cost and PV curtailment, even with small difference of auction result caused by the uncertainties in the day-ahead PV curtailment forecast, number of participants, and economic rationality of the customers. Although the auction

mechanism is used for the load shift of EV charging, it could be applied in other frameworks that require the equity of the customers' benefit and autonomy of customers' participation, such as the active power curtailment of PV inverters.

References

[4-1] Masuta T, Gari da Silva J, Fonseca, Ootake H, Murata A. Application of battery energy storage system to power system operation for reduction in PV curtailment based on few-hours-ahead PV forecast. 2016 IEEE Int. Conf. Power Syst. Technol., IEEE; 2016, p. 1–6. doi:10.1109/POWERCON.2016.7754068.

[4-2] Ueda Y, Kurokawa K, Tanabe T, Kitamura K, Sugihara H. Analysis results of output power loss due to the grid voltage rise in grid-connected photovoltaic power generation systems. IEEE Trans Ind Electron 2008;55:2744–51. doi:10.1109/TIE.2008.924447.

[4-3] Shayani RA, de Oliveira MAG. Photovoltaic generation penetration limits in radial distribution systems. IEEE Trans Power Syst 2011;26:1625–31. doi:10.1109/TPWRS.2010.2077656.

[4-4] Navarro-Espinosa A, Ochoa LF. Increasing the PV hosting capacity of LV networks: OLTC-fitted transformers vs. reinforcements. 2015 IEEE Power Energy Soc. Innov. Smart Grid Technol. Conf., IEEE; 2015, p. 1–5. doi:10.1109/ISGT.2015.7131856.

[4-5] Akagi S, Takahashi R, Kaneko A, Yoshinaga J, Ito M, Hayashi Y, et al. Upgrading the voltage control method based on the photovoltaic penetration rate. IEEE Trans Smart Grid 2017;PP:1–1. doi:10.1109/TSG.2016.2645706.

[4-6] Efkarpidis N, De Rybel T, Driesen J. Optimal placement and sizing of active in-line voltage regulators in flemish LV distribution grids. IEEE Trans Ind Appl 2016;52:4577–84. doi:10.1109/TIA.2016.2599148.

[4-7] Long C, Ochoa LF. Voltage control of PV-rich LV networks: OLTC-fitted transformer and capacitor banks. IEEE Trans Power Syst 2016;31:4016–25. doi:10.1109/TPWRS.2015.2494627.

[4-8] Kikusato H, Kobayashi M, Yoshinaga J, Fujimoto Y, Hayashi Y, Kusagawa S, et al. Coordinated voltage control of load tap changers in distribution networks with photovoltaic system. IEEE PES Innov Smart Grid Technol Eur 2016.

[4-9] Tant J, Geth F, Six D, Tant P, Driesen J. Multiobjective battery storage to improve PV integration in residential distribution grids. IEEE Trans Sustain Energy 2013;4:182–91. doi:10.1109/TSTE.2012.2211387.

[4-10] Marra F, Yang GY, Traeholt C, Larsen E, Ostergaard J, Blazic B, et al. EV charging facilities and their application in LV feeders with photovoltaics. IEEE Trans Smart Grid 2013;4:1533–40. doi:10.1109/TSG.2013.2271489.

[4-11] Brunner M, Rudion K, Tenbohlen S. PV curtailment reduction with smart homes and heat pumps. 2016 IEEE Int. Energy Conf., IEEE; 2016, p. 1–6. doi:10.1109/ENERGYCON.2016.7514075.

[4-12] Wang Y, Wang BF, So PL. A voltage regulation method using distributed energy storage systems in LV distribution networks. 2016 IEEE Int. Energy Conf., IEEE; 2016, p. 1–6. doi:10.1109/ENERGYCON.2016.7514050.

[4-13] Wang Y, Tan KT, Peng XY, So PL. Coordinated control of distributed energy-storage systems for voltage regulation in distribution networks. IEEE Trans Power Deliv 2016;31:1132–41. doi:10.1109/TPWRD.2015.2462723.

[4-14] Zeraati M, Golshan MEH, Guerrero JM. Distributed control of battery energy storage systems for voltage regulation in distribution networks with high PV penetration. IEEE Trans Smart Grid 2016;PP:1–1. doi:10.1109/TSG.2016.2636217.

[4-15] Ehsani M, Falahi M, Lotfifard S. Vehicle to Grid Services: Potential and Applications. Energies 2012;5:4076–90. doi:10.3390/en5104076.

[4-16] Zeraati M, Golshan MEH, Guerrero JM. A consensus-based cooperative control of PEV battery and PV active power curtailment for voltage regulation in distribution networks. IEEE Trans Smart Grid 2017;PP:1–1. doi:10.1109/TSG.2017.2749623.

[4-17] Vickrey W. Counterspeculation, auctions, and competitive sealed tenders. J Finance 1961;16:8–37. doi:10.1111/j.1540-6261.1961.tb02789.x.

[4-18] Hayashi Y. Development of distributed cooperative EMS methodologies for multiple scenarios by using versatile demonstration platform, CREST 2015. https://www.jst.go.jp/kisoken/crest/en/project/36/36_05.html (accessed January 14, 2018).

[4-19] Yamazaki T, Homma H, Wakao S, Fujimoto Y, Hayashi Y. Estimation method of prediction interval of solar irradiance based on just-in-time modeling for photovoltaic output prediction. IEEJ Trans Power Energy 2015;135:160–7. doi:10.1541/ieejpes.135.160.

[4-20] Yamazaki T, Wakao S, Fujimoto Y, Hayashi Y. Improvement of prediction interval estimation algorithm with just-in-time modeling for PV system operation. 2015 IEEE 42nd Photovolt. Spec. Conf., IEEE; 2015, p. 1–6. doi:10.1109/PVSC.2015.7355994.

[4-21] Fujimoto Y, Sugiura T, Murata N. K-nearest neighbor approach for forecasting energy demands based on metric learning. Int. Work Conf. Time Ser., 2014, p. 1127–37.

Chapter 5
Conclusion and Future work

5.1 Contribution

In this thesis, supply and demand side energy management schemes in the LVDSs were proposed for maximum utilization of PV generation. Supply side energy management is based on the voltage control using the LVR to mitigate voltage violation that causes PV curtailment. Demand side energy management focused on the EV charging management to adjust the amount of self-consumed PV output to reduce the PV curtailment and residential operation cost in the LVDS.

In chapter 2, a decentralized and coordinated voltage control scheme of MV OLTCs and LVRs was proposed. As a solution to the local voltage violation that cannot be avoided by using only MV OLTCs, installation of LVRs in the LVDSs instead of conventional transformers was investigated. The LVR is located downstream of the MV OLTCs in the radial DSs and its functionality is affected by their operation. In our proposed coordinated voltage control scheme, we specified the LVDSs where the MV OLTCs cannot alone avoid voltage violation and deployed the LVRs. In addition, the appropriate control parameters of the LVRs were determined considering the operation of the MV OLTCs located upstream of the LVRs. The effectiveness of the proposed scheme was evaluated based on numerical simulation using a DS model in terms of the number of houses with voltage violation. The simulation results suggested that the voltage control using LVRs whose location and control parameters are appropriately determined reduced the number of houses with voltage violation by 99% versus the voltage control by only using the MV OLTCs. Moreover, it was found that the LVR should be deployed at the LVDS with many customers, at the boundary of PV penetration, and at the boundary of pole transformers with different fixed tap.

In chapter 3, a method for rapidly determining the voltage control parameters of the LVR using classifiers based on the machine learning technique was proposed. Since voltage in the LVDS is varying due to PV generation, the voltage control parameters of the LVR that prevent the voltage violation are different depending on the weather. To mitigate the complex voltage fluctuation, an upgraded voltage control scheme that updates the control parameters in a short period on the basis of reliable power forecasting is presented. At the same time, the improvement of the calculation time required for determining the control parameters is necessary to meet the continuous update of control parameters. The proposed method built the classifier that learns the appropriate control parameters to the forecasted power profiles and rapidly classifies to narrow candidates of appropriate control parameters. The narrowed control parameters were precisely evaluated by the PFC. The proposed method was validated in the numerical simulation using an LVDS model in terms of calculation time required for determining the voltage control parameters and the number of days with voltage violation. The simulation results

showed that the proposed method successfully reduced the computation time for determination of control parameters by 96% while keeping a high performance voltage control.

In chapter 4, an EV charging management scheme based on an auction mechanism was proposed. The PV curtailment in the LVDS can be reduced by shifting the customers' EV charging period so as to adjust the amount of self-consumed PV generation. To aggregate the customers and obtain the appropriate amount of EV charging by some customers connected in the same LVDS, a reduction of the residential operation cost as well as the PV curtailment is needed. At the same time, the equity of the customers' benefit obtained by contributing to the EV charging shift and the autonomy to participate in the EV charging shift should be secured. In the proposed EV charging scheme, the application of the auction mechanism allows customers to secure the benefit equity by sharing the incentive with contributed customers. Additionally, it enables the customers to voluntarily determine comparting the benefit of EV utilization for contributing to the charging shift and for travel. The effectiveness of the proposed EV charging management scheme was evaluated by a numerical simulation based on an actual Japanese DS model and power measurement. The simulation results described the proposed scheme that reduced the PV curtailment and residential operation cost up to 20.1% and 45.1%, respectively. The reduction was found even under the condition with some uncertainties; the forecasting error of the day-ahead PV curtailment, the difference of opportunity cost of EV utilization, and the economic rationality of customers, which result in the different auction result.

Considering the world energy trend promoting PV penetration in the grid, the issue of PV curtailment will become more and more obvious in many countries all over the world in near future. We focused on the utilization of the LVR and EV for addressing the issue because the introduction of the LVR is relatively easy regardless of the location and the EV will be strongly promoted under the policy to preserve the environment in the world. Therefore, we believe our proposed methods for maximum utilization of PV generation can be useful worldwide in the near future.

5.2 Future work

This thesis focused on energy management in the DS with PV; voltage control using OLTCs including LVR in the supply side and EV charging management in the demand side. Although each side energy management scheme was individually verified to be able to contribute the maximum utilization of PV generation, further improvement of the energy management performance is expected through a coordination between the supply and demand side schemes. The coordinated energy management scheme between the supply and demand side should be studied in the future work. Moreover, these studies of the coordination scheme should include a consideration for various devices that will increase in the DS. Particularly, a smart inverter implemented in the PV and BESS will become a key device in both voltage control and residential load management. Due to the difference in operational time of OLTCs and smart inverters, a coordinated voltage control to avoid the mutual

interference is expected. In demand side energy management, the net-zero energy scheme will be required by effectively utilizing the PV, EV, and BESS, especially after the FIT is no longer valid.

An integrated consideration of the transmission system (TS) and DS should be studied as another future work. Large injection of active and reactive power from the PVs and BESSs in the DS will affect the TS operation and then in turn, voltage fluctuation in TS will affect the voltage control in the DSs. Therefore, the integrated evaluation framework of the TS and DS should be built and utilized as an assessment of the mutual effect and development of energy management considering both the TS and DS.

Furthermore, the effectiveness of the proposed schemes is evaluated based on the numerical simulation in this thesis. This assessment by the numerical simulation is only a, “simulation,” such that an assessment with real world hardware is essential for practical deployment.

Research achievements

* indicate the directly related researches with this thesis

[Journals]

1. *Hiroshi Kikusato, Jun Yoshinaga, Yu Fujimoto, Yasuhiro Hayashi, Shinichi Kusagawa, Noriyuki Motegi, "Deployment of Low-Voltage Regulator Considering Existing Voltage Control in Medium-Voltage Distribution Systems", Journal of International Council on Electrical Engineering, vol.6, no.1, pp.252-260, Dec. 2016
2. *Hiroshi Kikusato, Naoyuki Takahashi, Jun Yoshinaga, Yu Fujimoto, Yasuhiro Hayashi, Shinichi Kusagawa, Noriyuki Motegi, "Method for Determining Line Drop Compensator Control Parameters of Low-Voltage Regulator Using Random Forest", Applied Mechanics and Materials, vols.799-800, pp.1299-1305, Aug. 2015
3. *喜久里浩之，高橋尚之，吉永淳，藤本悠，林泰弘，草川慎一，茂木規行，「判別器を用いたLVRのLDC制御パラメータの高速決定手法」，電気学会論文B，vol.135，no.7，pp.446-453，2015.7
4. Yu Fujimoto, Hiroshi Kikusato, Shinya Yoshizawa, Shunsuke Kawano, Akira Yoshida, Shinji Wakao, Noboru Murata, Yoshiharu Amano, Shin-ichi Tanabe, Yasuhiro Hayashi, "Distributed Energy Management for Comprehensive Utilization of Residential Photovoltaic Outputs", IEEE Transactions on Smart Grid, vol.PP, no.99, pp.1-13, Jun. 2016

[International Conference Proceedings]

1. Masaya Kobayashi, Hiroshi Kikusato, Jun Yoshinaga, Yu Fujimoto, Nao Kumekawa, Shinji Wakao, Nao Kumekawa, Noriyuki Motegi, Yusuke Yamashita, "Method for Determining Voltage Control Parameters of Low-Voltage Regulator Using Forecast Interval of Photovoltaic Output", Proc. of 2017 IEEE PES Innovative Smart Grid Technologies Europe (ISGT-Europe), Sep. 2017
2. *Hiroshi Kikusato, Masaya Kobayashi, Jun Yoshinaga, Yu Fujimoto, Yasuhiro Hayashi, Shinichi Kusagawa, Noriyuki Motegi, "Coordinated Voltage Control of Load Tap Changers in Distribution Networks with Photovoltaic System", Proc. of 2016 IEEE PES Innovative Smart Grid Technologies Europe (ISGT-Europe), Oct. 2016
3. Masaya Kobayashi, Hiroshi Kikusato, Jun Yoshinaga, Yu Fujimoto, Yasuhiro Hayashi, Shinichi Kusagawa, Noriyuki Motegi," "Methods for Determining Line Voltage Drop Compensator Control Parameters of Low Voltage Regulator Considering Temporal and Spatial Resolution of Power Forecast Profile", Proc. of 2016 The International Conference on Electrical Engineering, Jul. 2016
4. *Hiroshi Kikusato, Masaya Kobayashi, Jun Yoshinaga, Yu Fujimoto, Yasuhiro Hayashi, Shinichi Kusagawa, Noriyuki Motegi, "Basic Study on Deployment of Low-Voltage Regulator Considering

Existing Voltage Control in High-Voltage Distribution Systems", Proc. of 2015 The International Conference on Electrical Engineering, Jul. 2015

5. Kohei Mori, Hiroshi Kikusato, Shinya Yoshizawa, Yu Fujimoto, Yasuhiro Hayashi, Akihiko Kawashima, Shinkichi Inagaki, Tatsuya Suzuki, "Information Exchange Between HEMS and GEMS for Effective EV Charge / Discharge Planning", Proc. of 2015 The International Conference on Electrical Engineering, Jun. 2015
6. *Hiroshi Kikusato, Naoyuki Takahashi, Jun Yoshinaga, Yu fujimoto, Yasuhiro Hayashi, Shinichi Kusagawa, Noriyuki Motegi, "Method for Determining Line Drop Compensator Control Parameters of Low-Voltage Regulator Using Random Forest", Proc. of 2014 3rd International Conference on Power Science and Engineering (ICPSE 2014), Dec. 2014
7. *Hiroshi Kikusato, Naoyuki Takahashi, Jun Yoshinaga, Yu fujimoto, Yasuhiro Hayashi, Shinichi Kusagawa, Noriyuki Motegi, "Method for Instantly Determining Line Drop Compensator Parameters of Low-Voltage Regulator Using Multiple Classifiers", Proc. of 2014 IEEE PES Innovative Smart Grid Technologies Europe (ISGT-Europe), Oct. 2014
8. Hayato Homma, Tomohide Yamazaki, Shinya Yoshizawa, Hiroshi Kikusato, Shinji Wakao, Yu Fujimoto, Yasuhiro Hayashi, "Fluctuation Range Prediction of PV Output by Using Just-In-Time Modeling", Proc. of the 6th World Conference on Photovoltaic Energy Conversion, Nov. 2014
9. Hayato Homma, Shinya Yoshizawa, Hiroshi Kikusato, Shinji Wakao, Yu Fujimoto, Yasuhiro Hayashi, "PV Output Prediction under Various Conditions of Time and Spatial Resolutions by Just-In-Time Modeling", Proc. of the 29th European PV Solar Energy Conference and Exhibition, Sep. 2014
10. Naoyuki Takahashi, Hiroshi Kikusato, Jun Yoshinaga, Yasuhiro Hayashi, Shinichi Kusagawa, Noriyuki Motegi, "Dynamic Control Method for LVR based on Predictive and Dynamic Controller", Proc. of 2014 The International Conference on Electrical Engineering, Jun. 2014
11. *Hiroshi Kikusato, Naoyuki Takahashi, Jun Yoshinaga, Yasuhiro Hayashi, Shinichi Kusagawa, Noriyuki Motegi,"Method for Determining Line Drop Compensator Parameters of Low Voltage Regulator using Support Vector Machine", Proc. of 2014 IEEE PES Innovative Smart Grid Technologies Conference (ISGT), Washington DC (USA), Feb. 2014
12. Naoyuki Takahashi, Hiroshi Kikusato, Jun Yoshinaga, Yasuhiro Hayashi, Shinichi Kusagawa, Noriyuki Motegi,"Dynamic Voltage Control Method and Optimization for LVR in Distribution System with PV Systems", Proc. of 2014 IEEE PES Innovative Smart Grid Technologies Conference (ISGT), Washington DC (USA), Feb. 2014

[Domestic Conference Proceedings (in Japanese)]

1. 喜久里浩之，小林将矢，小浦直洋，宮崎輝，藤本悠，若尾真司，林泰弘，茂木規行，山下裕輔，「需要家の電力データに基づく LVR の制御パラメータ決定手法の体系的評価」，平成 30 年電気学会全国大会，福岡，2018 年 3 月
2. *喜久里浩之，芳澤信哉，藤本 悠，林泰弘，花田真一，五十川大也，大橋弘，「配電系統シミュレーションによる EV 充電オークション制度の評価」，平成 29 年電気学会全国大会，富山，2017 年 3 月
3. 小林将矢，喜久里浩之，吉永淳，藤本悠，林泰弘，茂木規行，山下裕輔，「PV 発電量予測の信頼区間を利用した LVR の LDC 制御パラメータ決定手法」，平成 29 年電気学会全国大会，富山，2017 年 3 月
4. *喜久里浩之，小林将矢，吉永淳，藤本悠，林泰弘，草川慎一，茂木規行，「LVR を用いた協調電圧制御の評価」，平成 28 年電気学会電力・エネルギー部門大会，北九州，2016 年 9 月
5. 小林将矢，喜久里浩之，吉永淳，藤本悠，林泰弘，草川慎一，茂木規行，「LVR の制御パラメータの更新間隔が電圧制御効果に与える影響の評価」，平成 28 年電気学会電力・エネルギー部門大会，北九州，2016 年 9 月
6. 森皓平, 喜久里浩之, 芳澤信哉，藤本悠，若尾真治，林泰弘，川島明彦，稲垣信吉，鈴木達也，「EV 充放電計画のための PV 出力抑制量予測手法」，平成 28 年電気学会電力・エネルギー部門大会，北九州，2016 年 9 月
7. 小林将矢，喜久里浩之，吉永淳，藤本悠，林泰弘，草川慎一，茂木規行，「電力波形の時間分解能を考慮した LVR の LDC 制御パラメータの決定手法」，平成 28 年電気学会全国大会，仙台，2016 年 3 月
8. *喜久里浩之，小林将矢，吉永淳，藤本悠，林泰弘，草川慎一，茂木規行，「高圧配電系統の電圧制御を考慮した LVR の設置に関する基礎検討」，電気学会平成 27 年電力・エネルギー部門大会，名古屋，2015 年 8 月
9. 森皓平，喜久里浩之，芳澤信哉，藤本悠，若尾真治，林泰弘，川島明彦，稲垣信吉，鈴木達也，「電力予測精度と HEMS/Grid EMS 協調効果の関係の評価」，電気学会平成 27 年電力・エネルギー部門大会，名古屋，2015 年 8 月
10. 森皓平，喜久里浩之，芳澤信哉，藤本悠，林泰弘，川島明彦，稲垣信吉，鈴木達也，「HEMS による電圧制約を考慮した EV 充放電計画の決定と貢献の評価」，計測自動制御学会 システム・情報部門 学術講演会 2014，岡山，2014 年 11 月
11. *喜久里浩之，高橋尚之，吉永淳，藤本悠，林泰弘，「判別器を用いた LVR の LDC 制御パラメータの高速決定手法」，平成 26 年電気学会電力技術・電力系統技術合同研究

会，堺，2014 年 9 月

12. 高橋尚之，喜久里浩之，吉永淳，林泰弘，草川慎一，茂木規行，「JIT 電圧予測をもとにした動的電圧制御手法の開発」，電気学会平成 26 年電力・エネルギー部門大会，京田辺，2014 年 9 月
13. 森皓平，喜久里浩之，芳澤信哉，藤本悠，林泰弘，川島明彦，稲垣信吉，鈴木達也，「配電系統電圧制御を考慮したモデル予測型 HEMS による PHV 充放電計画の評価」，電気学会平成 26 年電力・エネルギー部門大会，京田辺，2014 年 9 月
14. *喜久里浩之，高橋尚之，吉永淳，藤本悠，林泰弘，草川慎一，茂木規行，「Random Forests を用いた LVR の LDC 制御パラメータ決定手法の改良及び実験による検証」，電気学会平成 26 年電力・エネルギー部門大会，京田辺，2014 年 9 月
15. *喜久里浩之，本間隼人，高橋尚之，吉永淳，藤本悠，林泰弘，草川慎一，茂木規行，「PV 出力予測を用いた LVR の LDC 制御パラメータ導出に関する検討」，平成 26 年電気学会全国大会，松山，2014 年 3 月
16. *喜久里浩之，高橋尚之，吉永淳，藤本悠，林泰弘，草川慎一，茂木規行，「LVR における SVM を用いた LDC 制御パラメータの決定手法」，平成 25 年電気学会電力技術・電力系統技術合同研究会，北九州，2013 年 9 月
17. *喜久里浩之，高橋尚之，吉永淳，林泰弘，草川慎一，茂木規行，「PV 連系配電系統における LDC 制御パラメータの動的決定手法」，平成 25 年電気学会電力・エネルギー部門大会，2013 年 8 月
18. *喜久里浩之，高橋尚之，吉永淳，林泰弘，草川慎一，茂木規行，「PV 連系配電系統における LVR の LDC 制御パラメータの決定手法」，平成 25 年電気学会全国大会，名古屋，2013 年 3 月

[Award]

1. *平成 25 年電気学会電力・エネルギー部門大会，Young engineer Poster Competition (YPC) 奨励賞，2013.8.28
2. *平成 25 年電気学会電力・エネルギー部門大会，Young engineer Poster Competition (YPC) 優秀発表賞，2013.8.28
3. *早稲田大学電力技術懇談会，田村記念賞， 2014.3.14
4. *平成 25 年電気学会電力・エネルギー部門大会，優秀論文発表賞，2014.9.11
5. *2014 IACSIT Barcelona Conferences, EXCELLENT ORAL PRESENTATION CERTIFICATE, 2014.12.19
6. *早稲田大学電力技術懇談会，田村記念賞，2015.3.20

7. *IEEE Power & Energy Society Japan Joint Chapter，IEEE PES Japan Joint Chapter 学生優秀論文賞，2017.1.10
8. *早稲田大学電力技術懇談会，田村記念賞，2017.3.2
9. *平成 27 年電気学会電力・エネルギー部門大会，優秀論文発表賞，2017.9.6